FUNDAMENTALS OF HYDROGEN THYRATRONS

by

S. J. Catalano
B.S. EE University of Colorado
Boulder, Colorado - 1949

Submitted to the Department of Electrical Engineering and to the Faculty of the Graduate School of the University of Kansas in partial fulfillment of the requirements for the degree of Master of Science in Electrical Engineering.

Advisor in charge

June, 1960

For the department

DISCLAIMER

ACKNOWLEDGMENTS

The writer is deeply appreciative of the help and encouragement given by a large number of people. Foremost of these was the writer's advisor, Dr. J. N. Warfield, who combined wisely the necessary experienced guidance with the maximum proportion of freedom in persuance of this study by the writer. A great help in performing some of the testing were two of the writer's co-workers, C.E. Heare and W. L. Purtee. J. E. Long of the Bendix Document Control Department was also generous with his time and effort in clearing the security aspects of this study. Gratefully acknowledged also are the excellent typing of the thesis masters by Berniece Schmedding and Patricia Gerling and the skillful offset reproduction by Ava Willey and Margaret Gates. Finally, my thanks must be expressed to my wife who contributed greatly to this manuscript by her patience in proof-reading as well as her continual encouragement and self-denial.

S. J. Catalano

THIS PAGE

WAS INTENTIONALLY

LEFT BLANK

TABLE OF CONTENTS

LIST OF TABLES

LIST OF FIGURES

CHAPTER I

Introduction

An attempt will be made to develop a logical series of discussions leading to and describing the type 1258 miniature hydrogen thyratrons. Various parameters of this tube will be shown in graph and oscilloscope trace forms.

Preceding the final discussion will be the following in the order stated:

I. Fundamental Theory of Electrical Conduction in Gases
   - A. This will consist of a basic and elementary discussion on the physical nature of gases and the processes by which electrical conduction takes place.

II. A General Description of the Fundamental Properties of Hydrogen Thyratrons
   - A. Some properties and advantages will be listed of hydrogen over other gases in switches for line type modulators.
   - B. Hydrogen thyratrons and their characteristic behavior will be delineated.

III. Some Specific Attributes of the Type 1258 Miniature Hydrogen Thyratron
   - A. As pointed out in the opening paragraph, the type 1258 hydrogen thyratron will be investigated

with an aim toward discovering some of its specific properties. These will be shown in the form of data, graphs and oscilloscope traces.

Chapter II

Fundamental Theory of Electrical Conduction in Gases

Kinetic Theory of a Gas

In the development of the classical kinetic theory of gases, a perfect gas will be assumed. This perfect gas would have the following properties:

1. It would consist of a great number of tiny elastic spheres in continual random motion colliding with one another and with the walls of the container.
2. In its normal stable state, its tiny spheres or molecules would all be of the same size, weight, elasticity, etc.
3. These molecules would move and behave in accordance with Newton's laws of motion.
4. The sizes of the spheres are small compared with the average distances they travel between collisions; therefore their volumes may be neglected.
5. Gravitational attraction between individual spheres and between the spheres and the walls is so small that it can be eliminated from further consideration.

In an elastic collision of gas molecules, the impact of the collision changes only the velocities of the molecules in accordance with the laws of conservation of energy and of momentum.

A molecule, having a large number of impacts in an additive direction, could reach a very high velocity. While such a series of opportune

collisions appears unlikely, it will be shown later that such occurrences do take place for a small number of gas molecules.

In an actual gas, collisions of molecules are not always elastic. The inelastic collision is one in which the internal energy of one or both of the molecules is changed. This results in the excitation or ionization of that molecule.

An atom can receive energy internally only in discrete amounts. In an energy exchange between colliding particles, that energy portion available for internal absorption by one or both of the particles must be equal to or more than the minimum discrete amount either particle can absorb, or the collision will be elastic.

Molecular Velocity Distribution

In the random motion of gas molecules, many collisions between these particles will occur producing changes in their velocities in both direction and magnitude. It is evident that a few of these collisions will result in leaving one of the particles with zero velocity. Conversely, some particles will, with a fortuitous number of collisions reach a comparatively high velocity. Most particles will have velocities between these extremes. The distribution of velocities of gas molecules under equilibrium conditions was derived by both Boltzmann and Maxwell, though by very different methods.

The derivation of the Maxwell-Boltzmann distribution function[1], as it

---

[1] Maxwell's derivation is shown in J. D. Cobine's "Gaseous Conductors" while Boltzmann's derivation is to be found in L. B. Loeb's "Kinetic Theory of Gases".

Chapter II

is often called, will not be performed here. Only the results of Maxwell's derivation will be stated. (The reader is invited to follow the step by step derivations in the references listed below in the footnote if he is interested.) The maxwellian distribution function can then be written in the form of the following expression:

$$\frac{dNc}{N} = \frac{4}{\sqrt{\pi}} \frac{c^2}{c_o^3} e^{-\frac{c^2}{c_o^2}} dc \qquad (1)$$

where c is the velocity of any gas molecule

dNc is the number of molecules having velocities between c and c + dc

N is the number of gas molecules under consideration and c_o is the most probable velocity

The quantity $\frac{dNc}{N}$ may be thought of as the probability of a velocity between c and c + dc. A useful form of the distribution function is given by the curve in fig. 1 [2].

---

[2] J. D. Cobine. Gaseous Conductors. Dover Publications Inc., New York, 1941, p. 15.

Chapter II

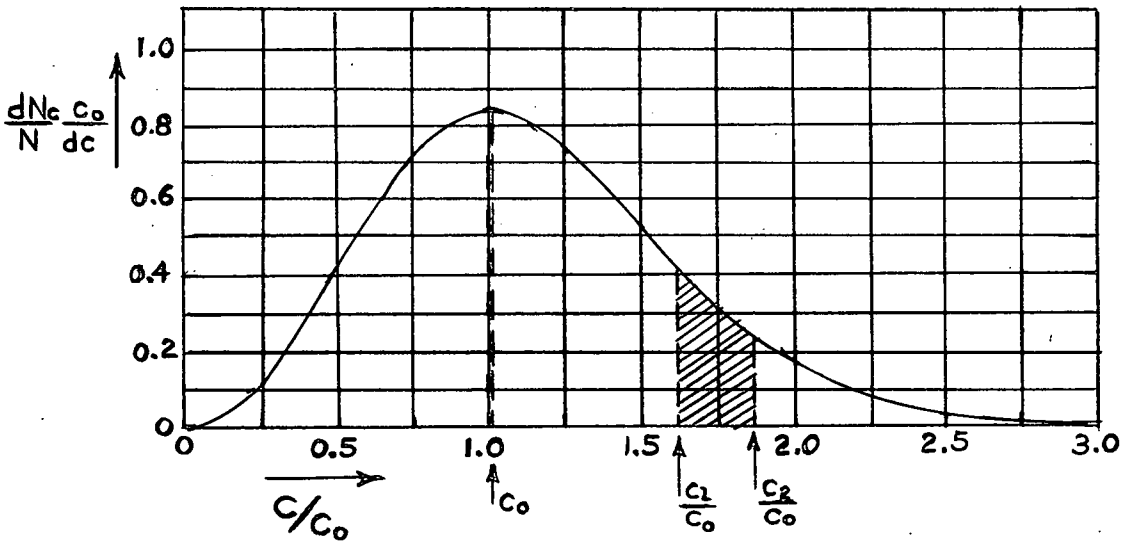

Fig. 1 Maxwellian Velocity Distribution Function.

The number of molecules having velocities within a given range, as between c_1 and c_2, is found by determining the area under the distribution curve between points c_1/c_0 and c_2/c_0 as indicated by the shaded portion of the graph.

It can be shown that the most probable velocity c_0 is proportional only to the mass of the gas molecules and to the temperature of the gas.

$$c_0 = \sqrt{\frac{2kT}{m}} \qquad (2)$$

where k is Boltzmann's gas constant

T is absolute temperature in degrees Kelvin

m is the mass of a molecule of gas

Using this new relationship for c_0, the distribution equation (1) becomes:

$$\frac{dNc}{N} = \frac{4}{\sqrt{\pi}} \left(\frac{m}{2kT}\right)^{3/2} c^2 e^{-\frac{mc^2}{2kT}} dc \qquad (3)$$

Chapter II

Mean Free Path of Electrons and Molecules

The distance that an electron moves between successive collisions with atoms in a gas is called the free path. Taking the average of a great many free paths traveled by electrons before colliding results in a quantity defined as mean free path of an electron. When electrons are traveling through a gas of molecular radius r, with N molecules per cubic centimeter, the mean free path of an electron can be found from the expression:

$$M.F.P. = \frac{1}{\pi r^2 N} \qquad (4)$$

Avogadro's number, 2.69×10^{19} molecules per cubic centimeter at $0^{\circ}C$ and 760 millimeters of mercury pressure will give the value of N under the conditions of pressure and temperature specified. However, as pressure and temperature values depart from these standard conditions, a modified form of the gas laws must be used to calculate N.

$$N = (2.69 \times 10^{19}) \frac{P\ T_o}{P_o\ T} \text{ molecules/cm}^3 \qquad (5)$$

where P_o & T_o are standard pressure and temperature conditions specified above with temperatures being expressed in degrees Kelvin.

Data on the molecular radius and the mean free path of an electron in various gases at several pressures are given in Table 1. [1]

---

[1] J. D. Ryder. Electronic Engineering Principles, Prentice Hall, Inc., New York, 1947, p. 272.

Chapter II

Table 1

Theoretical Mean Free Paths of Electrons in Gases at 25°C

Gas	M.F.P.(cm) P = 0.001 mm	M.F.P.(cm) P = 1mm	Molecular radius (cm)
Mercury	12.5	0.0149	1.82×10^{-8}
Argon	7.1	0.0450	1.43×10^{-8}
Neon	23.0	0.0787	1.17×10^{-8}
Hydrogen	77.0	0.0187	1.09×10^{-8}

Distribution of Free Paths

The length of the free paths of gas particles is determined by collisions which are random occurrences. Therefore some of these lengths will be long and some will be short. An expression will be sought for the "length distribution" of molecular free paths.

Consider a single gas molecule having an average velocity v, and an average of p collisions per second. Then the average number of collisions in one centimeter of travel [1] will be $a = p/v$ and the probable number of collisions made by this molecule in traveling a distance dx will be adx. If N molecules are released through a slit into a gas, let n be the number traveling a distance x without having a collision. Then it can be said that in the increment of distance between x and x+dx, the

[1] This is an average free path for one particle, and requires a knowledge of p and v, both of which vary from particle to particle and also with time.

amount of n molecules that will collide is proportional to the number entering this interval and the length of the interval.

That is, the change in n is

$$dn = -an\,dx$$

Integrating the above gives

$$n = Ae^{-ax}$$

At x=o, (at the slit), n=N; therefore

$$n = Ne^{-ax} \qquad (6)$$

To relate the constant a to the molecular m.f.p., let dN be the number of molecules with a free path of length between x and x + dx. The equation for the m.f.p. is

$$L = \int_0^N \frac{x\,dN}{N} \qquad (7)$$

Since $dN = |dn| = an\,dx = aNe^{-ax}\,dx$,

$$L = \int_0^\infty \frac{aNxe^{-ax}\,dx}{N} = \frac{1}{a}$$

From which the distribution of free paths can be expressed as

$$n = Ne^{-\frac{x}{L}} \qquad (8)$$

It can be seen from this equation that the number of free paths of length greater than a given distance is a decreasing exponential function of the distance. In figure 2,[1] it is evident that only 37% of the initial number

---

[1] Cobinc. op. cit., p.25

of molecules have free paths of length greater than one m.f.p.

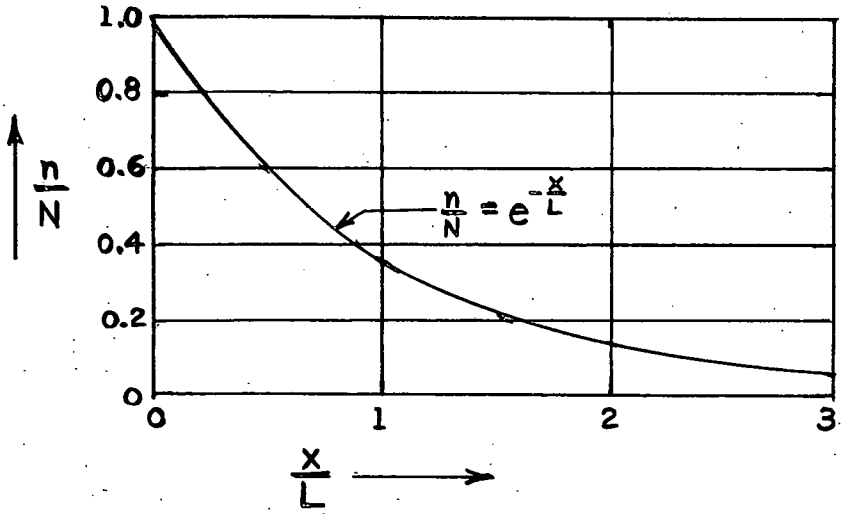

Fig. 2 Distribution of Free Paths

Mobility of Gaseous Ions

The dimensions of a high vacuum device are usually much smaller than the m.f.p. of ions. However, it is evident that the presence of gas will retard the motion of ions in an electric field, primarily because of the many collisions with the gas molecules. After each collision, the ions are accelerated by the electric field and gain some velocity in the direction of the field before the next impact. The average velocity component in the direction of the field of this stop and go motion is defined as the ion average drift velocity. This average drift velocity is directly proportional to the strength of the electric field and in an inverse manner upon the density of the gas under discussion. When the average drift velocity of an ion is determined for

a unit electric field, it is called the mobility K of the ion. The mobility K is mainly influenced by the type of gas through which the ion travels. Table 2 shows values of K obtained experimentally. [1]

Table 2

Mobility of Singly Charged Gaseous Ions at 0°C and at 760 mm hg.

Gas	K-	K+
Air (dry)	2.1	1.36
Air (very pure)	2.5	1.8
A	1.7	1.37
A (very pure)	206.0	1.31
Cl_2	0.74	0.74
CCl_4	0.31	0.30
C_2H_2	0.83	0.78
C_2H_5Cl	0.38	0.36
C_2H_5 OH	0.37	0.36
CO	1.14	1.10
CO_2 (dry)	0.98	0.84
H_2	8.15	5.90
H_2 (very pure)	7900.0	-
HCl	0.62	0.53
H_2O (at 100°C)	0.95	1.10
H_2S	0.56	0.62
He	6.30	5.09
He (very pure)	500.0	5.09
N_2	1.84	1.27
N_2 (very pure)	145.0	1.28
NH_3	0.66	0.56
N_2O	0.90	0.82
Ne	-	9.9
O_2	1.80	1.31
SO_2	0.41	0.41

[1] Ibid., p. 15

Chapter II

These experimental values are estimates of the most probable values for K since experimental measurements indicate a drift velocity distribution for ions. The table shows that, generally, the mobility of the negative ion is greater than that of the positive ion. Also evident in the table is the large difference in K values for pure and impure quantities of a given gas. The K^- value for ordinary hydrogen equals 8.15 while pure hydrogen possesses a K^- of 7900. It is thought that impurities lower K by tending to attach themselves to ions and forming clusters. The subsequent increase in effective mass and cross-section of such ions greatly reduces the average drift velocity. Therefore great care must be taken in proper selection of K for engineering calculations consistent with purities of gases used.

Theoretical considerations would lead to the conclusion that K should decrease with an increase in atomic or molecular weight of the gas. This is borne out by the results obtained experimentally and shown in figure 3.[1]

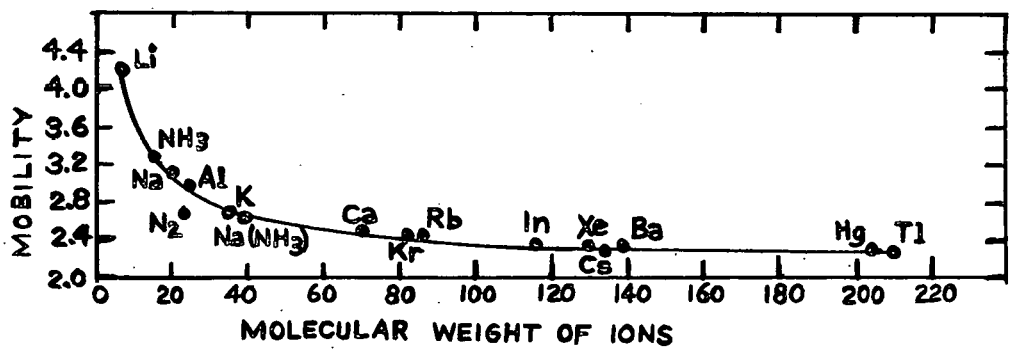

Fig. 3 Mobility of Positive Ions in Nitrogen (K in $\frac{\text{cm/sec}}{\text{volts/cm}}$)

---

[1] Ibid., p. 37.

Chapter II

Circuit Current Produced by Charge Motion

The creation of circuit current due to ion movement in a gas may be explained by studying the image charges in the electrodes. As an electric charge, $+q$, leaves one of the two electrodes shown connected in figure 4,[1] it induces an image charge of the opposite sign on the electrode from which it departed. Moving out further between the two electrodes, the charge, $+q$, has now shifted some of its lines of force from electrode A to electrode B, and correspondingly some portion of the original induced image charge on electrode A has flowed through the connecting conductor to electrode B. The proportion of negative charges induced on electrodes A and B at this time are $-\alpha q$ and $-(1-\alpha)q$ respectively.

Continuing to move, the charge, $+q$, arrives at electrode B. The total image charge, $-q$, also has reached electrode B simultaneously, traveling through the metallic conductors.

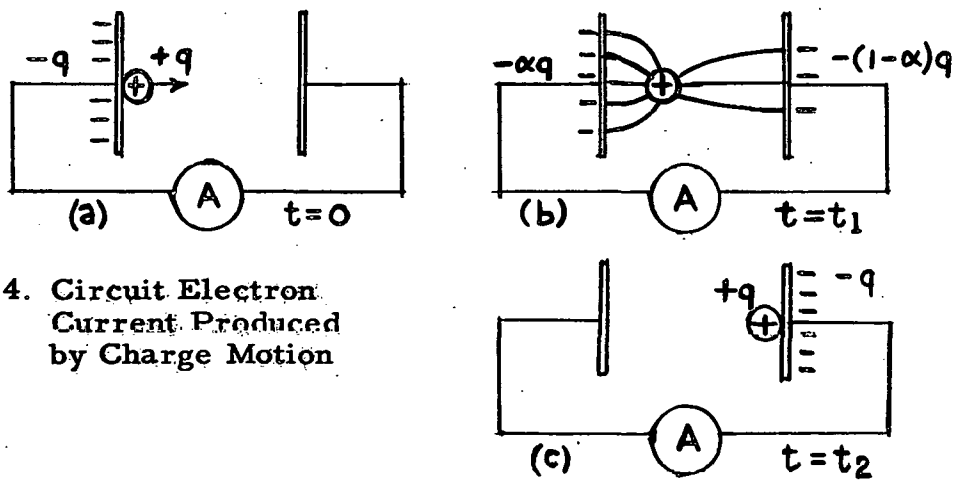

Fig 4. Circuit Electron Current Produced by Charge Motion

---

[1] Ibid., p. 55.

Chapter II

The Bohr Atom

It will be recalled that an assumption was made at the beginning of this chapter that gas molecules and atoms were tiny elastic spheres. This picture of gas particles was useful in explaining the phenomena of elastic collisions but is inadequate for describing the inelastic collision and its results. Therefore to better understand the concept of gaseous conduction, a fuller knowledge of the atom and its structure is needed. Early theories of the atom were proposed by Thompson and Rutherford. Sir J. J. Thompson's picture of the atom (shown in figure 5a [1]) consisted of a sphere, positively charged in which negative charges were scattered at random much like raisins in a muffin. Rutherford's experiments showed that such a proposed model was inconsistent with the data known at that time so he suggested a new model for the atom. (figure 5b [1]). In this configuration, a core of positive charge (nucleus) was surrounded by a sufficient number of fixed negative charges to make the atom neutral. Bohr extended Rutherford's conception of the atom and proposed a dynamic model much like the solar system (figure 5c [1]) in which the negative charges revolve around a nucleus of positive charge. Certain other conditions and properties were required for this proposed model and will be described later.

---

[1] J. D. Ryder, Electronic Engineering Principles - Prentice Hall, Inc., New York, 1947, p. 3

Chapter II

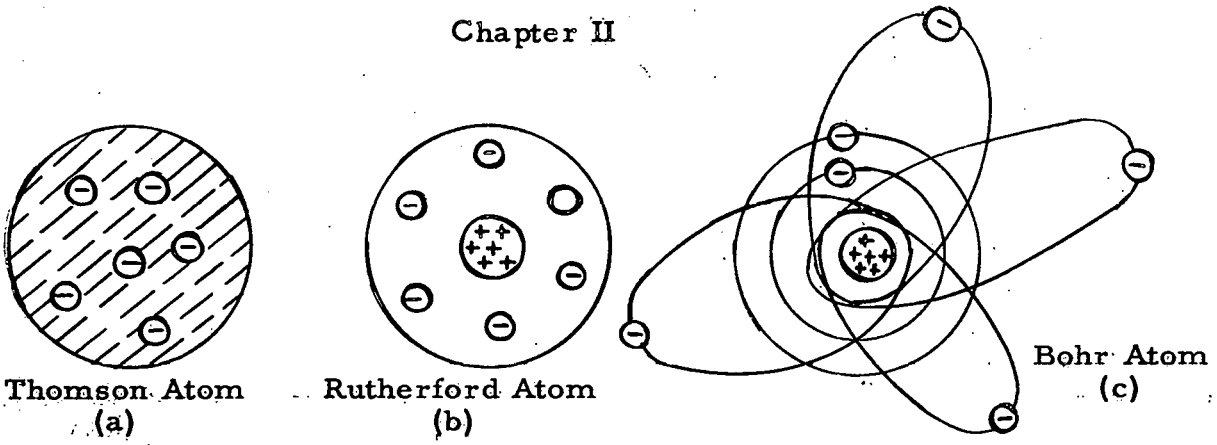

Fig. 5. Early Models of the Atom

Recent experimental results have led to some modification of the Bohr atom model in that negative charges have been given wave properties, orbits have given way to energy levels, and positions of electrons are expressed in terms of probabilities rather than in definite coordinates. However the definite physical picture of the atom proposed by Bohr will be useful for explaining gas conduction, so its special properties and conditions will be studied.

Max Planck established the quantum theory in attempting to find a satisfactory explanation for certain experimental results he obtained in the study of black box radiation. He theorized, in contradiction to classical mechanics that energy is radiated in a discrete quantities, $e = h\nu$ (The quantum of energy for light of frequency ν) This quantum of radiant energy is called a photon. With this initial premise, he went on to develop a theory to fit the experimental data resulting from his black box radiation study. Thus the quantum theory was evolved. Bohr applied Planck's quantum concept to his own problem and

proposed that atoms could radiate light only in these same discrete bundles of energy.

In addition, Bohr specified that electrons could revolve around the nucleus only in certain fixed orbits. An electron revolving about the nucleus follows roughly a circular path which necessitates a balance between the force of attraction of the nucleus and the outward centrifugal force due to rotation; but the continuous acceleration toward the center which is an inherent characteristic of circular motion must also be accompanied by radiation of energy from the accelerated particle according to classic electrodynamic theory. However, continued loss of energy from the electron due to the theoretically-required radiation would result in progressively smaller and smaller orbits around the nucleus with the eventual drop of the electron into the nucleus. Such an event would have long since occurred in all atoms, and matter would have ceased to exist in the form we know it today. It was apparent that classical electrodynamics gave answers inconsistent with observed results and Bohr, ignoring it, arbitrarily set up his first postulate:

1. An electron does not radiate or give up energy when it is in a stable orbit.

Bohr postulated two other basic requirements:

2. The angular momentum of the electron in the orbit could have only certain discrete values given by $nh/2\pi$ where h is Planck's constant and n may have only integer values, 1, 2, 3.....

Chapter II

3. An electron jumping to an orbit of lower energy radiates the excess energy only in certain discrete quanta of light. (photons) These three proposed properties gave Bohr a satisfactory atom model that agreed with experimental results and explained the existence of line spectra.

The First Bohr Postulate - Energy of an Orbit

To calculate the energy required by an electron to remain in a given orbit about the nucleus, let the simple case of the hydrogen atom be considered. With the single electron's mass equaling m, and the mass of the nucleus equaling M, the outward centrifugal force on the electron can be described in the following relationship:

$$f_c = \frac{mv^2}{r}$$

(M >> m therefore the affect of the electron's motion on the nucleus is negligible and can be ignored)

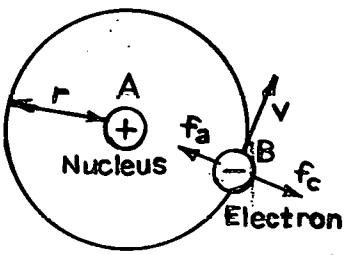

Fig. 6. Model of Hydrogen Atom

Coulomb's inverse square law gives the opposite and inward force on the electron resulting from the attraction force of the positively - charged nucleus.

Chapter II

$$f_a = \frac{e(-e)}{4\pi\epsilon_0 r^2} = -\frac{e^2}{4\pi\epsilon_0 r^2}$$

The net force on the electron is the algebraic sum of these two forces and since it is in equilibrium, this net force is zero.

$$\text{i.e.} \quad \frac{mv^2}{r} - \frac{e^2}{4\pi\epsilon_0 r^2} = 0$$

$$\text{or} \quad mv^2 = \frac{e^2}{4\pi\epsilon_0 r} \qquad (9)$$

The rotating electron can be said to have a kinetic energy equal to

$$\text{K.E.} = \frac{mv^2}{2} \qquad (10)$$

Combining equations (9) and (10) gives the relatibnship

$$\text{K.E.} = \frac{e^2}{8\pi\epsilon_0 r} \qquad (11)$$

The potential of any point in a field is defined as the work necessary to move a unit positive charge from infinity to the given point. To find the potential of point B (in fig. 6) due to the positive charge on the nucleus, we integrate

$$V = \int_{\infty}^{r} f\,dr = \int_{\infty}^{r} \frac{e^2}{4\pi\epsilon_0 r^2}\,dr = \frac{e}{4\pi\epsilon_0 r} \qquad (12)$$

where V is the potential from infinity to the orbit.

Chapter II

The energy gained by any electron moved through a potential V is v (-e) joules; therefore the potential energy acquired by the electron in moving from infinity to the orbit of radius r is

$$P.E. = \frac{e(-e)}{4\pi\epsilon_0 r} = -\frac{e^2}{4\pi\epsilon_0 r} \qquad (13)$$

(The negative sign shows that the electron has lost energy in moving from infinity to the orbit, having moved there under the attraction of a positive charge.)

The potential energy (equation (13)) and the kinetic energy (equation (11)) added together give the total energy of the electron in orbit.

$$W = -\frac{e^2}{4\pi\epsilon_0 r} + \frac{e^2}{8\pi\epsilon_0 r}$$

$$W = -\frac{e^2}{8\pi\epsilon_0 r} \qquad (14)$$

(The negative sign merely indicates an energy less than the zero reference energy possessed by the electron at zero.)

Second Bohr Postulate

In 1913, using Planck's earlier study of thermal radiation from hot bodies as a springboard, Bohr concluded that the angular momentum of an electron in orbit could possess only certain values as determined by the relation $nh/2\pi$.

Chapter II

DeBroglie reached the same conclusion in 1924 by an entirely different line of reasoning. He contended that electrons, though exhibiting corpuscular properties in many of the investigations made on these fundamental particles, also possessed wave properties similar to those of light. His equation defining the wavelength associated with the electron is

$$\lambda = \frac{h}{mv} \qquad (15)$$

where h is Planck's constant
v is velocity of the electron
m is the relativistic mass of the electron

This relationship states that electrons will have shorter wavelengths at higher speeds. In 1928 Davisson and Germer substantiated DeBroglie's hypothesis in an experiment involving electron beams and their diffraction from crystals.

The manner in which an electron might present wave-like characteristics orbiting around a nucleus can be explained by considering the circumference of a given orbit. The circumference of the orbit must be exactly an integral number of wavelengths long, - i.e., if an electron exhibits a positive wave value at a given point in its orbit, it must possess that same positive value at that point for every revolution made. The wave properties described can be clearly seen in figure 7a.[1]

---

[1] Ibid., p. 262

Chapter II

Figure 7b[1] shows the cancelling effect of a wave pattern in which the circumference is not an integral number of wavelengths. It is evident that with this kind of wave pattern, succeeding superimposed revolutions

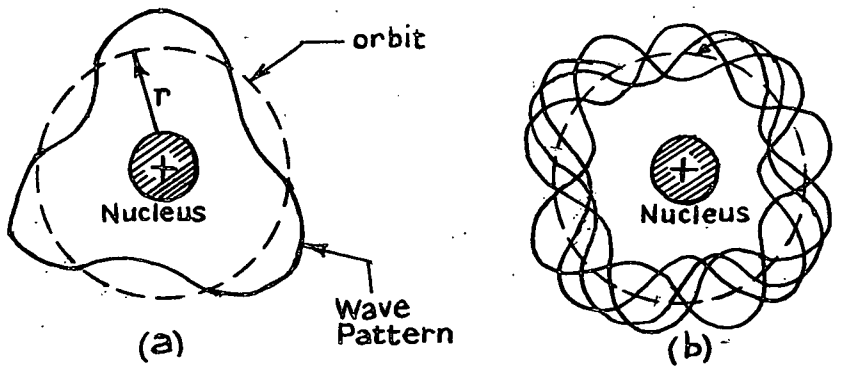

Fig. 7. Effect of Electron Patterns (a) Circumference of Orbit = $n\lambda$, (b) Circumference of Orbit not an Integral Number of Wavelengths.

will produce wave amplitudes of opposite polarity which will totally cancel out any electron wave effect. Therefore, if an electron wave length is to be realized, it must be assumed that the circumference of an orbit can be only an integral number of wavelengths in length. Stated mathematically, this relation would be

$$n\lambda = 2\pi r \tag{16}$$

where r is radius of the electron's orbit
λ is wavelength associated with the electron
and n is an integer value

If the value of λ given by equation (15) is substituted in equation (16) the result may be written

$$mvr = \frac{nh}{2\pi} \tag{17}$$

---

[1] Ibid., p. 262

Chapter II

The linear velocity of a revolving particle can be used to obtain its angular velocity ω by using

$$v = \omega r \qquad (18)$$

Substituting (18) into (17) gives

$$mr^2\omega = I\omega = \frac{nh}{2\pi} \qquad (19)$$

This relation states that the angular momentum of an electron ($I\omega$ is angular momentum) equals the quantity $nh/2\pi$ — so DeBroglie, having proposed wavelength properties for the electron, was able by this initial hypothesis to come to the same conclusions as Bohr in his second postulate.

Still considering only the simple hydrogen atom, a solution will be obtained for the radii of the allowed orbits in accordance with the angular momentum requirements stipulated above. If equations (10) and (11) are combined, the following relation results

$$\frac{mv^2}{2} = \frac{e^2}{8\pi\epsilon_o r}$$

The substitution of (18) into the above modifies it to

$$\frac{m\omega^2 r^2}{2} = \frac{e^2}{8\pi\epsilon_o r}$$

Finally, if ω^2 in the above equation is replaced by its equivalent value shown in equation (19), the resulting expression is

$$r_n = n^2 \frac{h^2 \epsilon_o}{\pi m e^2} \qquad (20)$$

The orbits allowed by the above expression have radii that are proportional to the squares of integers, 1, 2, 3..... These integers are known as the "quantum" numbers of the several orbits. The first orbit for hydrogen has a radius of 0.53×10^{-10} meters; its second orbit is four times as great, the third nine times as great, etc. Equivalent solutions involving heavier atoms are not obtainable, but the Bohr theory provides a qualitative picture of these more complex particles.

Equation (14) describes the energy possessed by an electron in any given orbit about hydrogen nucleus. If the permitted radii of equation (20) are inserted in the energy equation, the energy level of an electron in any permitted orbit may be expressed as:

$$Wn = -\frac{1}{n^2}\frac{m e^4}{8h^2 \epsilon_o^2} \qquad (21)$$

A hydrogen atom is in its normal and most stable state when its electron occupies the lowest energy orbit, that is, the first orbit. Likewise any atom is in its normal state when the electrons are in their lowest energy condition.

In all previous discussions, circular orbits have been considered but the general path an electron follows around a heavy nucleus is known to be elliptical. However this departure from actual Bohr theory and other details ignored in the forming of a qualitative picture of the Bohr atom are not important from an engineering standpoint.

Chapter II

A method of defining or describing an electron in any particular energy level has been developed and used by the spectroscopists. This relates quantum properties of the atom with its spectroscopic data. The various effects or forces associated with the electron in an atom may be stated as follows:

(1) An electron revolving in an orbit is an electric current and thus is accompanied by the necessary magnetic field with its direction determined by the electron direction of motion.

(2) The electron, as a negative charge, produces an additional magnetic field due to its rotation about its own axis.

These magnetic fields as well as the physical aspects of the electron in motion - i.e., its radial momentum and angular momentum are vectorial and quantal in nature.

The vector quantum numbers assigned to any electron in an atom are obtained from the following rules:

(1) The <u>total quantum number n</u> as determined in equation (16),

(2) The orbital angular momentum, described by the <u>orbital quantum number ℓ</u>, whose value can be integers from o to n-1,

(3) The spin quantum number s, resulting from the spin of an electron about its own axis, (Its magnitude is always equal to 1/2)

(4) The <u>total angular momentum quantum number</u> j of an electron - which is the vector sum of the orbital and spin quantum numbers ℓ and s.

Chapter II

When a magnetic field is present, two additional quantum numbers are necessary for complete description of an electron energy state in an atom:

(5) The magnetic spin quantum number m which is the projection of s on the magnetic axis. (The number m_s equals either 1/2 or -1/2 and is determined by the direction of spin of the electron.)

(6) The factor m_ℓ which is the magnetic orbital quantum number. (This factor is the projection of ℓ on the magnetic axis and can assume the integral values $(2\ell + 1)$ between -1 and +1 including zero.)

W. Pauli declared in his well-known Exclusion Principle that no two electrons in an atom can have the same values for each of the five quantum numbers n, ℓ, s, m_s, and m_ℓ. Stated in another manner, electrons returning to a completely stripped nucleus drop to the lowest allowed energy state, but at no time can any two of these electrons in the atom exist with exactly identical energy states as defined by the same five quantum numbers.

The Third Bohr Postulate - Radiation

It has been stated that electromagnetic radiation (light) emanates from an atom when an electron drops to an orbit of lower energy and that this radiating energy is released in discrete amounts or quanta (photons). An explanation of this phenomenon in terms of quantum mechanics theory will be attempted.

Chapter II

According to equation (21), the energy W_n of an electron is greater with larger values of quantum number, - i.e, with greater values of n. Therefore an electron in orbit of energy W_2 falling to an inner orbit of energy W_1 will lose energy of the amount

$$W = W_2 - W_1 \qquad (22)$$

The principle of conservation of energy leads to the inescapable conclusion that the energy W has either been radiated or converted to mass since energy can neither be created or destroyed. Some earlier work by Max Planck had resulted in the establishment of quantum size of energy versus frequency of the radiation relationship:

$$w = hf \qquad \text{joules} \qquad (23)$$

Concerning this equation John D. Ryder makes the following comment:

> This states that a quantum, or single bundle of radiant energy, has a definite size for every frequency, or color, of the radiation - that is, a quantum is not a fixed unit but varies with the frequency of the radiation. The name given to the bundle or particle of radiant energy is the "photon". All photons, therefore, are not alike.[1]

Bohr applied Planck's results to the initial premise he made on atomic radiation (equation (22)) and obtained

$$hf = W_2 - W_1$$

or

$$f = \frac{W_2 - W_1}{h} \qquad \text{cycles per sec.} \qquad (24)$$

---

[1] John D. Ryder, Electronic Engineering Principles, Prentice Hall, Inc., New York 1947, p. 265

Chapter II

An electron falling from an outer orbit of energy W_2 to an inner orbit of energy W_1 will emit radiation in the frequency described by equation (24). The corresponding wave length expression for (24) is

$$\lambda = \frac{hc}{W_2 - W_1} \quad \text{m}$$

$$\lambda = \frac{10^{10}\ hc}{W_2 - W_1} \quad \text{A}^{\circ} \qquad (25)$$

The foregoing equation gives the wavelengths of the photons radiated when electrons jump from higher energy orbits to lower energy orbits in the hydrogen atom. The complexity of the heavier atoms prevents the easy calculations of the emitted radiation frequencies but much can be learned through analogy with the simple hydrogen atom.

Metastable States

Experimental results have revealed the existence of certain energy levels from which orbital jumps in a lower direction occur very rarely. These levels have been named metastable levels or states. Electrons can leave these metastable levels only by gaining enough energy to leap to a higher energy level.

From this new position, the electron is then able to make any move to higher or lower normal levels. Since the metastable atom has a fewer number of ways to change energy level than a normal atom, its average life is longer in that state than in a normal state. A comparison of average lives of the two classes shows a length of 10^{-4} seconds for the metastable level as compared to 10^{-8} seconds for the normal excited level.

Chapter II

Excitation and Ionization Potentials

The nature of the excitation and ionization potentials of any gas can be more easily discussed by the use of an energy level diagram for the given gas atom. An energy level diagram consists of a number of horizontal lines spaced on an appropriate energy scale to represent the energy levels of the atom. Such an energy level diagram[1] (arranged according to an electron-volt scale) is shown for eleven different elements in figure 8. These are gases and vapors commonly used in discharge tubes.

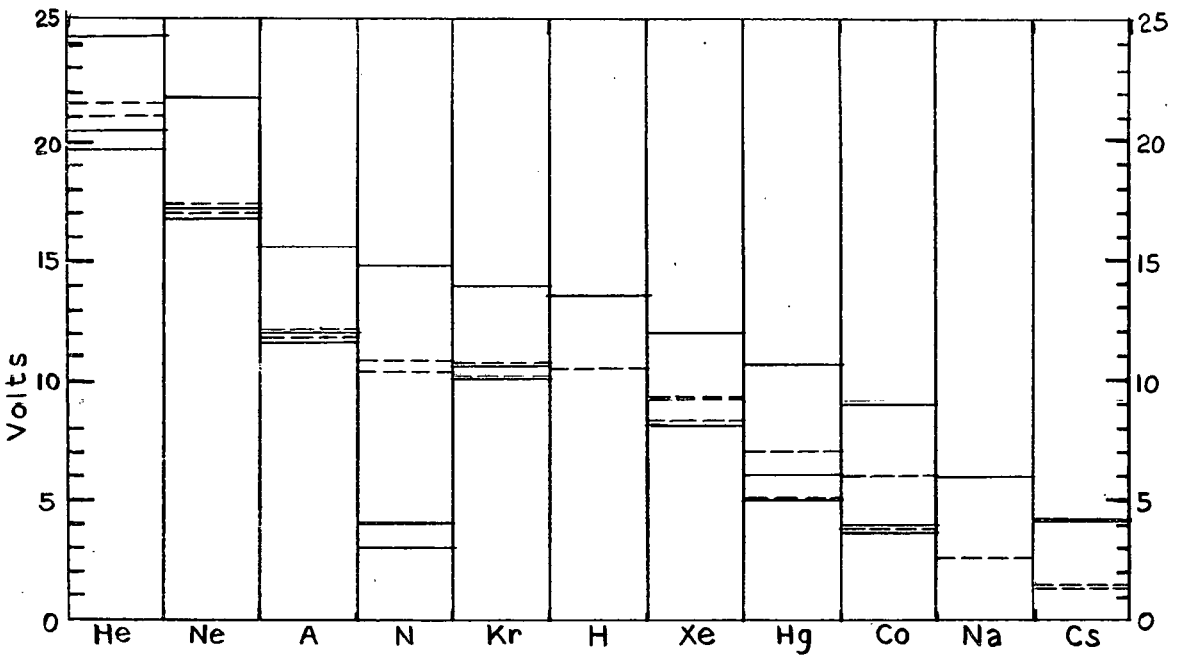

Fig. 8 Energy Level Diagram.

[1] H. Cotton, Electric Discharge Lamps 1946 p. 123

Chapter II

The diagram is constructed so that the normal, or unexcited, level is located at the bottom and, in the case where the electron-volt scale is used, this level is defined as zero. The top line in each case (solid line) indicates the potential energy level of an atom that has lost one electron. This is the ionization potential of the atom and is the amount of energy the normal atom must absorb to become ionized. Where an electrical discharge is concerned, this energy is provided in some manner by the electric field. One of the ways electric field energy is supplied to the atom is by the energy transfer, complete or partial from an electron to the atom in an inelastic collision between the two particles. The colliding electron had previously obtained its energy by being accelerated in the electric field. When the atom absorbs less energy than the amount required for ionization, it must accept an appropriate amount to raise it to one of that atom's excited levels. These excitation levels are shown as dotted lines on the energy diagram of figure 8 and are named resonance potentials. These shown in the figure are the lowest energy states from which the atom can quickly return to its normal unexcited state by releasing radiation. Of course this radiated energy must be equal to the energy absorbed by the atom previously when it was raised from the zero level to the levels under discussion. The lower solid lines in each atom's energy diagram are the lowest so-called forbidden energy states, i.e., those from which an electron is very rarely able to drop to a lower energy level. These are called metastable states.

Chapter II

Ionization

If an atom gains enough energy through some process, one of its electrons may jump from a normal or excited orbit to a point beyond the influence of the nucleus. This process of electron removal from an atom is called ionization. Electrons in the outermost orbit are held the most loosely by the nucleus and thus are the most easily lost by the atom. The minimum energy needed to remove an outer electron from its normal state in a neutral atom to a point not affected by the nucleus attractive field, is called the first ionization potential V_i of the atom. Adding sufficiently more energy results in the removal of additional electrons from the atom; however in this case a negative electron must be removed from a positive ion. Therefore the forces required for electron removal are much greater. Although ions of more than one electrical charge are rare, mercury ions have been observed with as many as eight positive charges.

Some of the more common gases and their ionization potentials are listed in table 3. [1]

TABLE 3

IONIZATION POTENTIALS OF CERTAIN COMMON GASES AND VAPORS

ELEMENT	IONIZATION POTENTIAL (e-v)
Argon	15.69
Helium	24.48
Hydrogen	13.6
Krypton	13.3
Mercury	10.39
Neon	21.47
Sodium	5.1
Xenon	11.5

[1] Ryder. op. cit., p. 268

Chapter II

The atom may acquire the appropriate energy for its excitation or ionization:

(1) by colliding with a high speed electron

(2) by absorbing a photon of correct energy

(3) by colliding with a positive ion

(4) by gaining so much thermal energy that its collision with another neutral atom is sufficient to produce ionization or excitation.

Ionization by Electron Collision

The velocity of the moving electron is a measure of its ability to ionize a molecule with which it may collide. Very slow moving electrons will not cause ionization but merely collide elastically with the molecule. Electrons with greater speed but insufficient energy to ionize an atom may accomplish the ionization in two steps, one electron first exciting the atom, the second electron providing enough energy to complete the ionization.

Further increases in electron speed will eventually lead to electrons of optimum energy for ionizing atoms. Very high speed electrons, however, are comparatively poor ionizers since many times they pass too quickly through an atom's sphere of influence to dislodge an electron. A plot is shown in fig. 9[1] of the numbers of ion pairs (equal amounts of positive and negative charges appear as ions) produced by an electron in traveling 1 cm. through air at a pressure of 1 mm.

---

[1] J. D. Cobine Gaseous Conductors Dover Publications, Inc., New York 1941, p. 79

Chapter II

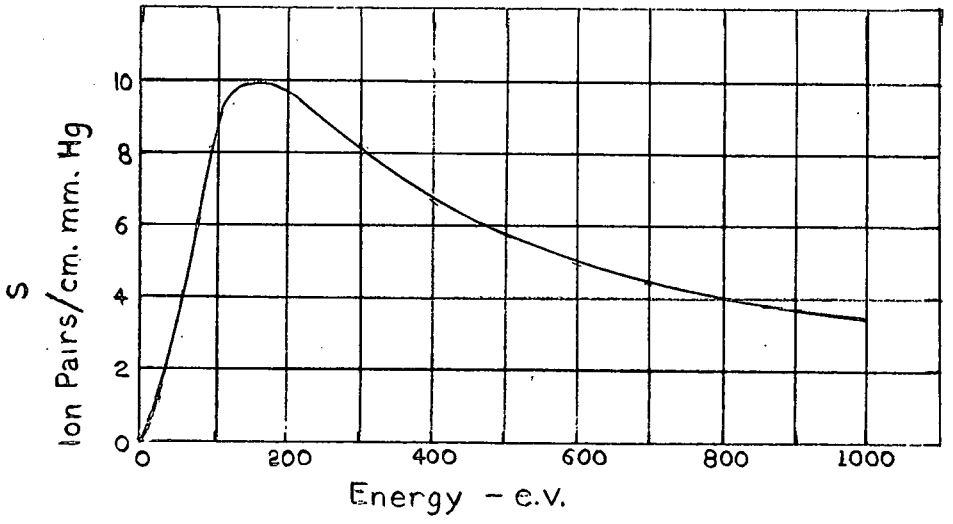

Fig. 9 Differential Ionization Coefficient for Electrons in Air (1 mm Hg 0°C)

Ionization by Radiation

It was stated earlier that an atom became ionized by absorbing the appropriate amount of energy provided by some outside source. This energy may be in the form of radiation (photons); however the quantum of light or photon must be of the appropriate kind, i.e., the h of the photon must be of greater magnitude than the eV_i of the atom. Unlike ionization by electrons, ionization by photons becomes rapidly less frequent with increase of photon energy beyond that required for ionization. Photoionization drops to zero at frequencies less than resonance. It is the general concensus of opinion that the amount of photoionization in gas discharges is considerably less than that of ionization by electron collisions.

Chapter II

Ionization by Positive-ion Collision

If positive ions possess great energies, they are effective ionizers. These energy levels are those which ions would have when their velocities are equal to those of electrons falling through the minimum ionization potential. Their kinetic energies are in the order of thousands of volts.

Thermal Ionization

It was stated earlier that neutral atoms or molecules could absorb so much thermal energy that collisions with one another at these thermally-induced high velocities would result in ionization. High temperature flames are a source of the required thermal energies and heat up the gases to produce the ionizing action of molecular collisions, radiation, and electron collisions. With increase in temperature, ionization is increased for the following reasons:

1. Many more ionizing collisions will occur as a result of an increase in high velocity atoms.
2. Greater photoionization takes place as a result of the higher radiation from the increasingly hot walls of the container.
3. The electrons freed from the molecules in the ionization process collide randomly with the increasingly-faster molecule and thus may gain enough energy to ionize another particle in a succeeding collision.

Chapter II

A measure of the degree of ionization with change in temperature is shown in fig. 10.[1]

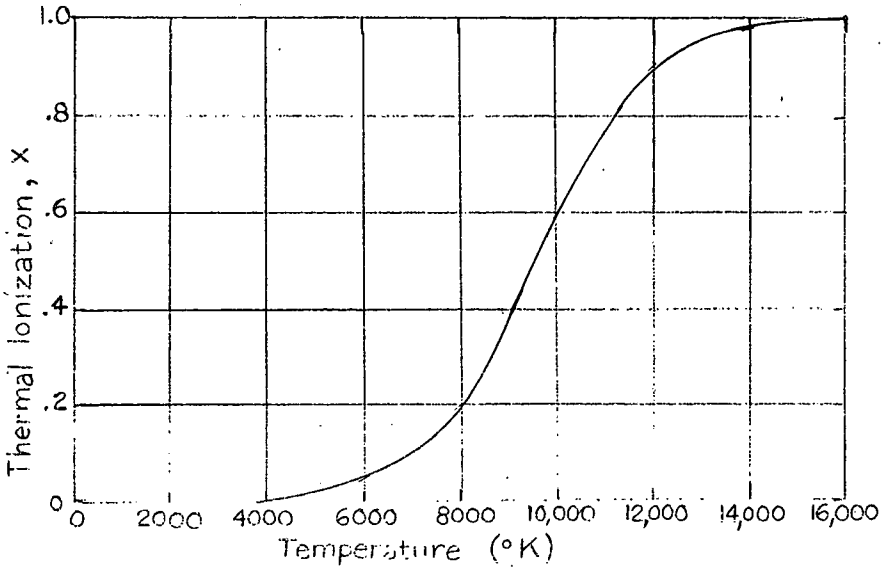

Fig. 10 Effect of Temperature on Degree of Thermal Ionization, x. (p = 760 mm. Hg, V = 7.5v.)

Deionization

Deionization takes place by two main processes:

1. ion diffusion to the walls of the container and
2. volume recombination of the positive and negative ions.

Deionization by Diffusion

The first process, ion diffusion to the walls consists of the movement of negative ions (or electrons) and positive ions to the walls as a result of concentration gradients. Stating this more generally, in any

---

[1] Ibid., p. 92

region containing a non-uniform density of ions, a migration of ions will take place from portions of the region with high ion density to other portions with lower densities. In this manner, diffusion produces a deionizing effect in the more dense areas and an ionizing effect in the areas of low ion density. At the wall, the positive ion is neutralized and leaves as a neutral atom. (See fig. 11[1].) Since ions lose their charges upon reaching the container walls, the concentration gradient drops from a high point in the discharge to a low at the walls. Thus the direction of diffusion is generally occurring from the discharge to the walls and results in eventual complete deionization of the entire volume if the source of ionization is removed. Since surfaces act as a vehicle in aiding neutralization of ions, certain tubes requiring rapid deionization

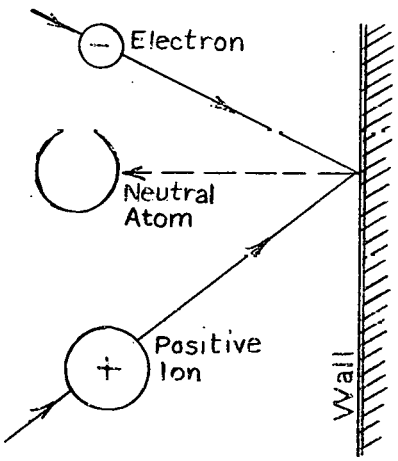

Fig. 11 Deionization at Surface

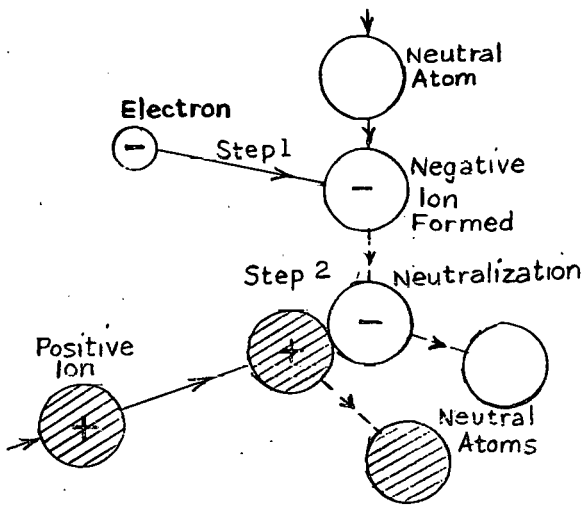

Fig. 12 Process of Volume Deionization

[1] Ibid., p. 96

are designed to have large electrode areas for greater recombining speed. While decreasing wall separation results in more rapid deionization, this change is not without some disadvantages. There will be an accompanying increase of ion loss from the steady discharge in a gas discharge device, and this represents a power loss.

Deionization By Recombination

The second process, volume recombination of ions, generally takes place in two steps. First, the electrons attach themselves to neutral atoms to form negative ions. Secondly these negative ions recombine with positive ions to produce two neutral atoms as shown in figure 12.[1] The forming of negative ions (by electron attachment to neutral atoms) does not occur in the noble gases or in pure hydrogen and nitrogen. On the other hand, the addition of impurities, such as chlorine and its compounds, enables relatively easy formation of negative ions. Other factors influencing formation of negative ions by electron attachment are:

(a) An electric field by speeding up the electrons makes their attachment to atoms more difficult and thus less likely to happen.

(b) High temperatures also increase electron velocities and thus reduce probability of electron attachment.

(c) Lower pressures mean fewer atoms (for a given temperature) and less likelihood of an electron meeting and attaching to an atom. Under these conditions, electrons are generally lost to the container walls.

---

[1] Ibid., p. 95

Chapter II

Electron and Positive Ion Emission From Solids

Emission of electrons from solids is a necessary requirement in any practical device involving electrical conduction through gas. Therefore the study of electron and ion emission shall be undertaken. Electron emission may be produced by the following means:

1. Thermionic - that is by heating the emitting surfact to high temperature
2. Electron bombardment of emitting surface
3. Positive ion bombardment of emitting surface
4. Bombardment of emitting surface by metastable atoms
5. High electric fields at the emitting surface
6. Photoemission.

Thermionic Emission

One of the earlier equations for thermionic emission of electrons was derived by Richardson. In his derivation he assumed that the electrons in a metal were governed by the laws of a perfect gas. His equation is:

$$J = aT^{\frac{1}{2}}\epsilon^{-\frac{b}{T}} \qquad (26)$$

where j is the saturation current density
T is the absolute temperature of the emitter
a & b are constants of the material.

Chapter II

Dushman proposed a thermionic-emission equation which has somewhat the same general form.

$$J = AT^2 \epsilon^{-\frac{\phi_o e}{kT}} \qquad (27)$$

where j & T are as described above
e is electronic charge
ϕ_o is the thermionic work function
k is Boltzmann's constant
and A is universal constant $= \frac{2\pi emk^2}{h^3}$
for which m is the mass of the electrons
and h is Planck's constant.

Because of their small work functions, electropositive metals provide considerably greater electron emission at any temperature than do the electronegative metals. Electronegative metals such as tungsten can can be covered with a layer, a single atom thick of such electropositive metals as thorium and caesium. These structures are emitters in the form of filaments. The thorium film is created by the high temperature heating of tungsten which causes thorium atom diffusion to the surface of the tungsten. When positive ion bombardment damages the thorium film, a new layer of thorium can be formed on the surface by operating the filament at higher-than-normal temperature with no anode voltage present.

The emission of electrons from a surface represents a loss of energy much as molecules evaporating from a liquid surface represent an energy loss in the form of heat of vaporization. This energy or heat loss as well as other heat losses are listed below. Included is the manner in which they vary.

Chapter II

1. The emission of electrons from a filament under saturation conditions results in a heat loss which varies exponentially with the filament temperature.
2. Heat losses from conduction are directly proportional to the temperature.
3. Losses resulting from radiation are related as the fourth power of the absolute temperature.

Thermionic emission is influenced by the presence of gas in two ways:

a. The emitters adsorb gas which covers the surface in the form of a film and generally reduces emission.
b. The gas molecules may become ionized and form positive ions which bombard and sputter the emitting surface. (Sputtering is the ejection of some of the metal surface by positive ion bombardment and will eventually lead to disintegration of the surface).

Plasma

Plasma is a dense concentration of positive and negative ions in nearly equal numbers existing in a gas discharge. This region of plasma has high conductivity so it has the corresponding low average voltage gradient. Because a plasma has generally equal numbers of electrons and positive ions (if a large enough region is considered) it is electrically neutral; however high electric fields can exist at local points. The plasma is kept in existence mainly by the ionization caused by electron collision, but photoionization contributes a portion of the ionization also.

Chapter II

Gas Discharge Between Cold Electrodes

If a gas or vapor contained no ions, it would be a perfect insulator. As a result, no current could flow in the case where two non-emitting electrodes, with a voltage applied between them, were surrounded by such an ion-free gas. However, all actual gases have some ions present due to the action of cosmic rays, radioactive materials in the walls of the containers, photelectric emission and other ionizing agents. In this gas, current would flow if a voltage were applied to two electrodes since the ions present would travel to the appropriate electrode. The nature of such current flow with a change in voltage will be studied. Consider the case of a gas discharge between cold electrodes as shown in the circuit of figure 13. [1]

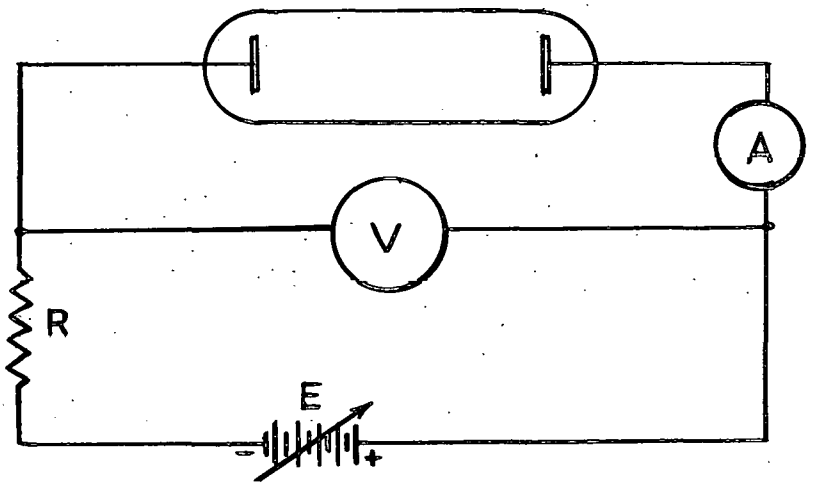

Fig. 13 Circuit for Obtaining the Volt-Ampere Curve of a Gas Discharge.

---

[1] J. D. Ryder - Electronic Engineering Principles - Prentice Hall, Inc., New York, 1947, p. 274

Chapter II

The gas within the envelope is at low pressure and there will be a few ions present between the two electrodes of the tube as a result of cosmic rays and applied ultra-violet light.

With the applied voltage slowly raised from zero value, a very small current will be noted on the current meter. This current will consist of some of the ions and electrons formed by the radiation. At this low potential, only part of the total ion and electron pairs being formed continuously by radiation reach the tube electrodes, the remaining pairs recombining to become neutral gas atoms again. This is the portion of the curve from O to A in figure 14.[1]

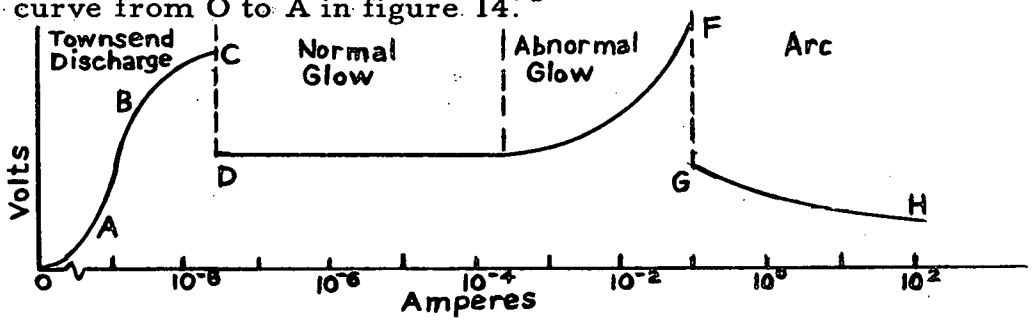

Fig. 14 Volt-Ampere Characteristic of a Gas Discharge Tube.

As the voltage source is increased, a point is reached where essentially all electrons and ions created by radiation are drawn to the electrodes rapidly before they can recombine. This saturation portion where an increase of voltage is not accompanied by a related increase in current is portion A to B.

---

[1] Ibid., p. 274

Increasing the voltage still further and thus the strength of the electric field, the accompanying greater forces on the electrons speed them up sufficiently to cause ionization of gas molecules when collisions between the two particles occur. The secondary electrons and ions produced by ionization constitutes an increase in current. The current continues to become larger as the voltage is increased as shown in the B to C part of the curve. Though this portion is also non-self-sustaining, amplification of the radiation-induced current is provided by the gas ionization occurring in the B to C portion of tube operation.

The area O to C is called the Townsend discharge as a result of investigations into this relationship made by J. S. Townsend in 1901.

At some point C, the electric field imparts enough energy to the positive ions so that ion bombardment of the cathode causes secondary electron emission. These emitted or secondary electrons are in turn accelerated sufficiently to produce ions upon colliding with gas molecules. The ions thus formed bombard the cathode and dislodge additional electrons. The process thus continues and repeats itself. The gas conduction then becomes self-maintaining and the gas is said to "break down". The voltage at which this occurs is described as the "breakdown potential".

At the breakdown point, the voltage drop across the tube decreases suddenly to point D. A visible glow emanates from the gas and from part of the cathode. The voltage drop remains substantially constant while the current increases from point D to E. The increase in current is accompanied by a spreading of the glow on the cathode until the entire

cathode surface is covered, maintaining during this increase an approximately constant cathode current density. This portion of the curve, D to E, is called the "normal glow" region and is the range where voltage regulator tubes are usually operated.

Continuing increase in current can be obtained only by an increase in cathode current density. The voltage drop also increases and a brighter glow is evident concurrently. This range of operation, E to F, is called "abnormal glow".

Further increase of current in the abnormal glow region results in increasingly heavier ion bombardment of the cathode, producing heavy secondary emission currents and heating of cathode. Finally, at point F, a sudden change takes place in which the cathode current density jumps to new high levels and the flow of current tends to concentrate at some point on the cathode. At that instant, the tube drop decreases and the abnormal glow operation changes to "arc" operation (shown as region G to H in figure 14). The heavily-concentrated current conduction may cause sputtering of the cathode surface by ionic bombardment. If operation in this region is allowed to continue, melting of the cathode may occur.

Law of Similitude

The law of similitude has great value in the study of gas discharge, especially in the spark phase of discharge. Its significant details may be described in the following manner. If a uniform field is assumed between plane-parallel plates, then when the gas pressure in this region is

multiplied by a constant K, and the linear dimensions are divided by the same constant,

$$P_2 = Kp_1 \qquad \text{and} \qquad d_2 = \frac{d_1}{K}$$

where P_2 is the new gas pressure
P_1 is the old gas pressure
d_2 is the new dimension
d_1 is the old dimension

Then with the applied voltages between the plates kept the same, i.e., $V_1 = V_2$, the respective electric fields E_1, and E_2, have the relationship

$$E_2 = KE_1$$

This set of conditions result in the currents remaining the same, $j_1 = j_2$. Thus the law of similitude states that with the applied voltage kept the same, the current also will remain the same if in multiplying the gas pressure by a factor K, all the linear dimensions are divided by K at the same time.

Spark Breakdown Potential

An equation for the spark breakdown potential of a gap in a uniform field may be written

$$V_s = \frac{Bpd}{\ln\left[\frac{Apd}{\ln 1/\gamma}\right]} \qquad (28)$$

where p is gas pressure in the gap region
d is gap separation
and A, B, & γ are constants

Chapter II

Paschen discovered in 1889 that the spark breakdown potential is related only to the product of the pressure and gap separation, pd. To be more rigorous, one should substitute gas density δ, for pressure p, in Paschen's Law. This would then include the effect of temperature at constant pressure on the mean free path in the gas. The spark breakdown potential for air[1] at atmospheric pressure and uniform field is

$$V = 30d + 1.35 \text{ (kv.)} \qquad (29)$$

The Paschen breakdown curves[2] for plane-parallel plates are shown in figure 15.

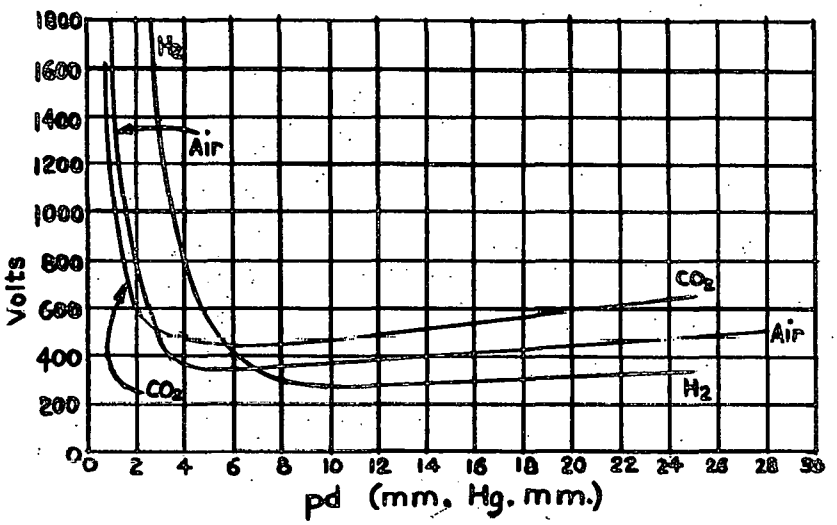

Fig. 15 Spark Breakdown Voltage for Plane-Parallel Electrodes (temperature = 20° C)

---

[1] J. D. Cobine. Gaseous Conductors Dover Publications, Inc., New York 1941, p. 163

[2] Ibid., p. 164

Chapter II

A study of the curves in figure 15 brings out these interesting and important facts:

(1) There is a minimum spark-breakdown voltage at a certain value of pd.

(2) If the pressure is lowered to put tube operation to the left of the minimum break-down point on the Paschen curve, then spark discharge will occur over the longer of two possible paths since the curve indicates a lower breakdown voltage for the longer path.

These minimum spark-breakdown voltages are shown in table 4 along with the appropriate pd.[1]

TABLE 4
Minimum Spark Breakdown Voltages

Gas	Vs minimum	pd mm. Hg x cm
Air	327	0.567
A	137	0.9
H_2	273	1.15
He	156	4.0
CO_2	420	0.51
N_2	251	0.67
N_2O	418	0.5
O_2	450	0.7
Na (Vapor)	335	0.04
SO_2	457	0.33
H_2S	414	0.6

Table 5[2] gives an indication of the comparative spark-breakdown strengths of several gases.

---

[1] Ibid., p. 165

[2] Ibid., p. 166

TABLE 5
Relative Spark-Breakdown Strength of Gases

Gas	N_2	Air	NH_3	CO_2	H_2S	O_2	Cl	H_2	SO_2
V/V_{AIR}	1.15	1	1	0.95	0.9	0.85	0.85	0.65	0.30

The table shows that N_2 has the highest breakdown with air and NH_3 closely following H_2 and SO_2 possess the lowest breakdown strengths of the gases listed.

Thirty kv/cm is a common figure given in engineering literature for the breakdown strength of air. Experimental data taken by Schumann shows that the apparent air breakdown strength is not a fixed value but appears to vary with separation distance of two plane-parallel electrodes. The word apparent is inserted before the phrase breakdown strength because the values for the field were calculated by dividing the breakdown voltage by the gap separation. This fails to take into account the high local fields and effects of space charges in the gap. Schumann's data is shown in the form of the curve in figure 16[1].

[1] Ibid., p. 173

Chapter II

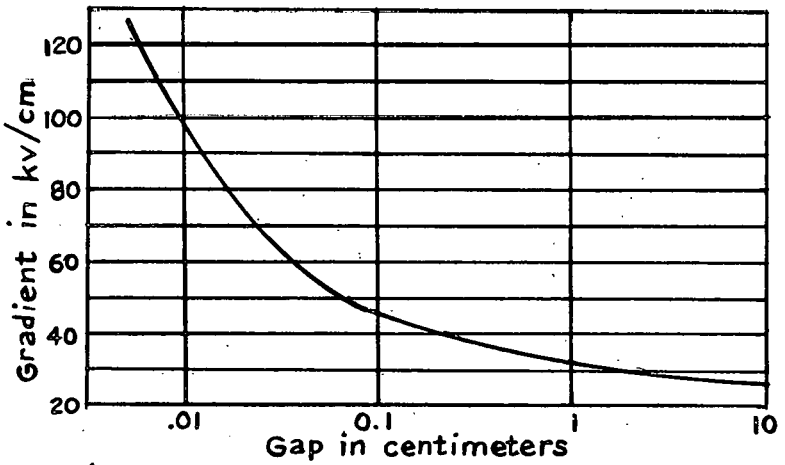

Fig. 16 Apparent Spark-breakdown Gradient of Air for Plane-Parallel Electrodes (760 mm Hg, 20°C)

The 30 kv/cm figure mentioned above for air field strength appears valid only for a gap of 2 cm according to the curve. Longer gaps result in lower field strengths while shorter gaps give much greater air field strengths.

Surge Breakdown

When there is a departure from the conditions studied previously, i.e., the application of a short-time impulse potential to a gap instead of the gradually-rising d.c. voltage, then a deviation from the previous results can also be expected. As stated by Cobine

> For an impulse the breakdown voltage may be considerably above the static breakdown voltage because of the finite time required to produce electrons and to establish the cumulative ionization processes. Thus a rapidly rising surge wave may reach a potential considerably above the normal breakdown voltage of the gap before the breakdown can occur.[1]

[1] Ibid., pp. 186 - 187

Chapter II

Mechanism of Spark Breakdown

A single electron leaving an electrode will produce a great number of free electrons by collision with gas molecules on its way to the other electrode. This large buildup of electrons, each of which also adds new free electrons during its travel to the positive electrode, would appear to be the complete breakdown mechanism occurring in the gas; however, this is not always the case. Breakdown time measurements made on gaps at high gas pressures are substantially smaller than those to be expected if electron avalanche were the only factor involved in the breakdown. Breakdown times resulting from electron action alone would be longer than the measured data because

(1) The observed mobilities of electrons are too low and thus would prevent electron traverse of the gap in such short times,

(2) the large positive-ion space charge (left behind by the growing electron avalanche) would create a high field which would slow down the advancing electrons.

Under certain applied set of conditions, an electron avalanche will require 1.5×10^{-7} seconds for its front to reach the anode. The new positive ions which are required for cumulative ionization take 1.2×10^{-6} seconds to arrive at the cathode from the instant the first electron originated the avalanche. Several electron avalanches starting from the cathode are required to produce a luminous streamer; so the time

involved in the first appearance of such a streamer would appear to be at least greater than the times listed above. Yet experimental data taken by Beams in 1928 and others at later dates indicate that definite luminous streamers are created in the middle of the gap in times of the order of 10^{-8} seconds. Cobine offers a possible explanation for the apparent contradiction between experimental data and theory.

> Thus it is evident that the simple mechanism of electron ionization and emission at the cathode by positive-ion bombardment is too slow to account for the observed speeds of spark formation. Loeb has proposed that the process can be brought up to the necessary speed by assuming photons formed in the avalanche ionize the gas well in advance of the head of the streamer and thus start new avalanches along the breakdown path. These avalanche-initiating photons bridge considerable distances at the speed of light, and thus high-speed propagation is possible by a succession of short avalanches. Of course, these new avalanches will not be in exactly the same path as the original one so that when the space-charge field between the head of one avalanche and the tail of a new one, somewhat ahead of it and to one side, becomes great enough, the intervening space is bridged and the irregular path observed in sparks is produced. The electrons formed near the anode are removed as soon as formed; the positive-ion field distortion, therefore, will be even greater at this point than it is at the head of a mid-gap avalanche. This favors the formation of a luminous streamer from the anode before the gap is bridged by the streamers from the cathode. The formation of an anode streamer is favored by high pressures and overvoltages where the positive-ion space charge slows down the advance of the cathode and mid-gap streamers.[1]

The amount of resistance in the external circuit can greatly influence the nature and degree of gap breakdown. A high resistance in series with the gap may hinder the complete breakdown of the gap. If a high

---

[1] Ibid., pp. 194-195

series resistance is present, the first streamer can be produced only by the partial discharge of the cathode electrode capacitance. The streamer's progress is stopped if the series resistance drops the voltage enough during the recharging of the cathode capacitance. During this recharging, the streamer column is losing the initial degree of ionization due to diffusion and recombination. The new streamer, starting when the voltage has been built up again, is likely to travel down the partly-ionized path of the old streamer and to extend it an additional amount. The presence of a high resistance therefore causes the breakdown to be comprised of a number of starts and stops, each start lengthening the conducting ionized column until the entire gap is traversed.

Self-Sustained Discharges

When a gap breaks down in an atmosphere of gas, the type of discharge resulting depends on

(1) gas pressure

(2) gap length and shape

(3) nature of applied voltage

(4) constants of the external circuit.

The static characteristics of these discharges will be discussed at this time. Repeated in figure 17 [1] are the volt-ampere characteristics of a discharge tube but with some additions such as resistance or "load" lines. This curve is obtained by using the circuit of figure 13 in which

---

[1] Ibid., p. 205

the discharge tube is in series with a resistance R and battery V.

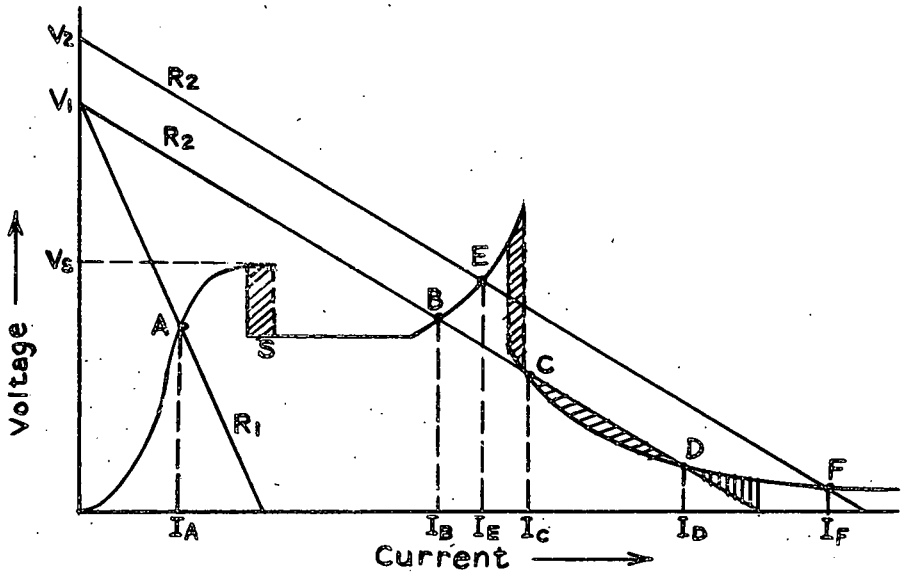

Fig. 17 Discharge Characteristics

Conditions for Existence and Stability of Discharges

An analysis will be made of the discharge resulting under certain external circuit conditions of d.c. voltage V and series resistance R. Figure 18[1] shows a hypothetical segment of a discharge curve with a resistance line drawn through it.

---

[1] Ibid., p. 208

Chapter II

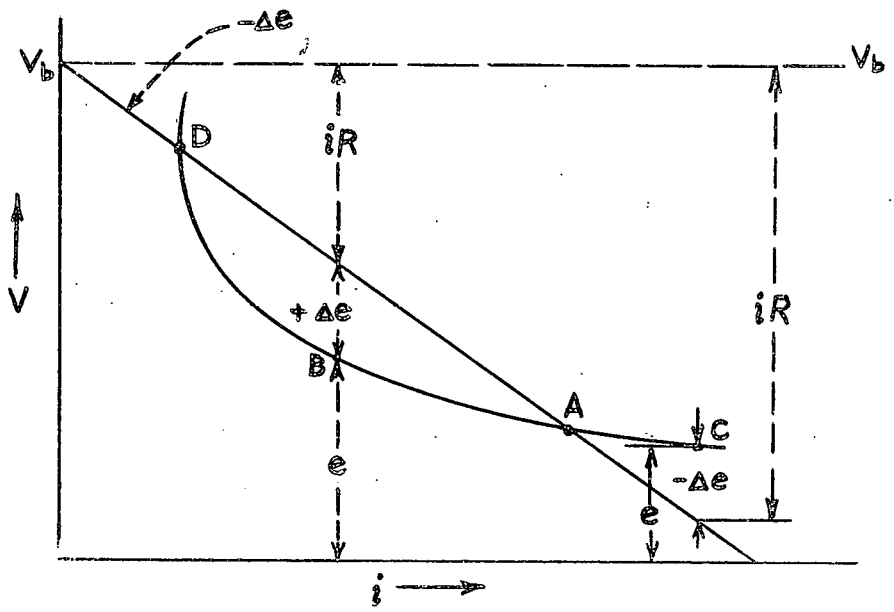

Fig. 18 [Hypothetical Segment of a Discharge Curve]

Point A, the intersection of the resistance or "load" line with the characteristic curve shows the following division relationship of voltages

$$V_b = e + iR \qquad (30)$$

where e is discharge voltage

and V_b is applied voltage.

A check will now be made to see if point A is a stable operating point. This will be done by supposing that in some manner a reduction in current is brought about, so that the new operating point is at B. Then the voltage equation will be

$$V_b - iR - e = \Delta e \qquad (31)$$

where Δe is the difference in voltage between the resistance line and the discharge characteristic.

It is seen that the applied voltage V_b, formerly equal to the quantity $(e + iR)$, has now in equation (31) become Δe amount larger than the new discharge-voltage-plus-resistance-drop total $(e + iR)$. Therefore, with the condition that no inductance is present in the circuit, Δe will cause the current i to grow larger until it becomes equal to i of equation (30). With that current increase tube operation will have returned to point A. Conversely, if current is increased beyond the point A value (to point C), $(iR + e)$ becomes greater than the applied voltage V_b. The current i must decrease until equation (30) again becomes the governing relation. Point A is thus a stable point of operation. A preliminary look at point D might result in the initial premise that it is a stable operating point since equation (30) is satisfied. A closer study however makes evident that increasing the current a small amount will result in a positive Δe and an accompanying continued increase in current until the tube operation reaches point A. The decreasing of current at point D causes Δe to become negative which results in further reduction of current. Therefore it is evident that point D is not a stable operating point. Since equation (30) is not sufficient in itself to determine stability of an operating point, some other standard must be found. A mathematical expression, sometimes called Kaufman's criterion for stability of a discharge, is a complete

and accurate stability criterion. It is

$$\frac{de}{di} + R > 0 \qquad (32)$$

where $\frac{de}{di}$ is the slope of the discharge characteristic at the point of its intersection with the resistance line.

In words, this may be restated that if $\frac{de}{di}$ is thought of as a resistance then the net circuit resistance must be positive for stable operation. If the above stability criterion is applied to the full discharge characteristic shown in figure 17, it is apparent that, with a load resistance R_1 and a voltage V_1, point A will give stable operation. Similar consideration of series resistance R_2 and applied voltage V_1 will lead to the conclusion that of the three intersection points B, C, and D, only B and D are stable. With two stable points of operation available, the tube will probably select B if it is ionized in a gradual manner by a slow reduction of series resistance. Point D operation will result if the discharge is initiated abruptly such as the bringing together of the electrodes in contact or by the opening of a fuse. Point D operation may also occur if the cathode of the tube operating at point B is heated sufficiently to supply a large number of electrons. Changing to a new applied voltage V_2 while keeping series resistance R_2 will move tube operation to two new stable points E and F.

Low Pressure Glow Discharge

If the pressure of a discharge tube in in the range of a few centimeters of mercury, a uniform glow emanates from the entire tube during

electrical operation. However, when the pressure is reduced to approximately one millimeter or so, (according to the gas), the continuous glow has changed to alternate dark and light regions. This is shown in figure 19a.[1] These light and dark areas of discharge operation are described as follows:

(1) The first space immediately adjacent to the cathode is a very short dark region known as the "Aston dark space".

(2) The "cathode glow" is the following space. The type of gas and the gas pressure determine the length of the cathode glow. The cathode glow seems to originate from the cathode surface and thus makes the Aston dark space practically unnoticeable.

(3) Next after the cathode glow is a dark space again. It has had several titles, among them "the cathode dark space", "the Crookes dark space", and "the Hittorf dark space".

(4) The brightest of all glow spaces succeeds the cathode dark space. It is identified as the "negative glow" and is relatively long.

(5) The dark space after negative glow has been called "the Faraday dark space".

(6) The next bright region, the "positive column" is a long one and occupies most of the discharge path length.

(7) With certain gases and certain values of discharge currents, an additional glow may exist, described as the "anode glow".

---

[1] J. D. Cobine, Gaseous Conductors, Dover Publications, Inc., New York, 1941, p. 213.

Chapter II

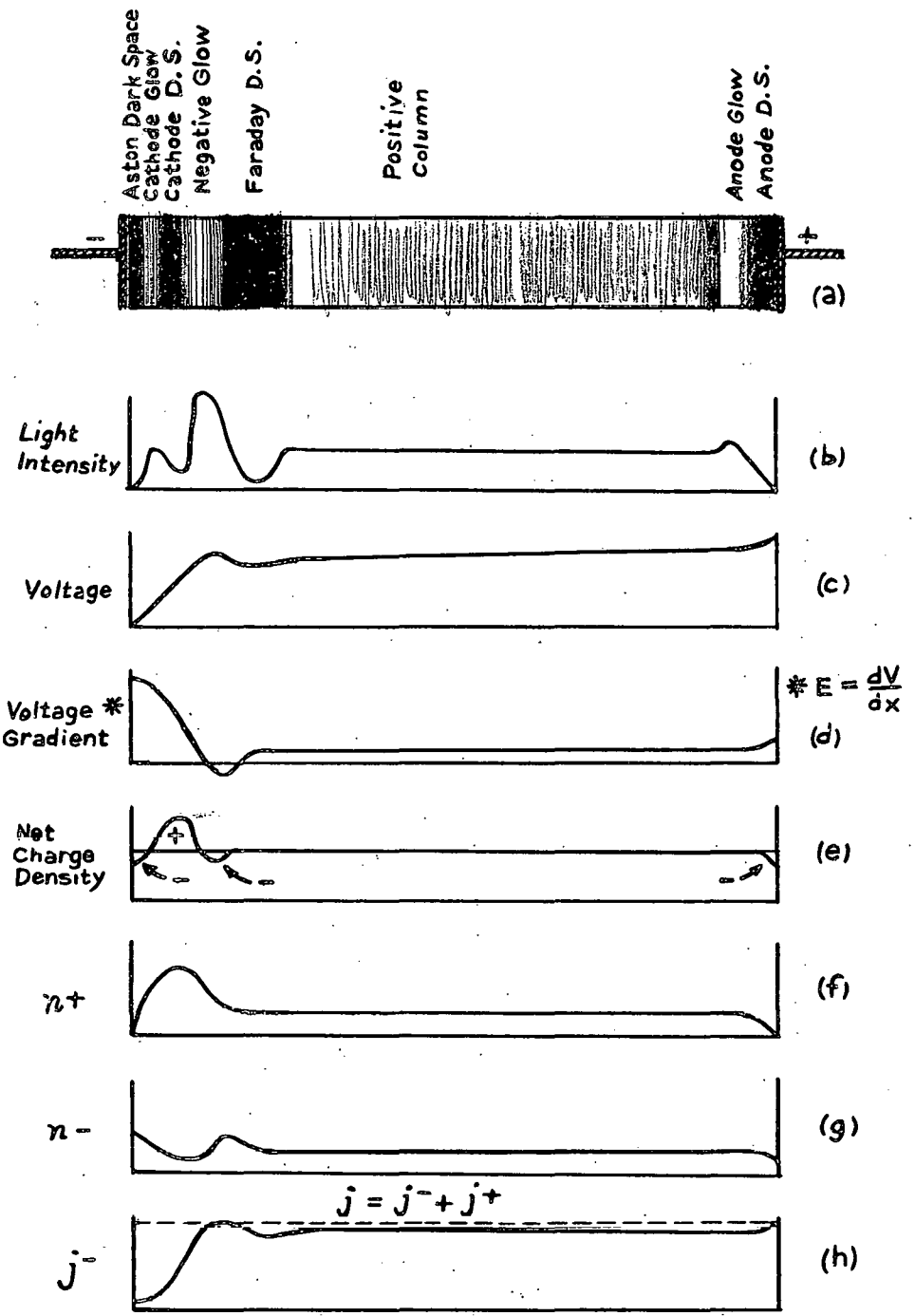

Figure 19 Approximate Characteristics of Glow Discharge

(8) The region of item (7) is accompanied by the last dark space adjacent to anode and appropriately titled "anode dark space". Figure 19b [1] gives the relative light intensities of the regions described in the previous paragraph and in figure 19a.

It is apparent from the curve of figure 19b that the so-called dark spaces are not fully dark but only in comparison with the "bright" regions where considerably more ionization and excitation exist. The manner in which these regions are affected by various conditions are described by Cobine.

> As the gas pressure is reduced, the negative glow and the Faraday Dark Space appear to expand at the expense of the positive column until at a sufficiently low pressure the positive column disappears completely. A similar effect is observed if the electrodes are moved together at constant gas pressure and constant current, when the region from the cathode to and including the Faraday dark space moves as a body and is unaltered in length, whereas the positive column decreases in length and finally disappears. This indicates that the phenomena at and near the cathode are essential to the discharge and that the positive column merely serves to maintain a conducting path for the current. This is further emphasized by the fact that if the electrodes are placed in a very large vessel instead of in a tube, the positive column disappears, and the current is carried throughout the entire volume by a relatively low density of ionization. The colors of the various glowing regions are different and vary with the gas. In air the negative glow is bluish and the positive column is a salmon pink. [1]

Figure 19 shows some of the relationships observed in the discharge tube. They may be summarized as follows:

---

[1] Ibid., p. 215

Chapter II

1. The major portion of the applied voltage is expended across the cathode dark space, as illustrated in figure 19c.

2. Figure 19d presents the voltage gradient across the discharge tube. It is interesting to note that the gradient may actually become negative in the negative glow side of the Faraday dark space.

3. Figures 19e, 19f, 19g, and 19h portray the distribution along the discharge tube axis of the net charge-density, positive-charge-density, negative-charge-density, and electron-current-density. Cobine elucidates on the foregoing phenomena:

> Just at the cathode there is a net negative charge produced by the electrons being emitted. Since their initial velocities are low, the electron current density at the cathode is relatively small so that the current is carried almost entirely by positive ions arriving at the cathode from the cathode dark space. The cathode dark space is a region of high positive-ion density. This high density of slow-moving positive ions produces the high value of cathode drop. Near the anode side of the cathode dark space, most of the current is carried by the electrons that have been accelerated by the cathode drop.
>
> The electron concentration increases to such an entent that in the negative glow the net charge density is nearly zero and the potential reaches a maximum value with a very low field. The electron and ion concentration may each be as high as 10" per cubic centimeter which is 10 to 100 times that of the positive column. In the Faraday dark space the field again increases with resulting acceleration of the electrons. The positive column is a region of almost equal concentrations of positive ions and electrons and is characterized by a very

> low voltage gradient. At the anode, there is a decrease in the positive-ion density and an increase in electron density such that the entire current at the anode is carried by electrons. There is an increase in the field strength at this point. The anode dark space is of the order of a mean free path; and the anode drop, when present is of the order of the least ionization potential of the gas. [1]

Cathode Phenomena

The normal cathode drop is directly related to both the kind of gas and electrode material used. The range in drop extends from 64 volts for potassium on an electrode in argon to 490 volts for a platinum cathode in carbon monoxide.

It is logical that the cathode drop varies almost directly with the work function of the cathode material since the discharge is maintained by emission of electrons from the cathode. This emission is caused primarily by bombardment of the cathode by positive-ions.

The ionization potential of the gas will affect the normal cathode drop.

Cathode Sputtering

If a discharge tube is operated in the glow region, positive ions bombard the cathode heavily enough to cause a knocking off or sloughing off of cathode surface material. This electrode disintegration is known as sputtering. Material removed from the cathode settles on all adjacent surfaces. When glass surfaces of the discharge tube are also included in the path of the sputtered electrode material, the typical darkening

---

[1] Ibid.

of the glass results.

Corona

Corona is generally defined as breakdown in the form of glow discharge at atmospheric pressure. This breakdown occurs between sharply-curved surfaces such as wires or points as the gap length between these surfaces is gradually increased.

The voltage at breakdown is less than the spark-breakdown voltage for the given gap length.

Corona on transmission lines causes damage to insulation by ion bombardment of insulation surfaces and by the chemical activity of certain substances created by the corona discharge. These substances include Ozone, oxides of nitrogen and when moisture is present, nitric acid.

Corona has a distinctive appearance on parallel electrical conductors and is described by Cobine.

> The corona on a positive wire has the appearance of a uniform bluish-white sheath over the entire surface of the wire. The corona on a negative wire is concentrated as reddish tufts of glowing gas as points along the wire. On the polished conductor, these glowing points are quite uniformly spaced along the wire, and their number increases with the current. [1]

General Properties of Arcs

The electric arc can be said in general to possess the following properties:

---

[1] Ibid., p. 252

(1) It is a self-maintaining discharge of high current capacity and low voltage drop.

(2) Its volt-ampere characteristic is usually represented with a negative slope.

(3) Arc operation is initiated by the pulling apart of contacts or by change from a higher voltage discharge.

(4) At atmospheric pressure and above, the arc consists of a small very bright center enveloped by a cooler region of incandescent gases sometimes known as the aureole. Under these conditions, the intense activity and energy involved in an arc discharge are easily great enough to bring the electrodes to their boiling temperatures.

(5) At low pressures, while some change is evident in the visual appearance of arc, the primary difference between low- and high-pressure arcs is the temperature of the positive column. A comparison of these temperatures shows a range of 5000 ^{o}K to 6000 ^{o}K for the high pressure column whereas the gas temperature of the low pressure arc has a maximum of a few hundred degrees centigrade.

Cathode Phenomena

Current density at the cathode of an arc is far greater than that of the glow discharge. An indication of the tremendously high current densities can be obtained from Table 6[1] which gives probable values

---

[1] Ibid., p. 301

of the arc-cathode current density.

Table 6

Probable Values of the Arc-Cathode Current Density

Cathode Material	Gas	Electron amp / cm^2	Positive ion am/cm^2	Current Range amp
Carbon	Air	470	65	1.5- 10
Carbon	N_2	500	70	4 -10
Iron	N_2	7000	-	< 20
Copper	Air	3000	600	< 20
Copper	Vacuum	14000	-	15- 30
Mercury	Vacuum	4000	-	5- 40

An investigation into the cathode mechanism causing high arc-current densities has been an ever continuing one by many workers in the field. Some have contended that thermionic emission is the primary source while others propose field emission as the principal process. Still others declare that a combination of both thermionic emission and field emission as the responsible agents for the observed high current densities.

A detailed account of the various cathode phenomena involved in an arc discharge is described by Cobine.

> Compton has used a heat-balance method to investigate the conditions at the cathode of an arc. The condition of thermal equilibrium is expressed by setting equal to zero the net rate of generation of heat at the cathode. The fraction of the current at the cathode carried by the electrons is taken as f, and the fraction carried by positive ions is (1-f). The various processes involved at the cathode are shown in figure 9.12. [Note: This is figure (20) in this thesis.] In (1) positive ions fall through the cathode potential drop Vc and give up the fraction a of

their energy to the cathode. The fraction (1-a) is the average proportion of the incident energy that is carried away by the neutralized atoms. This may be one source of the high-speed particles found in vapor arcs. The quantity a is known as the accomodation coefficient. The heat of neutralization ϕ' of the positive ions is

$$\phi' = V_i - \phi_o + L$$

where V_i is the ionization potential of the gas molecule, ϕ_o is the normal work function of the cathode surface, and L is the heat of condensation of the neutral molecule on the cathode surface. L is zero if the ion does not actually condense on the surface. The presence of a strong electric field which reduces the effective work function of the surface for electron emission, does not affect the value of ϕ'. [1]

The individual contributions and affects of various physical processes and mechanisms at the cathode are illustrated in figure 20. [2]

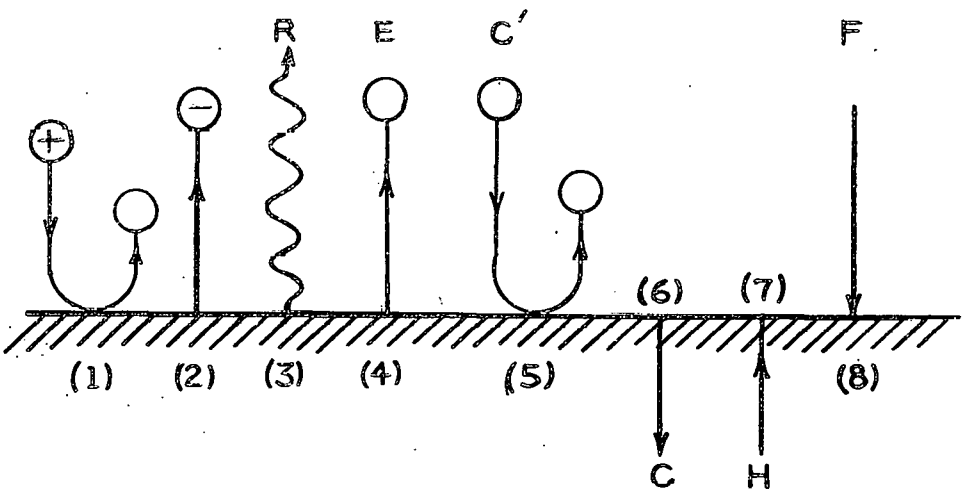

Fig. 20 Processes occurring at an arc cathode

[1] J. D. Cobine Gaseous Conductors Dover Publications, Inc., New York 1941, p. 308.

[2] Ibid.

These phenomena might be described in detail as follows:

Process (1) shows the net heating caused by arrival of the positive ion and may be expressed in equation form as $H(1) = (1-f)(a\ V_c + V_i - \phi_o)$

Process (2) represents electron emission which results in cooling of the cathode. Its mathematical relationship is $H(2) = -f\phi-$ where $\phi-$ is the effective work function of the cathode surface. (An electric field drops the work function of the surface from ϕ_o to $\phi-$) Thus, each electron possesses an energy $V_c - \phi_o + \phi-$ when it leaves the cathode-fall space.

Process (3) illustrates the radiation emanating from the cathode. This energy loss from radiation is presented in the form $H(3) = -R$, where R is the energy radiated per ampere-second.

Process (4) accounts for the heat loss resulting from evaporation of material from the cathode surface. In the mathematical equivalent expression for the foregoing statement $H(4) = -E$, the term E is the product of the mass of material lost by evaporation per ampere-second multiplied by its latent heat of evaporation.

Process (5) provides for the heat $H(5) = -C'$ lost by gas conduction and convection.

Process (6) pictures the amount of heat $H(6) = -C$ drained away from the cathode by direct heat conduction through the cathode and its supports.

Chapter II

Process (7) diagrams the heat the cathode may possibly gain through some external source.

Finally Process (8) is an attempt to portray the energy given up to the cathode by such unelectrified carriers as radiation, metastable atoms, excited atoms and high velocity neutral atoms which reach the cathode.

Glow-Arc Transition

Cathode current density is relatively low under glow discharge conditions and is accompanied by the characteristic high voltage. The arc discharge has high current density flow while its voltage drop decreases to comparatively low values. It can thus be seen that radical changes in the cathode emission mechanism must take place when transition from glow to arc discharge occurs. It is thought that in the higher current portion of abnormal glow, positive ions gain enough extra energy to raise the cathode temperature sufficiently (by positive ion bombardment of the cathode) to produce thermionic emission. This is the case when the cathode is made of refractory materials as carbon and tungsten. Cobine observes

> The increased current produced by thermionic emission increases the number of positive ions formed in the cathode-drop space which further increases the cathode heating so that a lower voltage will maintain a given current than were emission by positive-ion bombardment alone. Under these conditions the falling volt-ampere characteristic of the arc is established.[1]

---

[1] Ibid., pp 311-312

Where the cathode is composed of low melting material, Cobine indicates that the cathode emission increases as a result of localized increase of vapor pressure. He declares:

> For cathodes of materials of low melting point the transition from the glow to the arc is sudden instead of continuous as for the thermionic arc. Since for arcs with these materials the current density at the cathode is very high, the sudden transition from the low-current glow to the arc represents a high rate of change in the emission process. For the mercury arc, v. Engel and Steenbeck suggest that the transition from the abnormal glow to the arc is induced by localized increases in vapor density. By the similarity law, an increase in vapor density must be accompanied by an increase in the current density. A local increase in current density will result in increased heating and consequent further increase of vapor pressure; thus, the process could quickly become cumulative for a material that is easily vaporized and result in the formation of an arc cathode spot. Plesse found that if the metals are arranged according to their heat of sublimation, the order of the metals is the same as then arranged according to the least current at which the glow is observed to change to the arc. The metal having the lowest heat of sublimation, mercury, has the lowest current at which the glow changes to the arc. This series is Hg, Cd, Zn, Ca, Mg, Pb, Al, Ag, Cu, Sn, Ni, Fe, Pt, W, C.[1]

Anode Phenomena

The conditions existing at the anode of a low pressure glow discharge are repeated at the anode of a low pressure arc. The range of values to be expected for anode drop of potential is presented in Table 7[2].

---

[1] Ibid., p. 314

[2] Ibid., p. 300

Table 7
Arc Cathode and Anode Voltage Drops

Electrodes	Gas	Current Range Amp.	Cathode Drop volts	Anode Voltage volts
Cu	Air	1 - 20	8 - 9	2 - 6
C	Air	2 - 20	9 - 11	11 - 12
Fe	Air	10 - 300	8 - 12	2 - 10
Hg	Vacuum	1 - 1000	7 - 10	0 - 10
Na	Vacuum	5	4 - 5	- - 10

Just as the cathode-drop region is one of very high positive-ion space charge so the anode drop region has a similar counterpart, i.e., a high electron space charge. The electron space charge is created by the action of the anode in collecting electrons. The concentration gradient of positive-ions increases in the direction of the cathode so that the electron space charge existing at the anode end of the anode-drop region is nearly neutralized at the cathode end of the anode-drop region by the increasing positive-ion concentration. It is at this nearly neutral point that the plasma of the positive column begins.

Oscillations in DC Arcs

When an alternating current is super-imposed on a d-c arc, the total arc current can be expressed as

$$i = I + I_m \sin \omega t$$

where I is the normal value of d-c arc current and I_m is the peak alternating component of arc current.

With this type of current flow, the characteristics exhibit a dynamic behavior that is different from that of the static characteristics resulting

from d-c current flow alone. It is evident that with the frequency ω close to or equal to zero, the dynamic operation of the discharge tube is substantially the same as its static operation. This is illustrated by trace 1 in figure 21.[1]

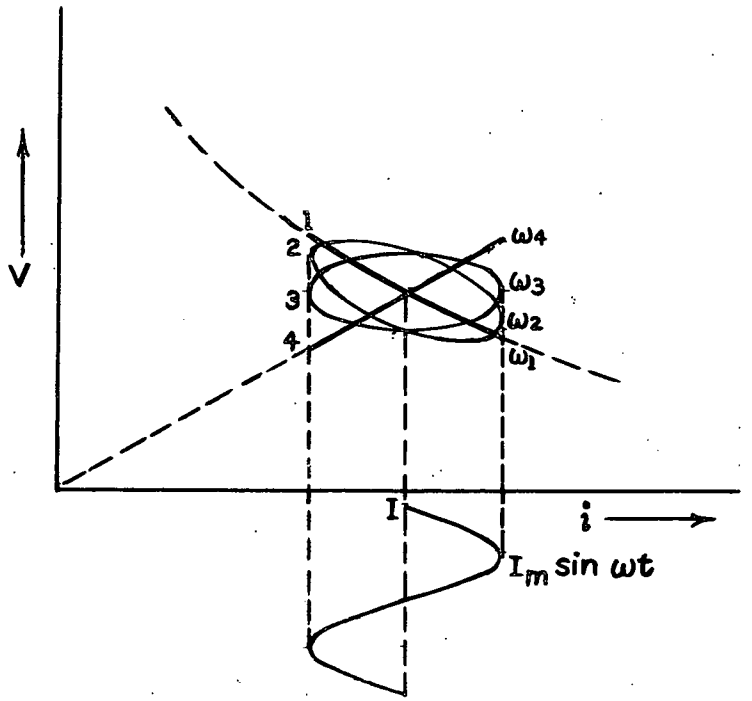

Fig. 21 Dynamic Characteristic of d-c Arc
$(\omega_1 < \omega_2 < \omega_3 < \omega_4)$

As ω is gradually increased, tube operation is denoted by elliptic trace 2 which shows an increasing voltage with a decreasing current. A further increase in ω results in tube operation tracing out ellipse 3. In this case an increase of voltage is accompanied by a corresponding increase in current. The reason for higher voltages with increasing

---

[1] Ibid., p. 345

current at these higher frequencies is given by Cobine

> The higher voltage with increasing current is due due to the fact that ionization of the column is less than normal so that a higher voltage gradient is required to increase the ionization and supply the required current. Similarly, on decreasing current the ionization lags behind the current and the arc has a greater ionization than is required so that the current flows with a lower voltage gradient.[1]

When the frequency ω is made quite high, the characteristic pattern made by tube operation possesses a positive slope and is practically a straight line. This can be interpreted as saying that at high frequencies the arc volt-ampere characteristic are practically identical to that of pure resistance.

Adsorption, Absorption, Occlusion and Sorption

Gas molecules may leave their free state and become "imprisoned" in a solid by at least three processes:

(1) The gas and the solid may react chemically. An example of chemical "cleanup" of gases by solids is the removal of water vapor by phosphorus pentoxide ($P_2 O_5$) in a chemical reaction to form phosphoric acid ($H_3 PO_4$).

(2) Gas molecules may also be "lost" in the presence of an evacuated solid by two physical processes. One of these is adsorption which is defined as the condensing of the gas as a layer (having a thickness

---

[1] Ibid.

of one or more molecules) on the surface of the solid.

(3) Another physical cleanup method is absorption. This is the case in which the gas molecule moves into the interior of the solid just as gas molecules dissolve in a liquid. The term occlusion has been used to describe the same general process but has fallen in disuse, having been supplanted by absorption.

For those instances where both adsorption and absorption actions are taking place, a combination term sorption was introduced by J. W. McBain in 1909.

Several definitions on this general subject will be helpful.

Adsorbent - The solid which takes up the gas.

Adsorbate - The gas or vapor removed from the gas phase.

Desorption - The process of removing gas from an absorbent.

An absorbent possesses a sorptive capacity that is essentially proportional to its surface per unit mass. Therefore porous adsorbents such as charcoal, silica gel, etc. are much more efficient at cleaning up gasses than such substances as glass, mica, metal surfaces which are composed of smooth plane surfaces. It should be noted that adsorption increases with decrease in temperature. In contrast absorption or true solution of gases in metals increases with increase in temperature.

It has been found by researchers that, in general, adsorption is greater at any given temperature for those gases which condense more readily

or have the higher boiling points. Table 8[1] illustrates this relationship.

Table 8
Adsorption of Gases by Charcoal
(Volume per gram adsorbent, temperature 15°C

Gas	Volume Adsorbed, cm^3	Boiling Point, °C	Critical Temperature *
$COCl_2$	440	+ 8.3°C	182°C
SO_2	380	-10.0	157.2
CH_3Cl	277	-23.7	143.1
NH_3	181	-33.35	132.4
H_2S	99	-61.8	100.4
HCl	72	-83.7	51.4
N_2O	54	-89.5	36.5
C_2H_2	49	-88.5	36
CO_2	48	-78.5	31.1
CH_4	16	-161.5	-82.5
CO	9	-192	-139
O_2	8	-183	-118.8
N_2	8	-195.8	-147.1
H_2	5	-252.8	-239.9

* Values given in Handbook of Physics and Chemistry, 1945 Edition

A theory on the nature of adsorption phenomena was developed by Langmuir in which he attempts to describe the nature of the forces existing at the surfaces of solids and liquids. Dushman quotes from Langmuir's

[1] Saul Dushman Scientific Foundations of Vacuum Technique John Wiley & Sons, New York 1949, p. 389.

original paper "Surface Chemistry", published in 1933.

> During the year 1914, in connection with studies of electron emission and chemical reactions at low pressures, I became much interested in the phenomena of adsorption, and developed a theory which has been strikingly verified by a large number of experiments carried out since that time. According to this theory there is an abrupt change in properties in passing through the surface of any solid or liquid. The atoms forming the surface of a solid are held to the underlying atoms by forces similar to those acting between the atoms inside the solid. From Bragg's work on crystal structure and from many other considerations we know that these forces are of the type that have usually been classed as chemical. In the surface layer, because of the asymmetry of the conditions, the arrangement of the atoms must always be slightly different from that in the interior. These atoms will be unsaturated chemically and thus they are surrounded by an intense field of force.
>
> From other considerations, I was led to believe that when gas molecules impinge against any solid or liquid surface they do not in general rebound elastically, but condense on the surface, being held by the field of force of the surface atoms. These molecules may subsequently evaporate from the surface. The length of time that elapses between the condensation of a molecule and its subsequent evaporation depends on the intensity of the surface forces. Adsorption is the direct result of this time lag. If the surface forces are relatively intense, evaporation will take place at only a negligible rate, so that the surface of the solid becomes completely covered with a layer of molecules. In cases of true adsorption this layer will usually be not more than one molecule deep, for as soon as the surface becomes covered by a single layer the surface forces are chemically saturated. Where, on the other hand, the surface forces are weak the evaporation may occur so soon after condensation that only a small fraction of the surface becomes covered by a single layer of

> adsorbed molecules. In agreement with the chemical nature of the surface forces, the range of these forces has been found to be extremely small, of the order of 10^{-8} cm. That is, the effective range of the forces is usually much less than the diameter of the molecules. The molecules thus usually orient themselves in definite ways in the surface layer since they are held to the surface by forces acting between the surface and particular atoms or groups of atoms in the adsorbed molecule.[1]

Evolution of Gases by Glass

A number of investigators have come to the same conclusions, namely, that products liberated below 300°C from various kinds of glasses are adsorbed gases whereas at greater temperatures, actual chemical decomposition of the glass itself supplies the gaseous substances. Further study in this direction led to the following interpretation of the results

> It is seen (the investigators state) that the adsorbed gases for the lime and lead glasses are practically all given up at a temperature of 200°C, while 300°C is required in the case of the borosilicate glasses. The absorbed gases begin to come off at the softening points of the various glasses, 400°C for the lead and lime glasses, and 600°C for the borosilicate glasses. In this connection, it should be stated that the amount of absorbed gases found in the above experiments represents only that portion of the dissolved gases which lies nearest the surface of the glass. Owing to the great viscosity of the glass at the temperatures used, the rate of diffusion of the gas would be altogether too slow to permit any considerable portion to reach the surface.[2]

---

[1] Ibid., p. 402

[2] Ibid., p. 520

Chapter III

Hydrogen Thyratrons

History

The hydrogen thyratron was developed primarily to satisfy the need for a switch with certain properties. This switch was to be used in pulse generators capable of producing a train of high power and high voltage pulses of very short time duration. Radar systems utilize these pulse generators to modulate the transmitter and, as a result, such generators have been variously referred to as "modulators", "pulsers" and "keyers". Rotary spark gaps were used in radar modulators in the early periods of radar development and were generally satisfactory, however, several disadvantages were present in these switching devices:

(1) They were not well suited for high recurrence frequencies.

(2) A variation in time of firing as high as 50 μsec was an inherent characteristic.

(3) They could not be easily used in designs involving air-tight enclosures.

Therefore, studies were begun on the feasibility of using other devices as pulse generator switches. One of the general areas in which investigations were carried out was that of thyratrons. Extensive experimentation at the Radiation Laboratory resulted in the successful design of the hydrogen thyratron, which had been proven

more satisfactory than other types of thyratrons. The hydrogen thyratron is the principal type modulator switch used in present day radar design.

General Requirements

It was noted in the previous paragraph that hydrogen thyratrons were successfully developed to function as switches in radar pulse generators or modulators. The specific type of modulator for which the thyratron was best suited was the "line-type" pulser, so-called because the energy-storage device in the pulser is essentially a lumped-constant transmission line. This energy-storage device is not only a source of electrical energy but also is the pulse-shaping component. Accordingly, it is known as a pulse-forming network, PFN, and is made up of inductances and capacitors in a variety of connections.

A line-type pulser with the power supply and an isolating element are shown in schematic form in figure 22 [1].

If the capacitive portion of the PFN is charged up by the power supply, the energy thus stored can be transferred to the load by closing the switch. The switching action involved imposes certain strict requirements on the switch itself. The switch must have the following characteristics:

---

[1] Glasoe and Lebacqz, Pulse Generators, McGraw-Hill, Inc., New York, 1948, p. 11.

Chapter III

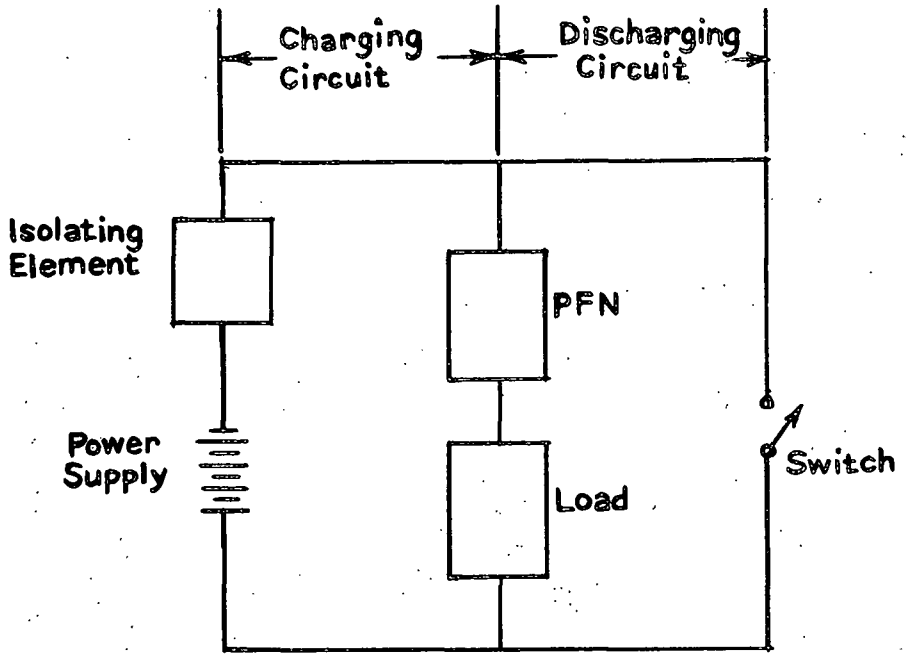

Fig. 22 Charging and Discharging Circuit for a Voltage-fed Network.

(1) high-current-carrying capacity

(2) lowest possible resistance during discharge of network

(3) capability of closing very rapidly at predetermined times

(4) ability to regain a nonconducting state rapidly after the end of the pulse

(5) retain that non-conducting state during the entire charging period.

In addition to meeting the above requirements, the thyratron possesses such advantages as:

(1) relative small size

(2) relative little weight

(3) high efficiency

(4) ability to operate over wide range of plate voltages

(5) accurate triggering with low voltage pulses to the grid.

Comparison of Gas Fills

Several readily-available gases could be used for the thyratron fill. Their various advantages and disadvantages are listed in table 9.

Table 9

Comparison of Gas Fills for Thyratrons

Gas	Relative Advantages	Relative Disadvantages
Mercury Vapor		1. Temperature-sensitive 2. Long deionization time 3. Low destruction voltage* (30v)
Zenon		1. Long deionization time 2. Low destruction voltage* (in 30 volt range)
Argon		1. Long deionization time 2. Low destruction voltage* (in 30 volt range)
Helium	1. Short deionization time	1. Low destruction voltage* (in 30 volt range)
Hydrogen	1. Short deionization time 1/10 that of Mercury, Argon or Zenon 2. High Destruction Voltage (600v) 3. High voltage breakdown strength	1. Gas cleanup

* Destruction voltage is the voltage corresponding to the ion velocity at which destruction of an oxide cathode sets in.

The advantages listed in the above table for hydrogen appear to result from its low molecular weight. This low weight allows more rapid ion movement and the accompanying short recovery time. Another benefit accruing from hydrogen's lightness is the comparatively slight harm to cathode surfaces resulting from positive ion bombardment.

Structural Features of the Hydrogen Thyratron

A cross-section of a type of hydrogen thyratron is shown in figure 23.[1]

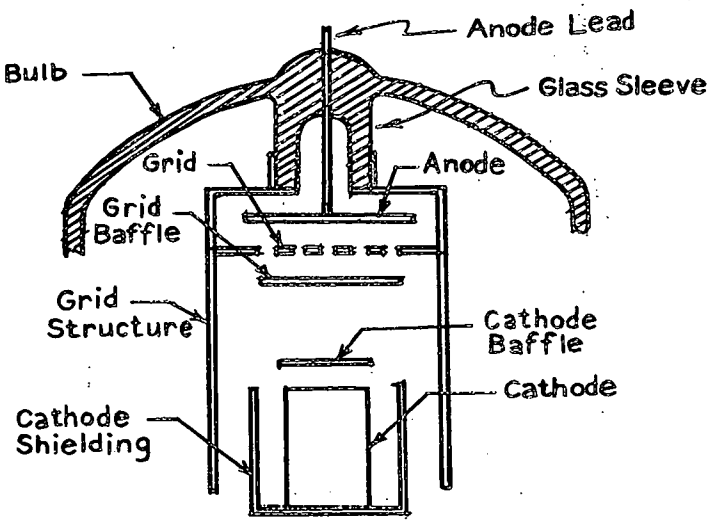

Fig. 23 Structure of Hydrogen Thyratron

The drawing makes the following facts evident.

(1) The plate at all points is approximately equi-distant from the enclosing grid structure. The purpose of this constructional feature is twofold.

---

[1] Ibid., p. 338

Chapter III

(a) Thyratron gas pressures and electrode spacing design place the operating point on the lefthand part of the Paschen curve shown in figure 24[1]. In this region, the breakdown voltage is increasing rapidly as the product of pressure and spacing is reduced; therefore a design incorporating unlike gap distances would sustain gaseous discharge breakdown at lower voltages across the longer gap distances.

(b) The shorter gap distances on the other hand allow breakdown to occur by the field emission process. It must be noted however that field emission breakdown does not depend on gap dimensions alone but is also affected by electrode surface conditions. Conducive to field emission breakdown is the lowering of surface work function (by deposit of evaporated cathode emitting material, for example) as well as the concentration of electric fields at sharp surface irregularities.

---

[1] Ibid., p. 337

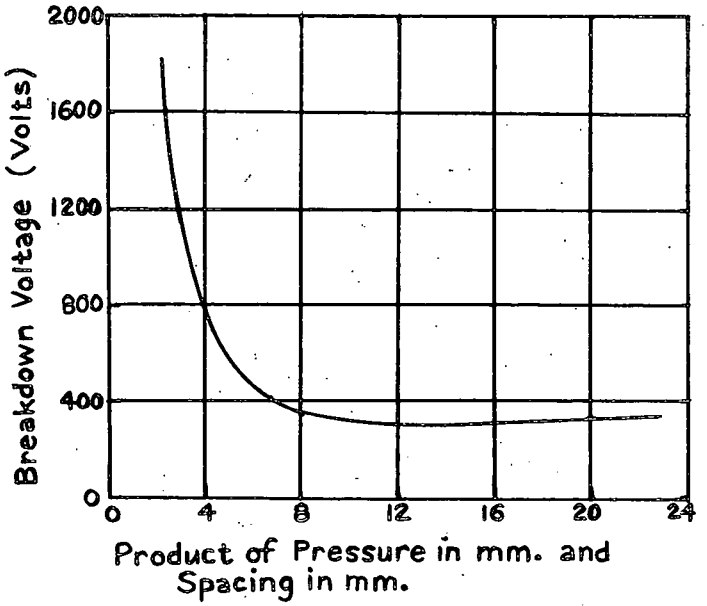

Fig. 24 Plot of Breakdown Voltage in Hydrogen as a Function of the Product of Spacing and Pressure.

It can thus be seen that dimensions from the thyratron anode to other electrodes are determined by compromising between long path lengths, to prevent field emission breakdown, and short path lengths, needed to prevent gaseous electrical breakdown.

(2) Extensive baffling surrounds the cathode. This accomplishes the following:

(a) blocks a direct path from cathode-to-anode so that breakdown between these two electrodes is unlikely to occur spontaneously (i.e. without initiation by grid.)

(b) minimizes heat loss from the cathode by reducing radiation losses.

(c) decreases possibility of sputtered emissive material from the cathode depositing upon surfaces in the grid-anode region where high electric fields might bring about field emission breakdown.

Because gas cleanup (permanent or temporary removal of gas molecules from their "free" gaseous state by chemical combination, adsorption or absorption) is accelerated by such reducing agents as carbon, silicon, etc., materials free of these substances must be used in hydrogen thyratron cathodes. Electrolytic nickel is a material meeting these specifications and is commonly used for hydrogen thyratron cathodes. Grade A nickel is used for most of the other tube parts except for the anode. Molybdenum is used for anode construction to minimize anode sputtering.

Some additional constructional features of hydrogen thyratrons are illustrated in figures 25 and 26. [1]

Figure 25a shows the typical plane parallel electrode arrangement of hydrogen thyratrons in general. Mr. Goldberg[2] enlarges on this matter.

> In this design the anode, grid, and cathode are essentially coplanar, ---. The essential features of this design, and in fact of any thyratron design, are:

---

[1] Seymour Goldberg, Research Study on Hydrogen Thyratrons Vol II, Edgerton, Germeshausen, & Grier, Inc., Boston, 1956, pp. V-4 and V-5.

[2] Ibid., p. V-3

Chapter III

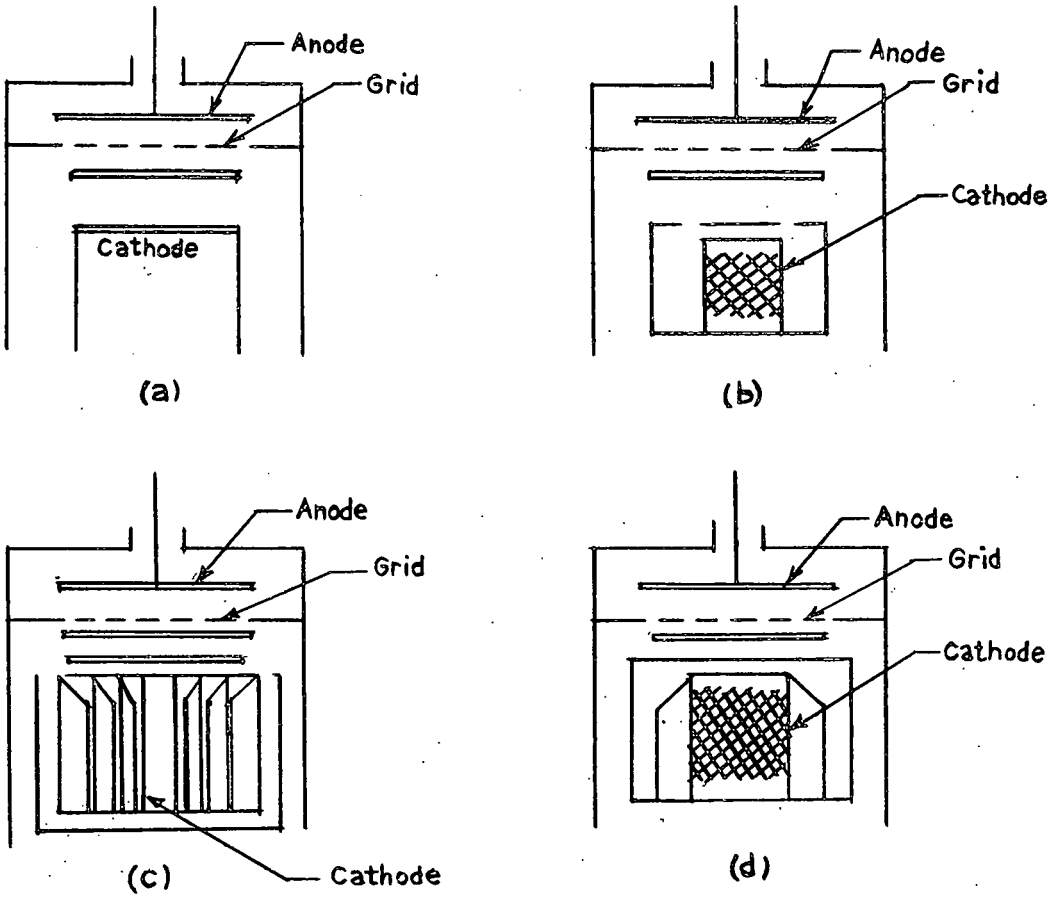

Fig. 25 Plane Parallel Thyratron Structures with Different Cathode Arrangements

1. Anode surrounded by close-fitting shield (in this case the grid) to prevent long path breakdown.

2. Grid-cathode spacing about five times anode spacing to allow breakdown in grid-cathode space.

However figure 25a is the idealized electrode arrangement which must be modified to the practical configuration of figure 25b. This cathode design, used on the 4C35 and 5C22, provides greater emitting cathode

area and lessens the possibility of cathode emissive deposit on grid surfaces. The cathodes of figures 25c and 25d are examples of increased cathode area design accomplished by the addition of cathode vanes. These cathode structures are used in the 1907 and larger thyratrons. An evident common geometrical feature of the tube structures shown in fig. 25 is the placement of the anode lead at one end of the envelope while the grid and cathode leads come out at the other end. This double-ended arrangement is used for the larger higher-voltage tubes to provide large external leakage paths from anode to cathode. On smaller low-voltage tubes this requirement is not necessary and results in the single-ended structure shown in figure 26. In this instance all electrode leads are brought out through the base.

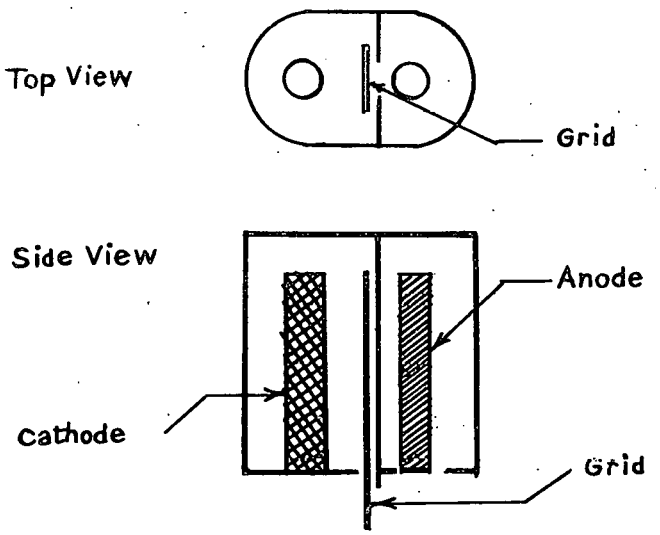

Fig. 26 Single Ended Thyratron Structure

Chapter III

Hydrogen Thyratron Operation

It has been previously mentioned that hydrogen thyratrons were well suited to operation in voltage-fed line-type pulsers. An example of this type of circuit is reproduced in figure 27. D.C. resonant charging is used in this instance to provide the necessary energy

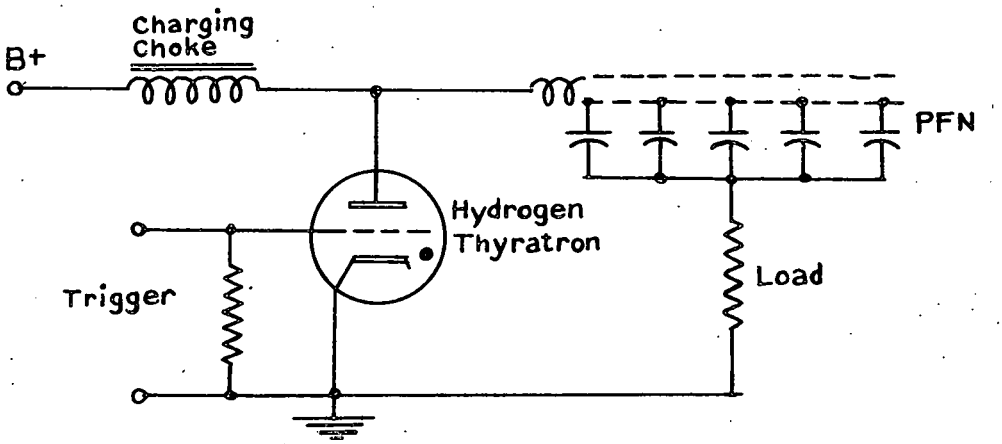

Fig. 27 Line Type Pulser

to the PFN capacity. This permits the selection of a lower voltage anode supply since D.C. resonant charging will supply nearly twice this power supply voltage to the PFN capacitors. The voltage and current waveforms encountered at various points in the circuit are presented in figure 28.

Chapter III

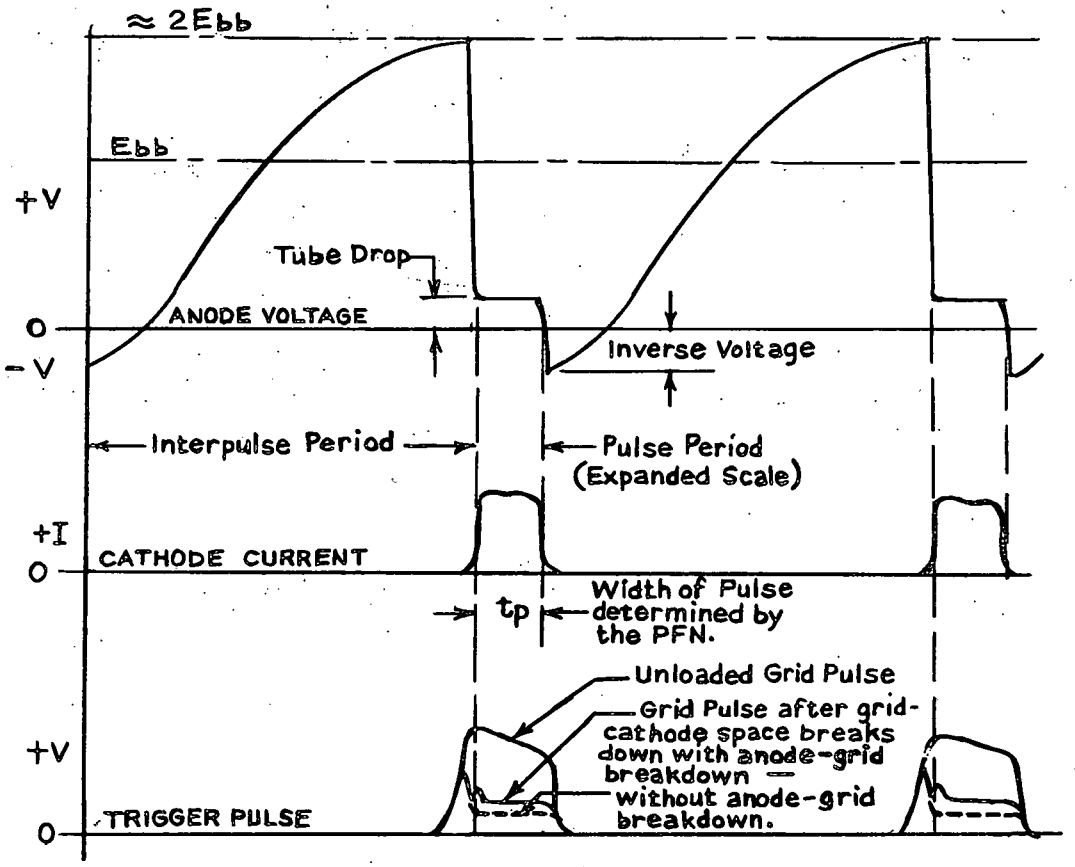

Fig. 28 Voltage and Current Waveforms of Line Type Pulser in Figure 27.

A complete cycle of the wave forms in figure 28 will now be studied in greater detail. Such a study made by Goldberg[1] proposed that the complete pulse cycle be divided into four portions which were defined by him as follows:

---

[1] Ibid., p. II-3

Chapter III

1. triggering
2. commutation
3. steady state conduction
4. recovery.

These four distinct operation modes are shown in figure 29[1] in the order of times in which they occur.

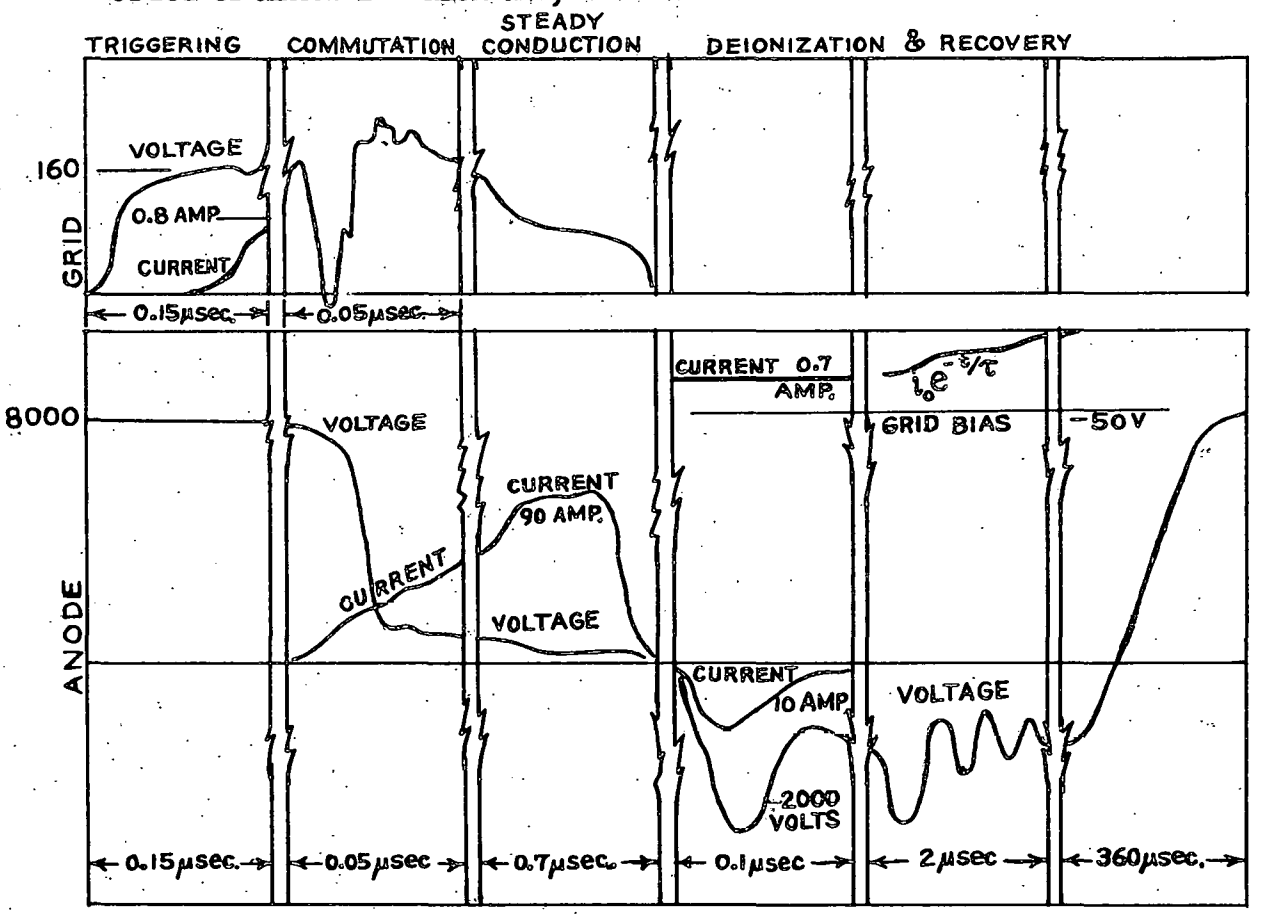

Fig. 29 Typical Events in the Pulsed Operation of a Hydrogen Thyratron.

---

[1] Ibid.

Goldberg describes tube action taking place during each of these intervals.

> .....The voltages and current shown are typical for the 4C35 thyratron.
>
> The triggering interval is initiated by the application of the positive grid trigger pulse. Following a delay in the order of tenths of a microsecond from the application of voltage, grid current is observed to increase exponentially with time. After the grid current reaches a certain critical value, conduction is transferred to the anode region and the commutation interval starts. The anode voltage then falls rapidly with a time constant of a few hundredths of a microsecond. The cathode current rises at a rate determined by the modulator circuit time constant and the rate of fall of anode potential.
>
> The course of the grid voltage during the commutation interval is somewhat erratic, principally because of self and mutual inductive effects of the rapidly rising current in the cathode circuit. Under certain conditions these inductive effects can give rise to a voltage spike on the grid in the order of kilovolts. During the steady conduction interval which follows, the current is substantially constant and the anode voltage is at some low value equal to the steady state tube drop. At the end of this time the pulse network has delivered the charge it received and the current falls to zero.
>
> Next, a negative or inverse voltage appears at the anode because of the normal mismatch in impedance between the load resistance and the pulse network. This starts the deionization or recovery interval, during which the plasma remaining in the tube as a result of the discharge decays to the tube walls by means of a diffusion process. The anode voltage slowly increases from its inverse value to the peak forward voltage. Oscillations are superimposed on this because of transients reflected back and forth along the pulse line. Because of losses in the transmission line, these normally decay to a negligibly small value after some tens of microseconds. At the end of 360 microseconds,

> which corresponds to a repetition rate of 2,800 cycles per second for the example shown, the anode voltage reaches its full peak forward voltage called epy. If the grid is maintained negative during the deionization period, a current made up of positive ions will flow to it. Diffusion losses of the plasma cause the current to decay exponentially with time as the plasma decays.[1]

The following paragraphs will expand in detail on the four arbitrary divisions of pulsed tube operation.

Triggering

The triggering action occurring in most hydrogen thyratrons may be divided into three steps:

(1) Positive pulse voltage is applied to the grid.

(2) Electrons from the cathode are accelerated to the grid, colliding with gas molecules enroute and ionizing them. Thus a build-up of grid current ensues and, in the process, a plasma is created in the grid-cathode region.

(3) Electrons from the newly-formed plasma diffuse to the grid regions penetrated by the anode field (at the grid openings or beyond the anode-field "shadow" cast by a solid grid).

In the next step, these electrons, diffusing to regions within the influence of the anode field, are accelerated by the field toward the anode. The resultant ionization and breakdown of the grid-anode region is defined as commutation and is expanded upon more fully

---

[1] Ibid., pp. II-3 and II-4

in the next paragraph.

A definite time interval is required between the initial application of a positive pulse to the grid and the occurrence of commutation. This time interval appears to be affected by the initial location of the grid-to-cathode discharge. The location of the grid-to-cathode discharge path is shown in figure 30 [1] for a 4C35 type tube.

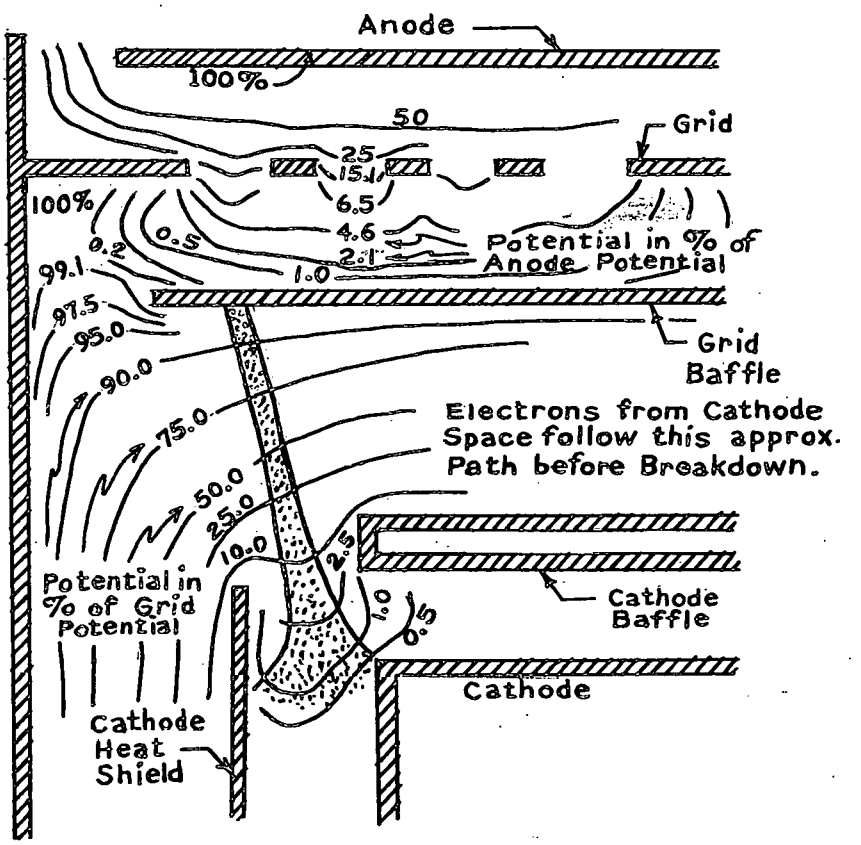

Fig. 30 Equi-potential lines in the grid-cathode space and in the space between the grid baffle and anode of 4C35. Lines are identified in percentage of grid voltage (in grid space) and in percentage of anode voltage (in anode space).

---

[1] Ibid., p II-12

Chapter III

Goldberg enumerates some of the various factors affecting time of commutation:

> The focusing action is indicated by the shaded paths shown in figure II-6. [our figure 30].
>
> Since the initial electrons flow in this path, we might expect the plasma to be initially located here also. Because of the high degree of shielding of the anode, electrons must, in order to contribute to anode breakdown, appear at the annular opening leading to the anode. We must rely on diffusion or some other mechanism to allow electrons to move here.
>
> . . . . . .
>
> Since the time of commutation is affected by the initial location of the grid-cathode discharge, we might expect factors that influence the initial course of the electrons to be of importance in determining this time. The presence of magnetic fields originating from the filament windings has been shown to have an effect on the commutation time and to introduce a source of jitter which corresponds in frequency to the alternating filament voltage. Magnetic fields of this nature would, of course, affect the initial path of electrons as well as the manner in which they diffuse.[1]

Commutation

In his attempt to explain the mechanism of anode breakdown, Goldberg[2] discarded as not agreeing with the known experimental facts both a plasma front theory developed by Langmuir and a diffusion process.

---

[1] Ibid., pp. II-10 and II-13

[2] Ibid., pp. II-15 to II-42

Chapter III

Instead a picture has been developed in which an increasing apparent area of the anode and accompanying potential change in the grid-anode space continue to the point where breakdown takes place. This may be described in detail as follows. When the anode voltage is raised to the level where the anode space potential is greater than that of the triggering plasma by an amount at least equal to the ionization potential, then some ionization occurs in the space between the anode and plasma. The resulting positive space charge in the anode region leads to the raising of space potentials at all points in the grid-anode region. Thus the equi-potential line representing the ionization potential moves closer to the grid, and the apparent electron collecting area of the anode is enlarged. This process is cumulative, for more electrons are gathered in by the anodes' greater collecting area. This increased electron current in turn multiplies the formation of positive ions which again elevate anode space potentials. The accompanying anode area enlargement starts the process all over again, and the cycle is repeated until breakdown is accomplished.

The Steady State Discharge

The steady state discharge, occurring immediately after commutation, lasts for a period of time as determined by the PFN. The thyratron passes the required current by the following tube action.

Figure 31[1] shows the existence in the tube of two plasmas separated by a double sheath. The cathode plasma is the one established during

---

[1] Ibid., p. II-44

the triggering phase and has been previously referred to as a triggering plasma. The anode plasma (six times the density of the cathode plasma)

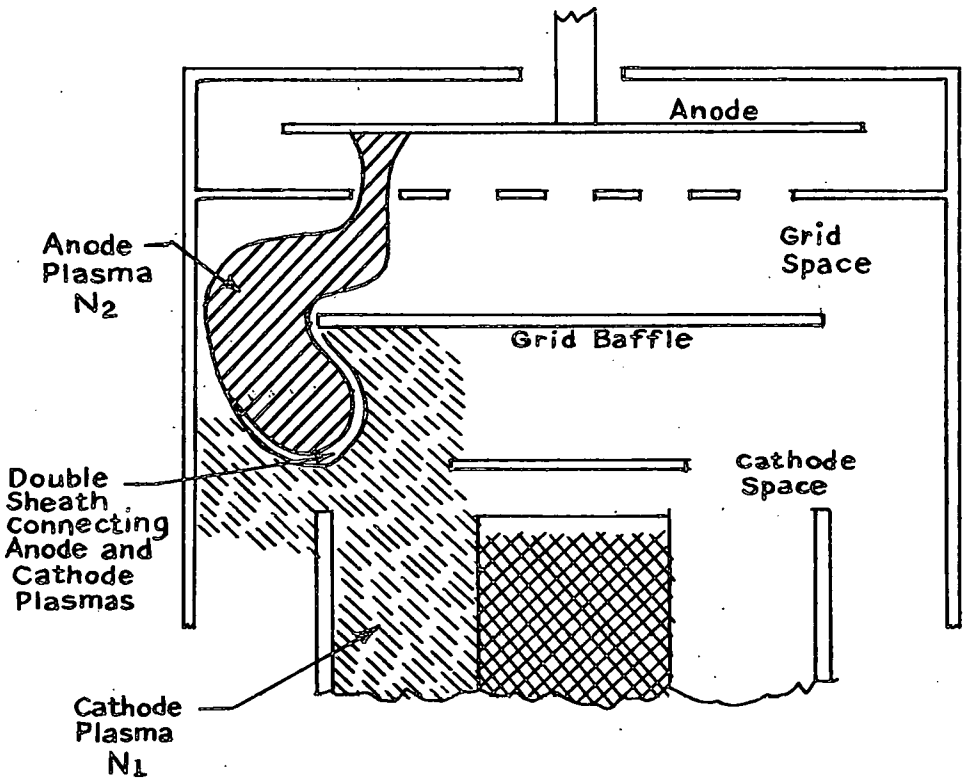

Fig. 31 Double Sheath Bounding Anode and Cathode Plasmas during Steady Discharge.

is formed during commutation and is surrounded by a double sheath which is also designated as the anode collecting area. This double sheath may be considered to be the anode itself projected out to the cathode plasma since nearly all electrons arriving at the double sheath also reach the anode itself.

Chapter III

Deionization and Recovery

The steady-state discharge phase is completed with the depletion of the energy in the PFN capacitance. At this time the discharge region in the tube still possesses a substantially large number of free electrons and positive ions. It has been shown (in figure 28) that the anode voltage at this point of the cycle is negative due to mismatch in impedance between the pulse forming network and the resistance load. The anode voltage then slowly becomes more positive as the PFN charges up. If the plasma in the thyratron has not reduced to a sufficiently low level by the time the anode voltage reaches a critical value of positive voltage, tube breakdown may occur without application of trigger voltage. With regard to this, the term "recovery time" has been used to denote the interval between the end of the current pulse and the time at which positive voltage may be reapplied without causing breakdown.

Recovery times are influenced by:

(1) negative bias on the grid. (Recovery time is a logarithmic function of negative bias.)

(2) peak current during the discharge. (The amount of ionized particles present in the discharge path at the start of the deionization period is proportional to the peak currents passed by the tube.

While inverse voltage at the anode will quickly sweep positive ions in the grid-anode region to the anode, the cathode plasma requires a relatively long time to disappear since the grid-cathode region is shielded from the anode field. Therefore inverse voltage at the anode does not measurably change recovery time.

The primary manner in which the plasma is removed from the discharge region appears to be diffusion of the charged particles to wall and electrode surfaces. Goldberg discusses this subject more fully.

> The diffusion is termed ambipolar, meaning that both the ions and electrons leave the plasma at an equal rate. If the ions and the electrons were to leave at their free diffusion rates, the electron loss would predominate, leaving the plasma charged positive. This positive charge, in turn, would restrain the free loss of electrons. An equilibrium state then results wherein a small field is set up in the plasma to hold back the faster electrons so that the loss of ions and electrons proceeds at an equal rate. Ion loss by recombination of ions and electrons in the gas volume is highly improbable because of the improbability of an ion and an electron colliding and because of the tendency, even when collision occurs, of the electron to enter a diverging orbit around the ion without radiating or entering into an orbit of the ion.
>
> . . . . . .
>
> The theory of ambipolar diffusion to the walls thus appears to account fairly well for the rate of disappearance of the plasma. Accordingly, shortening the diffusion distances would be a means of reducing the deionization and recovery times. [1]

---

[1] Ibid., pp. II-75 and II-79

Chapter III

Hydrogen Thyratron Operation Limits

Thyratron operation limits are determined principally by the degree of dissipation occurring in the various parts of the tube. This dissipation is encountered mainly at the anode, grid, and cathode.

Anode Dissipation

Anode dissipation takes place during two portions of the operating cycle:

(1) An energy loss results during commutation when the anode voltage, though dropping, is still relatively high while the anode current is rising. Figure 32[1] illustrates the time relationship of these parameters. This condition of initial high anode-voltage and simultaneous existence of anode current produces a spike of dissipation which accounts for the major portion of energy given up at the anode. The initial spike is clearly demonstrated in figure 33.[2]

(2) Another cause of energy loss at the anode appears shortly after the end of the steady discharge or at the beginning of the deionization and recovery period. At this time inverse voltage on the anode brings on anode bombardment

---

[1] Glasoe and Lebacqz, Op. Cit., p. 344

[2] Glasoe and Lebacqz, Op. Cit., p. 345

by positive ions which are still present in the grid-anode region at the end of the steady discharge interval. The positive-ion current flow exhibits the following characteristics:

(a) It lasts for only a few tenths of a microsecond but can produce serious damage to the anode by the sputtering of the electrode's surfaces.

(b) The peak amplitude of this inverse current is directly proportional to the value of the coincident inverse voltage on the anode. The latter voltage value is directly affected by the degree of impedance mismatch between the PFN and its load.

(c) The peak amplitude of this inverse current is also directly affected by the amplitude of the main forward current pulse, since the latter establishes the multiplicity of ions in the anode region.

(d) The inverse current remains unchanged with change in tube pressure.

(3) Anode dissipation can also be brought about by the emission of electrons from the grid to the anode during the interpulse period when the anode potential is increasing to high voltage levels.

Chapter III

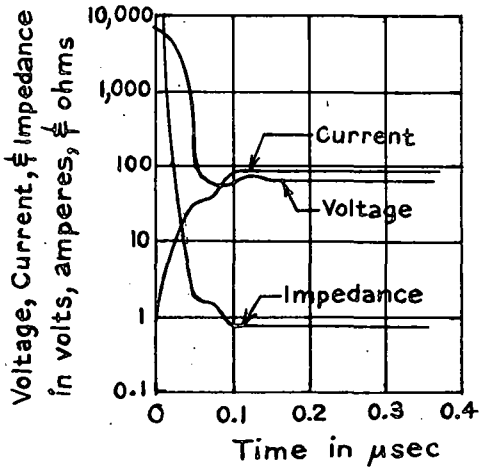

Fig. 32 Tube Drop, Current, and Impedance as a Function of Time for a 4C35 Hydrogen Thyratron (V_N = 8kv, Ip = 90 amp., = 1.1 usec)

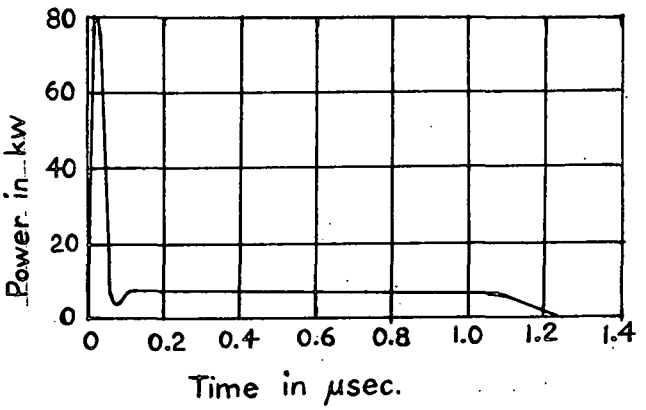

Fig. 33 Plot of Tube Dissipation vs. Time for a Single Pulse (4C35, V_N = 8kv, Ip = 90 amp, = 1.1 usec)

Grid Dissipation

Grid dissipation takes place during the steady-state discharge. The electrons gain energy from acceleration across the cathode sheath and across the double sheath existing in the grid region. Because of large grid electrode area and the constriction of the main discharge at the grid apertures, a large amount of the gas energy is transferred to the grid electrode surfaces.

Chapter III

Cathode Dissipation

Concerning cathode dissipation, Goldberg provides the following explanation.

> Cathode dissipation also occurs during the steady state discharge because of i^2R losses resulting from the resistive nature of the cathode coating.
>
> . . . . . .
>
> Dissipation in the cathode results primarily from passage of the emitted electron current through the resistive cathode coating. The principal effect of cathode dissipation is to heat the cathode which increases the rate of evaporation of cathode coating and depletes the active emitting surface. The dissipation resulting from ion bombardment of the cathode is generally negligible, since the cathode sheath through which the ions are accelerated is only about 20 volts compared to resistive voltages in the order of 100 volts in the cathode coating, due to primary electron current. In addition, the ion currents are only about 2% of the electron current. It is only in cases where the cathode has become considerably deactivated and sheath voltages far in excess of 20 volts develop that ion bombardment becomes an appreciable source of dissipation.[1]

Goldberg's analysis led to the conclusion that generally cathode dissipation is proportional to the RMS cathode current squared.

Hydrogen Thyratron Operational Parameters

Typical characteristics of hydrogen thyratrons will be enumerated in an attempt to provide a general background on practical thyratron operation.

---

[1] Goldberg, Op. Cit., pp. III-4 and III-23

Chapter III

Cathode Temperatures

Thyratron cathode temperatures must be kept within a relatively narrow range in order to avoid undesirable results. On the one hand, cathode temperatures of 900°C and higher lead to thermal evaporation of cathode coating plus its possible chemical reaction with hydrogen at these increased temperatures. Too low cathode temperatures, beginning at 800°C, bring about diminished cathode emission, and further drop in cathode temperature is accompanied by rapidly-decreasing cathode emission, high tube drop and high tube dissipation. Therefore, cathode temperatures of 800°C to 850°C are the appropriate temperature boundaries within which proper tube operation lies.

Ionization Time

Ionization time may be defined as the time taken for anode voltage to fall from maximum anode voltage before conduction to the start of the steady-state discharge. This process appears to require 0.02 to 0.07 μsec to be completed and is affected primarily by two factors, gas pressure, and tube geometry. Gas pressure is a measure (at constant temperatures) of the number of gas molecules present in the enclosed volume; therefore higher pressures mean greater numbers of gas molecules, and greater probabilities of electron collision with these molecules. Higher gas pressures are thus conducive to faster rate of ion buildup-or shorter ionization times. Ionization time is also

approximately proportional to tube dimensions according to Germeshausen.[1] The larger tubes, such as the 5C22, have longer ionization times (approximately 0.07 μsec) while the smaller 3C45 and 4C35 require times to ionize of 0.03 μsec and 0.045 μsec respectively. Such factors on the other hand as anode current, rate of rise of anode current, and initial plate voltage fail to influence the time of gas ionization. In addition, Krulikoski found among other things that ionization time was unchanging for different pulse lengths, repetition rates, and operating power levels.[2]

Tube Drop

Tube drop of a hydrogen thyratron can be considered to exhibit two distinct aspects. The first portion of each pulse or the ionization interval of commutation is one of relatively high tube drop. This initial phase of tube conduction is illustrated in the first 0.05 μsec of the voltage curve in figure 32. The tube drop values generally listed in hydrogen thyratron specifications are those measured during the steady-state discharge part of the pulse. In figure 32 this is represented by the part of the voltage curve to the right of the 0.05 μsec time. During this period, the amount of tube drop is influenced by the emissive quality of the cathode and by the value of peak cathode current conducted through the tube. The latter relationship is

---

[1] Glasoe and Lebacqz, Op. Cit., p. 345

[2] S. J. Krulikoski, Jr., Hydrogen Thyratrons in Pulse Generator Circuits, Radiation Laboratory Report No. 953, March, 1946, pp. 953-4 & 953-16.

shown in figure 34.[1]

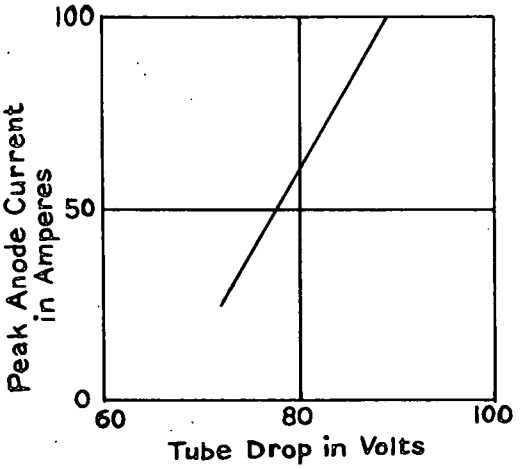

Fig. 34. Variation in Tube Drop during the Pulse with Anode Current.

Tube Dissipation

The dissipation occurring in a hydrogen thyratron during a pulse is shown in figure 33 and again in figure 35.[2]

The peak of dissipation at the beginning of the power dissipation curve in figure 35B results from a product of rising anode current and comparatively-high anode voltage. A smaller but substantial spike of dissipation is evidenced at the end of the pulse, and is caused by a high inverse anode voltage in conjunction with the inverse current flowing at that time. The portion of the curve between these two peaks

---

[1] Glasoe and Lebacqz, Op. Cit., p. 345

[2] R. S. Whitlock, Techniques for Application of Electron Tubes in Military Equipment, Vol. I, Wright-Patterson Air Force Base, Ohio, December 1958, p. 3-15.

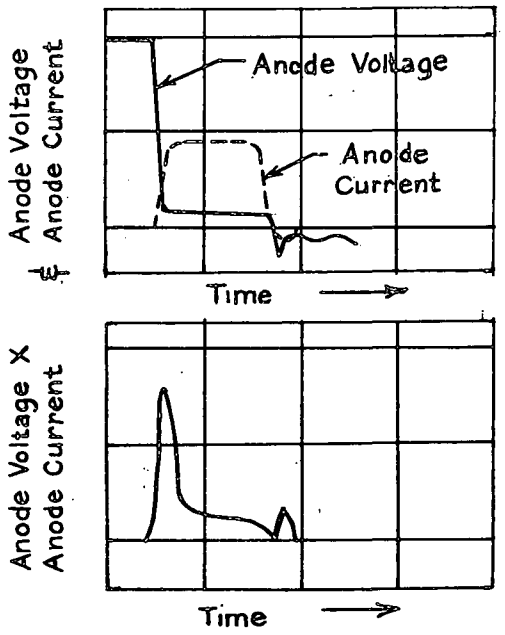

Fig. 35 Power Dissipation at the Anode of a Type JAN-5C22/HT 415 Hydrogen Thyratron. (A) Anode Voltage and Anode Current vs. Time. (B) Product of Anode Voltage and Anode Current vs. Time.

is the amount of energy dissipated in the tube during the steady-state conduction. Tube dissipation per pulse will in general change with change in such circuit parameters as pulse current, pulse duration, anode voltage, and rate of rise of anode current.

The variations in average power dissipation with a number of operating conditions were measured by Kruliskoski.[1] He found that average power dissipation:

(1) varies approximately linearly with pulse repetition frequency

---

[1] Kruliskoski, Op. Cit., pp. 953-32 to 953-46.

(2) decreases with decrease in operating power level.

Triggering Time

Triggering Time might be considered to be that interval of time from the attainment of 6 volts by the grid to the instant of anode breakdown. As has been mentioned before, one of the requirements for modulator switches is the capability of closing very rapidly at predetermined times. Extremely short trigger time or capability of closing very rapidly is a hydrogen thyratron characteristic. To this performance capability must be added the advantage of low "jitter" or variation in triggering time from pulse to pulse. Some external operating conditions that would tend to modify triggering times are the amplitude and rate of rise of the trigger pulse and the thyratron anode voltage. The relationship of rate of rise of grid-voltage vs grid-to-cathode breakdown voltage is graphically illustrated in figure 36.[1]

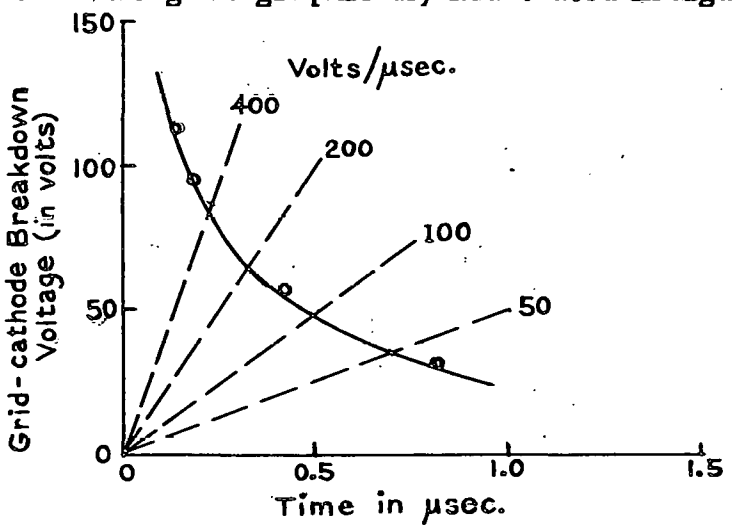

Fig. 36 Grid-to-Cathode Breakdown Voltage as a Function of the Rate of Rise of Grid Voltage for a 4C35 Thyratron.

[1] Glasoe and Lebacqz, Op. Cit., p. 350

Chapter III

Goldberg investigated triggering phenomena and obtained results shown in fig. 37.[1] In this case the point of anode breakdown is observed for various values of applied grid voltages. It is readily apparent from this figure that higher grid voltages bring about shorter triggering times.

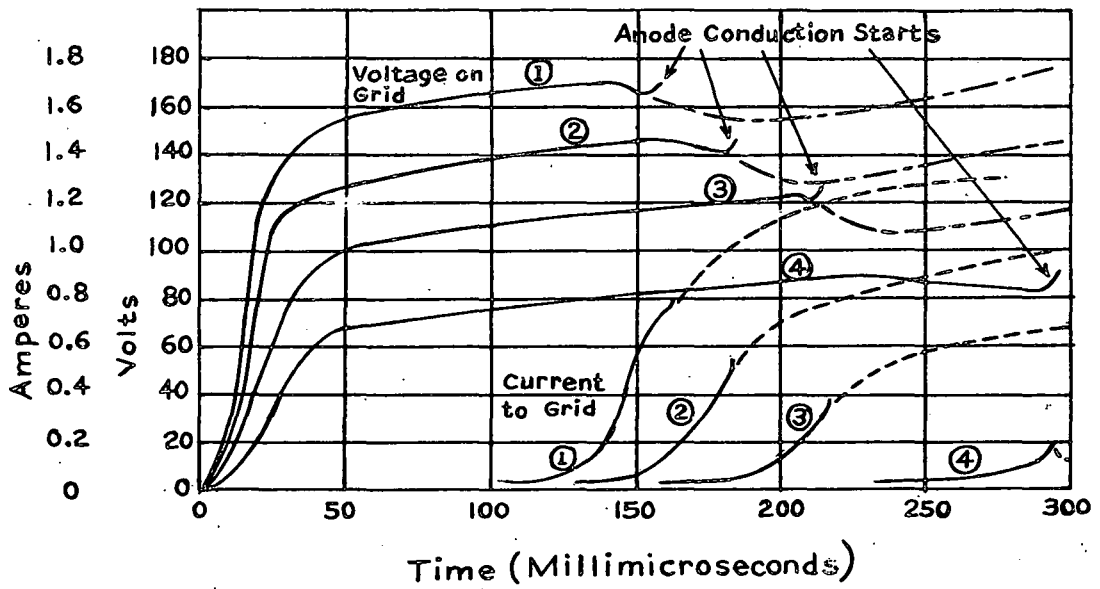

Fig. 37 Grid Current During Breakdown of the Cathode-Grid Space and Commutation to the Anode as Functions of Time at Various Voltages. Anode Voltage 3 KV.

Within the broader classification of Triggering Time will be included the subject of Anode Delay time. Anode delay time as discussed by Germeshausen[2] is described as the period of time measured between

---

[1] Goldberg, Op. Cit., p. II-6

[2] Glasoe and Lebacqz, Op. Cit., pp. 350 to 352

grid-cathode breakdown and the breakdown of grid-anode. Anode delay time's variation with several factors may be summarized as follows:

(1) Anode delay time increases slightly with decrease in anode voltage. (A representative measurement is a 0.07 μsec increase in delay time with a change of anode voltage from full to 1/4 maximum anode voltage.)

(2) Anode delay time decreases with decrease in trigger impedance. The time reduction amounted to 0.1 μsec with a 2000 ohm to 200 ohm change in trigger impedance. For generally-used trigger circuits, the internal impedances lie in a 300 to 500 ohm range.

(3) Anode delay time decreases with an increase in rate of rise of trigger voltage. The manner in which the two are interrelated is presented in figure 38.[1] The curves indicate that rate of rise of trigger voltage affects delay time a lesser amount beyond trigger voltage rise rates of 200 to 300 volts/μsec.

---

[1] Glasoe and Lebacqz, Op. Cit., p. 352

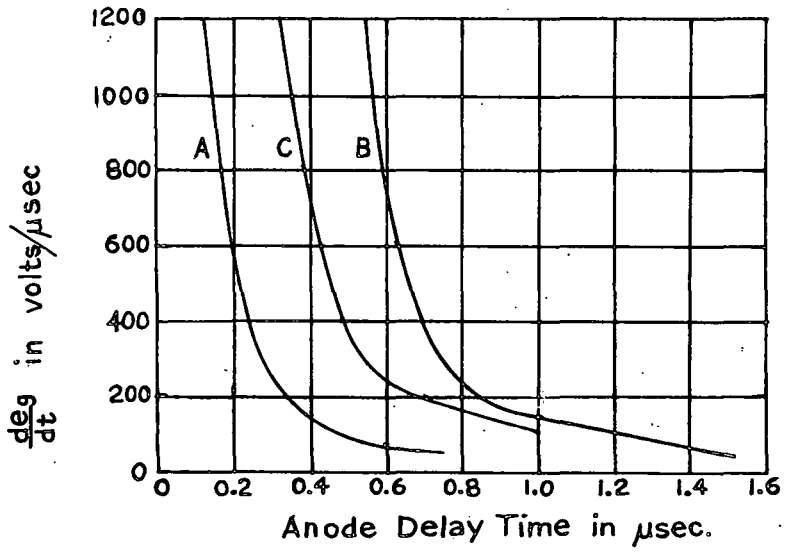

Fig. 38 Effect of the Rate of Rise of Trigger Voltage on the Anode Delay Time. Curve A is for the shortest delay, curve C is for the longest delay and curve B is an average based on A and C and statistical data. (4C35 V_N = 8 Kv, trigger amplitude - 150v)

Summary of Thyratron Operation

In the interest of providing a single compact source of information on operation characteristics, the preceding four sections will be summarized in table 10.

TABLE 10

SUMMARY OF THYRATRON OPERATION CHARACTERISTICS

PARAMETER	DEFINITION	VARIES WITH	REMARKS
1. Ionization Time	Time interval from start of anode voltage fall (from maximum voltage before conduction) to start of steady-state conduction	(a) Tube geometry (b) Gas pressure	Typical values of ionization times: .02 to .07 μsec
2. Tube Drop	Anode-to-cathode drop	(a) Cathode emission (b) Cathode current (c) Gas pressure (slightly)	Typical values: 80 to 120 volts
3. Tube Dissipation Per Pulse	Product of tube drop and tube current	(a) Pulse current (b) Pulse duration (c) Anode voltage (d) Rate of rise of anode current	Typical values are dependent on anode current since tube drop is nearly the same for most hydrogen thyratrons.
4. Triggering Time	Interval of time from attainment of 6 volts by the grid to the instant of anode breakdown	(a) Amplitude of trigger (b) Rate of rise of trigger (c) Anode voltage	
5. Anode Delay Time	Period of time from grid-cathode breakdown and breakdown of grid-anode	(a) Anode voltage (b) Anode delay time (c) Rate of rise of trigger voltage	

Chapter IV

Some Specific Attributes of Type 1258 Hydrogen Thyratron

Introduction

A study of several characteristics of a reliable version of the type 1258 hydrogen thyratron was initiated. It was expected that a fuller knowledge of the tube's operating parameters would be gained through a number of investigative tests. To that end, the following relationships were sought:

(1) filament current vs. time

(2) tube drop vs. filament voltage

(3) tube drop vs. time

General Description

The type 1258 thyratron has a single-ended structure -- that is, the tube leads exit through one end of the glass envelope. The glass envelope is the standard T $6\frac{1}{2}$ miniature size and is composed of a hard glass, Corning 7720 or similar. The hard glass is necessary as a result of the high bulb temperatures encountered in regular operation of the thyratron. To match the temperature coefficient of hard glass, tungsten is used for the tube base pins. Since tungsten is a hard and relatively unbending material, the insertion of a tube with base pins made of this metal into a tube socket with slight misalignment of socket receptacles can result in glass base cracks or breakage. The tungsten pins, instead of bending to fit the misaligned socket receptacle, remain rigid and transmit nearly the full side forces to the glass base. To

minimize the possibility of glass base damage, sockets with "floating" receptacles -- that is, receptacles, allowing a limited amount of lateral movement, should be employed. The usual jigs for straightening tube base pins should also be avoided to reduce glass base damage. The general constructional features of the type 1258 reliable version are illustrated in figure 39.

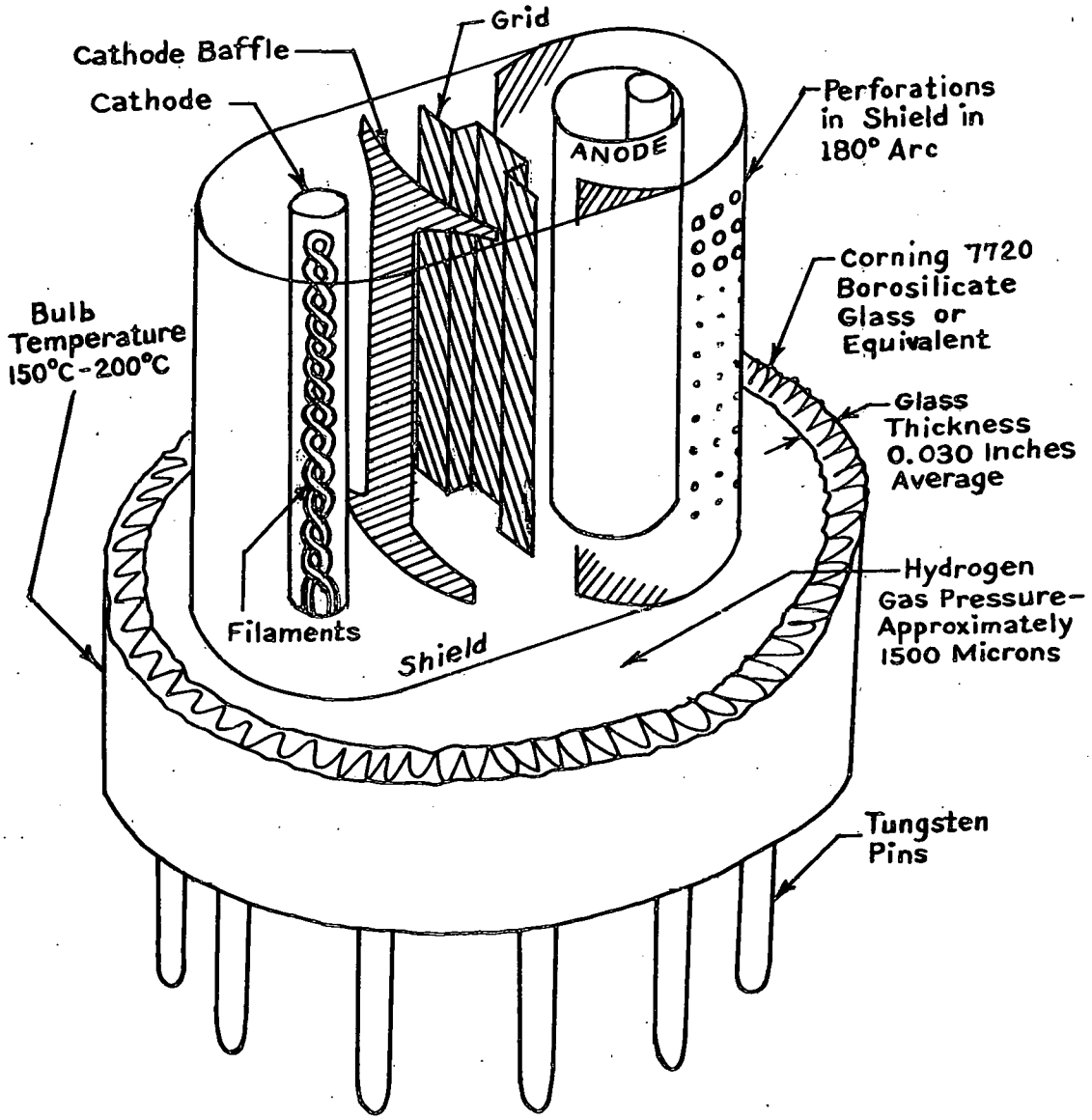

Fig. 39. General Constructional Features of the Type 1258 Hydrogen Thyratron.

Chapter IV

Filament Current vs. Time

The initial peak of filament current through cold tube filaments can impose severe starting loads on the heater power supplies and also place considerable electrical and mechanical strains on the tube filaments themselves. In the latter case, life tests can be performed utilizing the worst combination of conditions in which filaments are cold-started in regular cycles with appropriately selected high filament voltages. The results of this type of life testing will indicate the extent to which the tube may be affected in similar actual circuit use.

It is the intent in this instance, however, to investigate only the characteristic affecting filament power supply loading -- i.e., the initial surge value of filament current through cold tube filaments. This was accomplished by employing the circuit and procedure shown in Appendix A.

Photographs of oscilloscope traces were obtained of various filament surge current values under different conditions of applied voltages with respect to the latter's amplitude, rise time, and frequency. These are shown in figures 40 and 41.

Figure 40(A) to 40(C) show the effect of the application of a controlled rate of rise of filament voltage on a cold tube and a warm tube. The surge current rises to 7.4 amperes on the cold tube.

Chapter IV

The initial surge of RMS current in figure 40 (D) to 40 (F) appears to be approximately 7 amperes in value. The A.C. filament voltage used in this instance was the standard 6.3 volts.

In figure 41 (A) through 41 (F), the filament current surges were obtained using a "stiff" filament power supply -- i.e., one with low internal impedance and good regulation. With an internal impedance of 0.001 ohms, filament voltage rise times of approximately 8 to 10 milliseconds were obtained with the filaments of one Type 1258 thyratron as a load. The surge currents under these conditions of applied voltage are shown as approximately 9 amperes and 10 amperes for filament voltages of 6.3 and 7.1 volts respectively. The steady state value of filament current generally measured in a Type 1258 after one minute operation will lie in the range of 1.70 to 1.95 amperes.

Tube Drop vs. Filament Voltage

Since filament voltages may vary during thyratron operation, a knowledge of the degree of accompanying tube drop change would be useful. The measurements were made with the plate voltage and trigger voltage set at the normal values and with the filament voltage only being varied. The details of the procedure, circuit schematic, and graphical results are shown in Appendix B.

The curves for this relationship emphasize how much tube drop depends on cathode emission. The low filament voltages, which produce low temperatures and subsequent poor emission from the cathodes, result

in high tube drop. High filament voltages bring about the opposite result. It is interesting to note that tubes with the higher tube drops at low filament voltages are improved a greater amount with increase in filament voltage than the remaining tubes. This suggests that high tube drop thyratrons at low or normal filament voltages may have relatively poor low temperature cathode activity.

Tube Drop vs. Time

It will be recalled that a previous discussion on tube drop took place in Chapter III. In that discussion tube drop was described as possessing two distinct portions, the first consisting of a relatively high but rapidly decreasing voltage value occurring during the commutation period of operation, and the second part being of relatively long duration and low constant voltage level. The latter division is present during and is part of the steady-state discharge. It is this latter portion of the tube drop that will be elaborated upon with regard to the change of its level with time. More specifically, the change in tube drop level with time will be investigated during intervals immediately after application of voltages to thyratron electrodes.

The rate of gas ionization affects the voltage values observed in the initial or commutation portion of the tube drop waveform; however cathode emission is the principal parameter influencing the steady-state portion of tube drop. Additional factors causing change in steady-state tube drop are cathode current levels and tube gas pressure.

Chapter IV

Preliminary Test Attempts

Means by which tube drop could be measured with respect to time took several directions of investigation. One of the methods tried involved the use of the line-type pulser circuit shown in figure 44 of Appendix B. In place of the voltmeter V_1, an X-Y recorder was connected across the variable power supply which serves as a bias source for the oscilloscope lower deflection plate. Immediately after anode voltage is applied to the TUT (tube under test), a waveform similar to that illustrated in figure 45(A) is noted on the oscilloscope tube face. The operator attempts to vary the bias power supply so that the tube drop porch section is positioned on the zero reference line previously located on the oscilloscope tube face. As the thyratron under test warms up, the tube drop decreases in value, so the operator must vary the bias supply in an appropriate manner to keep the porch at the zero reference line. This changing bias supply voltage is applied to the X-Y recorder, and a plot of tube drop vs. time results. While this method proved satisfactory for the later portions of the plot, the initial portions were not only ragged and erratic but in the case of the first five seconds after anode voltage turn-on were practically impossible to record. The operator was physically incapable of reacting quickly or smoothly enough to get correct representations of the initial levels of steady-state tube drop. This test procedure was therefore abandoned for others showing more promise.

Chapter IV

Description of Test Method Used

Another method with an entirely different approach was analyzed. A high power pulse generator was used to apply a pulse voltage to the Type 1258 thyratron sufficient to cause cathode pulse currents of approximately 13 amperes peak value. Several variations of this method were tried before a satisfactory version was obtained. A description of the circuit and procedures used can be found at the end of Appendix C. The circuit is shown in figure 49. A pulse generator utilizing a 4C35 hydrogen thyratron serves as the high power pulse voltage source for the anode circuit of the Type 1258 thyratron under test. A blocking oscillator, designed with a Type 5814A twin triode, triggers a small line-type pulser which in turn triggers the 4C35 pulse generator. A similar blocking oscillator applies a trigger pulse to the grid of the Type 1258 TUT. This trigger pulse and the plate pulse to the TUT delivered by the 4C35 pulse generator are held in proper phase relationship by a synchronizing signal from the 1258 trigger generator to the TUT's trigger source. The 4C35 pulse generator was left operating constantly during the tests, so that its initial warmup and corresponding initial changing output would not affect the measurements taken. Instead, a relay (with mercury contacts to eliminate circuit interruptions due to contact bounce) was used to switch on pulse voltages to the TUT. The tube drop was simultaneously recorded on the X-Y recorder and viewed on an oscilloscope through a voltage divider circuit across TUT anode-to-ground.

Chapter IV

Test Results

Appendix C includes some of the X-Y recordings made with the foregoing circuitry.

Figures 46(A) through 46(C) portray for three tubes the tube drop vs. time curves obtained at various recorder speeds. In each instance the tube was allowed to cool to normal room temperature before proceeding with the next measurement. Procedure 1 described at the end of Appendix C was the test method providing the results of figure 46. It can be seen that initial peak tube drops as high as 265 volts were obtained on tubes that normally measure in the 100 to 120 volt range after several minutes operation. This occurred at a time of five seconds after filament voltage had been applied so that cathode emission was understandably low with a cathode warmup time of only five seconds.

Figures 47(A) through 47(C) represent tube drop vs time measurements similar to those of figure 46 except that filament warmup times of 10 seconds were provided to the tube under test in this instance. The lower initial tube drops are evident and resulted from the higher temperature and subsequent better emission of the cathodes. Although great care had been taken in calibrating the entire equipment at the beginning of these tests, an additional check was made to compare tube drop vs time readings by two methods. At the same time that the X-Y recording was being traced out, a photographic print was made of the initial tube drop waveform present at 10 seconds on the oscilloscope.

Visual oscilloscope readings at the noted times were also read. These have been added to the X-Y recordings for comparison purposes. In addition, tube drop readings of these tubes after three minutes operation were obtained using the oscilloscope deflection plate method described in Appendix B. In all instances comparison of the data showed that correlation was satisfactory.

Figures 48(A) through 48(C) include the effect of cold temperature on initial tube drop values. The three tubes were stored in an environmental chamber in which the ambient temperature (TA) was decreased to -62°C. After a waiting period sufficient to bring the entire inner structure of the tube to this low temperature, each tube was in turn removed from the chamber, inserted in the test socket, and measured for its tube drop data. The results were not unforeseen. It was to be expected that colder initial temperatures would slow cathode warm-up and produce the subsequently higher tube drops.

Summary

The results of the tube drop vs. time tests may be summarized in the form of table 11. This affords easy comparison of the drop values obtained under various conditions of operation time, ambient temperature, and warm-up time.

Chapter IV

Table 11

Tube Drop vs Time for Several Test Conditions

Time after Filament Voltage Turn-on (sec.)	TA = 25°C W/U Time = 5 sec. Tube No.			TA = 25°C W/U Time = 10 sec. Tube No.			TA = -62°C W/U Time = 10 sec. Tube No.		
	8A	9A	29A	24A	336	340	24A	336	340
5	256	170	265	--	--	--	--	--	--
10	188	99	205	210	180	165	230	205	175
60	98	79	116	132	98	87	183	96	90
300	103	78	102	--	--	--	--	--	--

Conclusions

A review of the tests described in Chapter IV and their results lead to a few general and some specific conclusions regarding the Type 1258 hydrogen thyratron.

(1) The peak filament current at first turn-on of filament voltage:

(a) for controlled rate-of-rise D.C. filament voltage equals 7.4 amperes, (V_f = 8.0 volts; 0-90% value in 400 msec.)

(b) for 60 cps A.C. filament voltage equals 7.0 amperes, (V_f = 6.3 volts)

(c) for a "stiff" source of D.C. filament voltage (Z_{int} = 0.001 ohms) equals 9 and 10 amperes at V_f = 6.3 and 7.1 volts respectively.

Since for Type 1258 hydrogen thyratrons normal filament currents range from 1.70 to 1.95 amperes at V_f = 6.3 volts, peak currents four to six times the usual measured values can be expected at first

turn-on; therefore design considerations should take this fact in account.

(2) Tube drop varies inversely with filament voltage and:

(a) is more noticeable in high tube drop tubes possibly indicating in these tubes poor low-temperature cathode activity which is strongly improved during high filament voltage operation,

(b) may differ, in the range of filament voltages of 6.2 to 6.4 volts, from two volts (Tube #20A) to 10 volts (Tube #28A).

If tube drop must be closely controlled in a particular circuit application, filament voltages should be well regulated.

(3) Tube drop at initial times immediately after anode voltage turn-on:

(a) varies inversely with warm-up time,

(b) varies inversely with ambient temperature,

(c) may have values at first turn-on approximately two to three times greater than that after one minute operation.

To minimize initially high tube drops, longer warmup times and controlled ambient temperatures would appear to be two factors helping to achieve this goal.

BIBLIOGRAPHY

BIBLIOGRAPHY

Books

Cobine, J. D. Gaseous Conductors. Dover Publications, Inc., New York, 1941.

Condon, E. U. and Odishaw, Hugh. Handbook of Physics. McGraw Hill, Inc., New York, 1958.

Cotton, H. Electric Discharge Lamps. Chapman and Hall, London, 1946.

Dushman, Saul. Scientific Foundations of Vacuum Technique. John Wiley and Sons, New York, 1949.

Glasoe, G. N. and Lebacqz, J. V. Pulse Generators. McGraw Hill, Inc., New York, 1948.

Reich, H. J. Theory and Applications of Electron Tubes. McGraw Hill, Inc., New York, 1944.

Ryder, J. D. Electronic Engineering Principles. Prentice Hall, Inc., New York, 1947.

Technical Reports

Goldberg, Seymour. Research Study on Hydrogen Thyratrons, Volume II. Edgerton, Germeshausen, and Grier, Inc., Boston, 1956.

Krulikoski, S. J. Hydrogen Thyratrons in Pulse Generators, Radiation Laboratory Report no. 953, Cambridge, March, 1946.

Marshall, F. R. and Hauser, S. M. Development of Hydrogen Thyratrons for High Power Millimicrosecond Operation, Third Quarterly Report, (ASTIA no. AD 206229), Electro-Optical Systems, Inc., Pasadena, 1958.

Proceedings of the Fifth Symposium on Hydrogen Thyratrons and Modulators. U. S. Army Signal Research and Development Laboratory, Fort Monmouth, 1958.

BIBLIOGRAPHY

Technical Reports

Schaffer, Allan. An Analysis of the Glow Discharge. (ASTIA no. 216 845), Space Technology Laboratories, Los Angeles, 1958.

Whitlock, R. S. Techniques for Application of Electron Tubes in Military Equipment, Volume 1. Wright-Patterson Air Force Base, December, 1958.

APPENDIXES

APPENDIX A

Filament Current vs. Time

Appendix A

Fig. 40. Initial Surge Values of Filament Current at First Turn-on of Filament Voltages

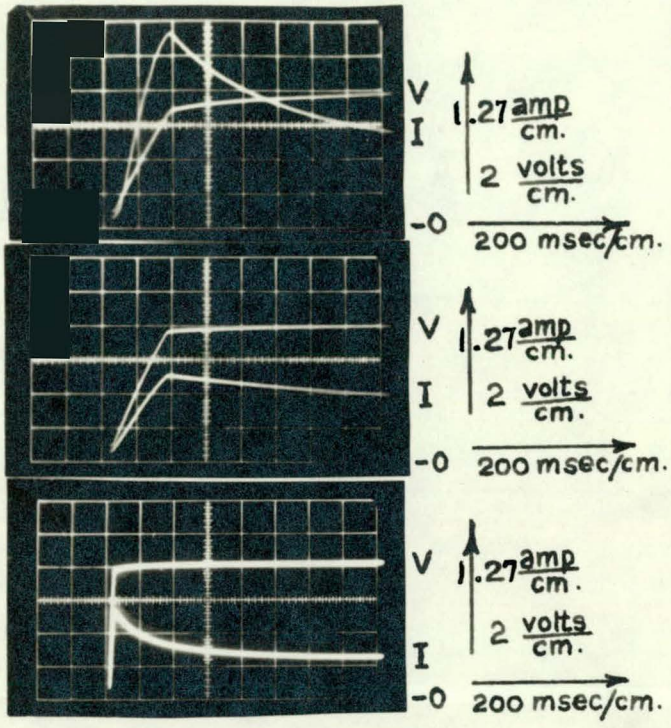

(A.) Application to Cold Tube of D.C. Filament Voltage with Controlled Rate of Rise (0 to 90% in 400 msec). Initial $I_f \approx 7.4$ Amp.

(B.) Same as (A) except tube is warm.

(C.) Same as (B).

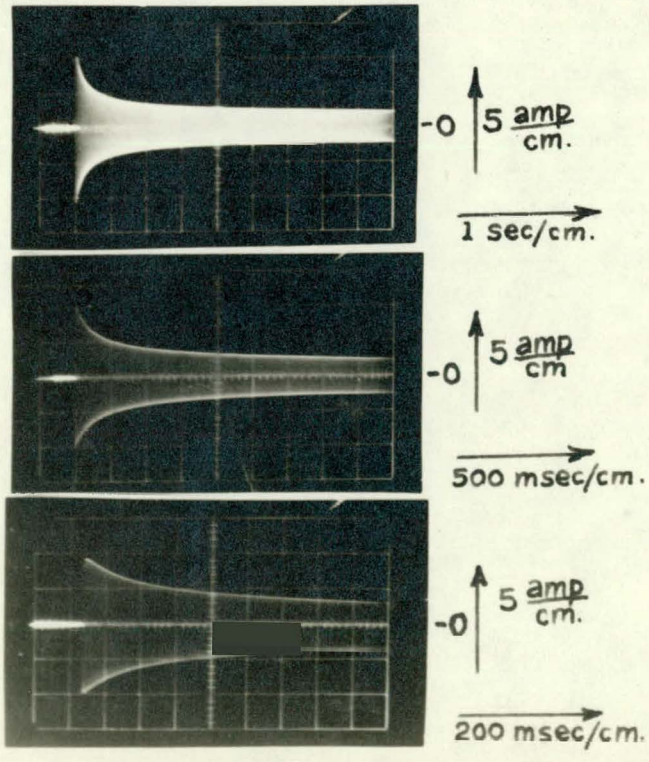

(D.) Filament Current Waveform (Peak-to-Peak) of Cold Tube with 60 cps A.C. Voltage Applied. Initial RMS $I_f = 7$ Amp approx.

(E.) Same as (D).

(F.) Same as (D.).

Appendix A

Fig. 41. Initial Surge Values of Filament Current at First Turn-on of Filament Voltages.

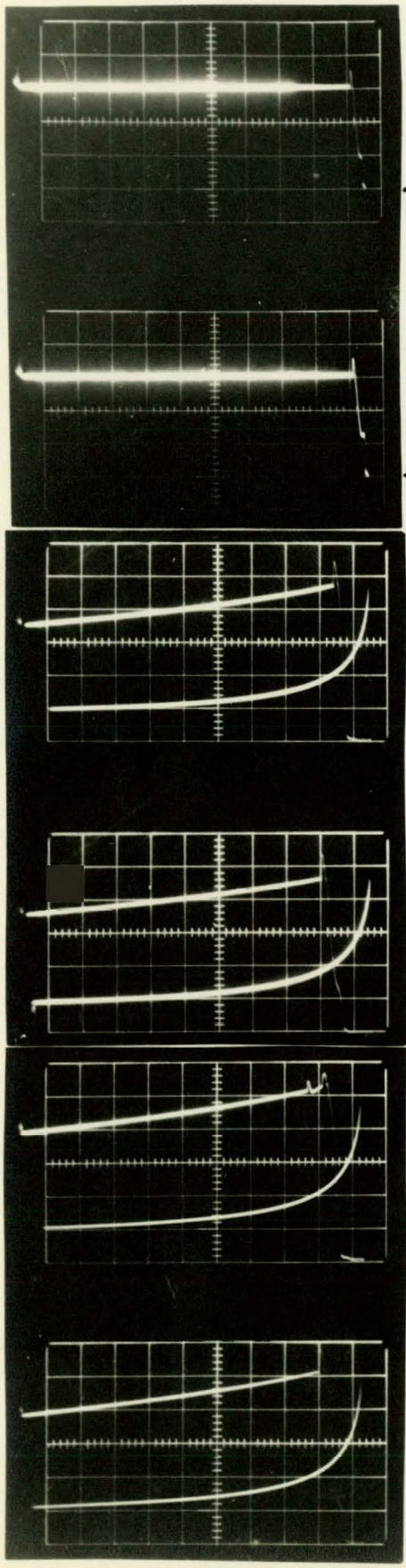

(A.) Waveform of Applied Filament Voltage to Cold Filaments of Tube.

(B.) Same as (A) Showing Uniformity and Repeatability of Applied Voltage Rise Time.

(C.) Waveforms of Initial Filament Current through Cold Tube with Applied Voltage V_f = 6.3 v. as in (A).

(D.) Same as (C) Showing Uniformity and Repeatability of Filament Current Waveform.

(E) Same as (C) except V_f = 7.1 v.

(F.) Same as (E).

APPENDIX A

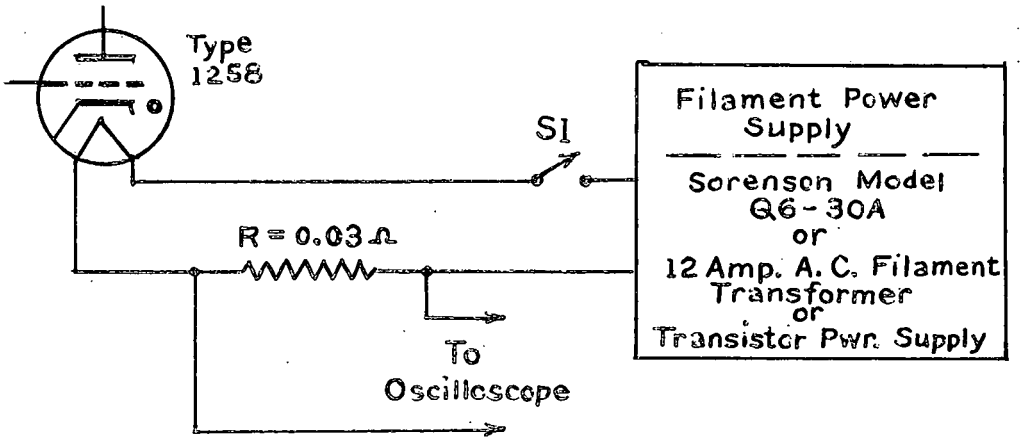

Fig. 42. Circuit for Measuring Filament Current vs. Time

Procedure

(1) Immediately before closing switch S1, the shutter on the oscilloscope camera is opened. (The shutter setting is on "Bulb" position.)

(2) Switch S1 is closed.

(3) The shutter is closed after the appropriate interval, depending on the oscilloscope sweep speed being used.

(a) The Sorenson power supply was used to obtain the 20 millisecond rise time in filament voltage shown in figures 41(A) through 41(F).

(b) The AC filament current waveforms in figures 40(D) through 40(F) were photographed when the AC filament transformer was selected for the heater power supply.

APPENDIX A

(c) A transistor power supply provided the controlled rate-of-rise waveforms illustrated in figures 40(A) through 40(C).

APPENDIX B

Tube Drop vs. Filament Voltage

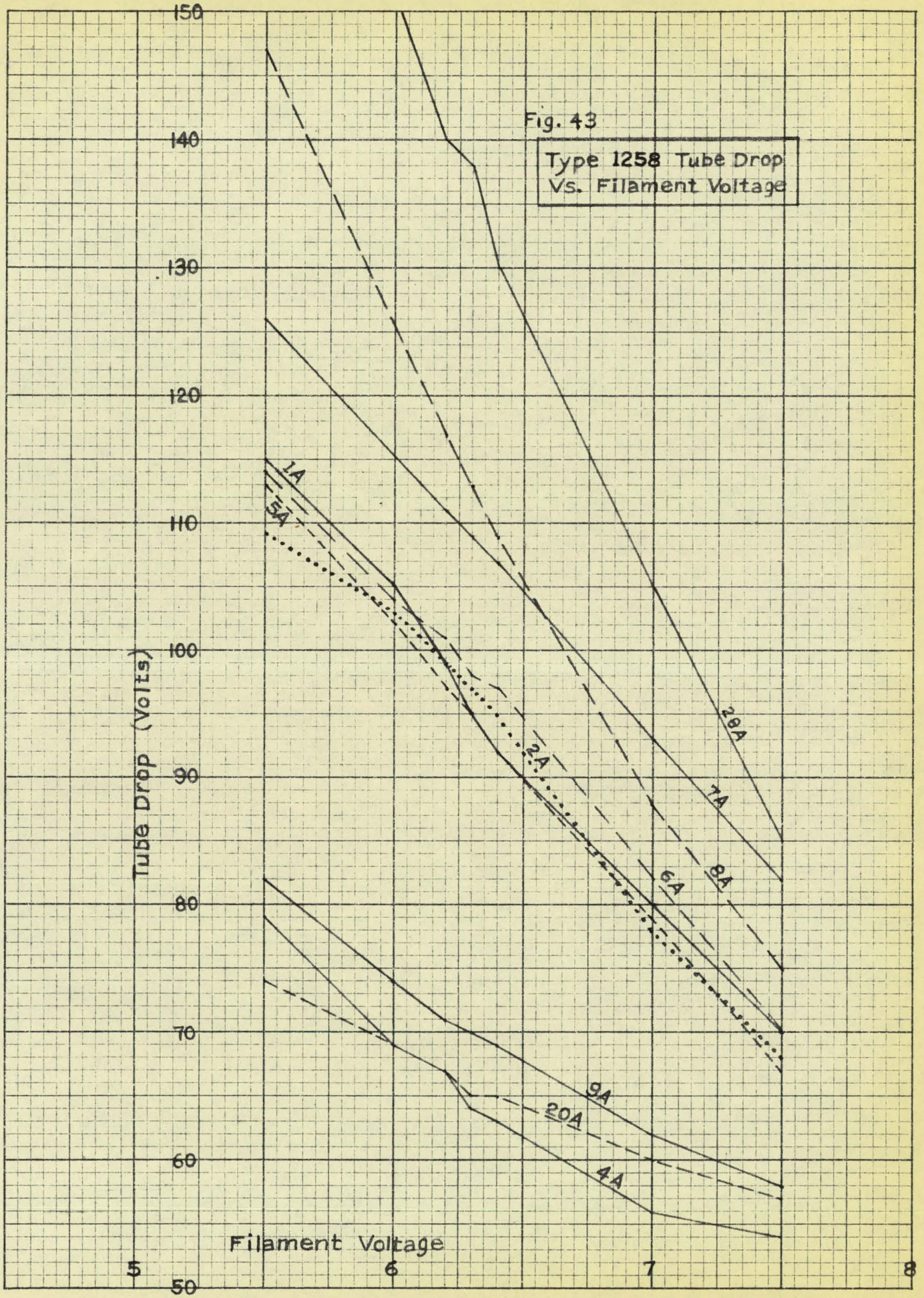

APPENDIX B

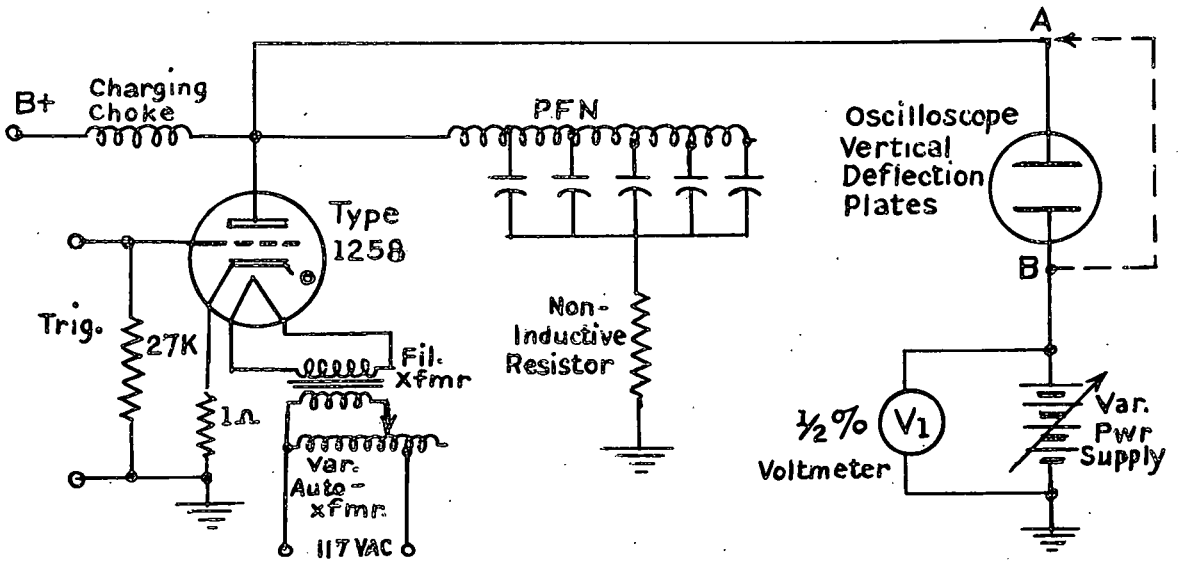

Fig. 44. Circuit for Measuring Tube Drop vs. Filament Voltage

Procedure

(1) Before turning on any voltages, point A should be temporarily connected to point B in order to place the upper and lower deflection plates at the same potential. This establishes the zero voltage reference line since the electron stream sweeps the oscilloscope tube face at a line approximately midway between the two deflection plates.

(2) With point A disconnected from point B, voltages are applied to the tube, i.e., normal plate, trigger, and filament voltages.

(3) With the tube stabilized, the trace illustrated in figure 45A is observed.

(4) Tube drop is measured by applying sufficient positive voltage to the oscilloscope's lower deflection plate to move the tube drop "porch",

APPENDIX B

i.e., the horizontal flat portion down to the zero reference line. (This is shown in figure 45B.) The tube drop value is that amount read on the meter V1.

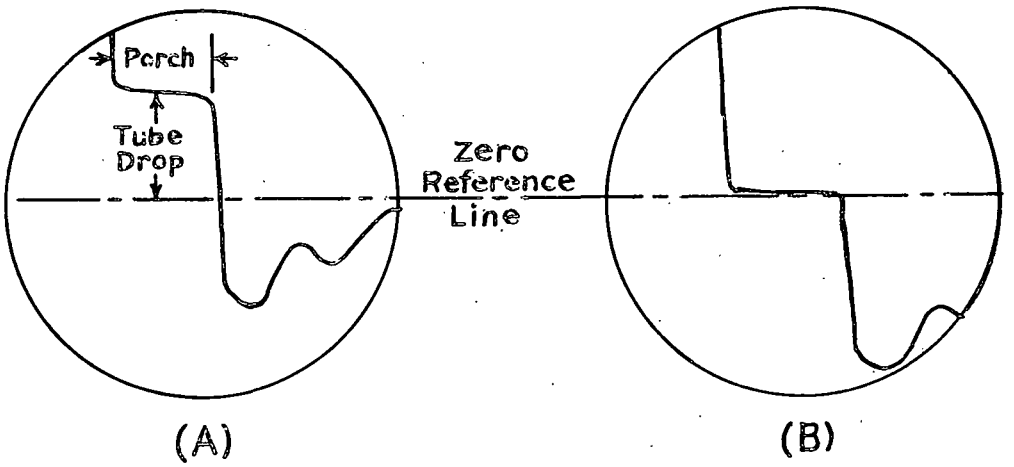

Fig. 45. Oscilloscope Traces of Anode Voltage during Commutation, Steady State Conduction, and Portion of Recovery.

(5) The filament voltage only is adjusted to a new value and the tube is allowed to stabilize. Steps (3) and (4) are repeated. This procedure is repeated until the readings at all the desired filament voltages are obtained.

APPENDIX C

Tube Drop vs. Time

ELECTRO INSTRUMENTS, INC.
SAN DIEGO, CALIFORNIA
NO. R100-10
MADE IN U.S.A.

Fig. 46 (A)

X-Y RECORDING OF TYPE 1258 TUBE DROP VS. TIME

TUBE # 8A

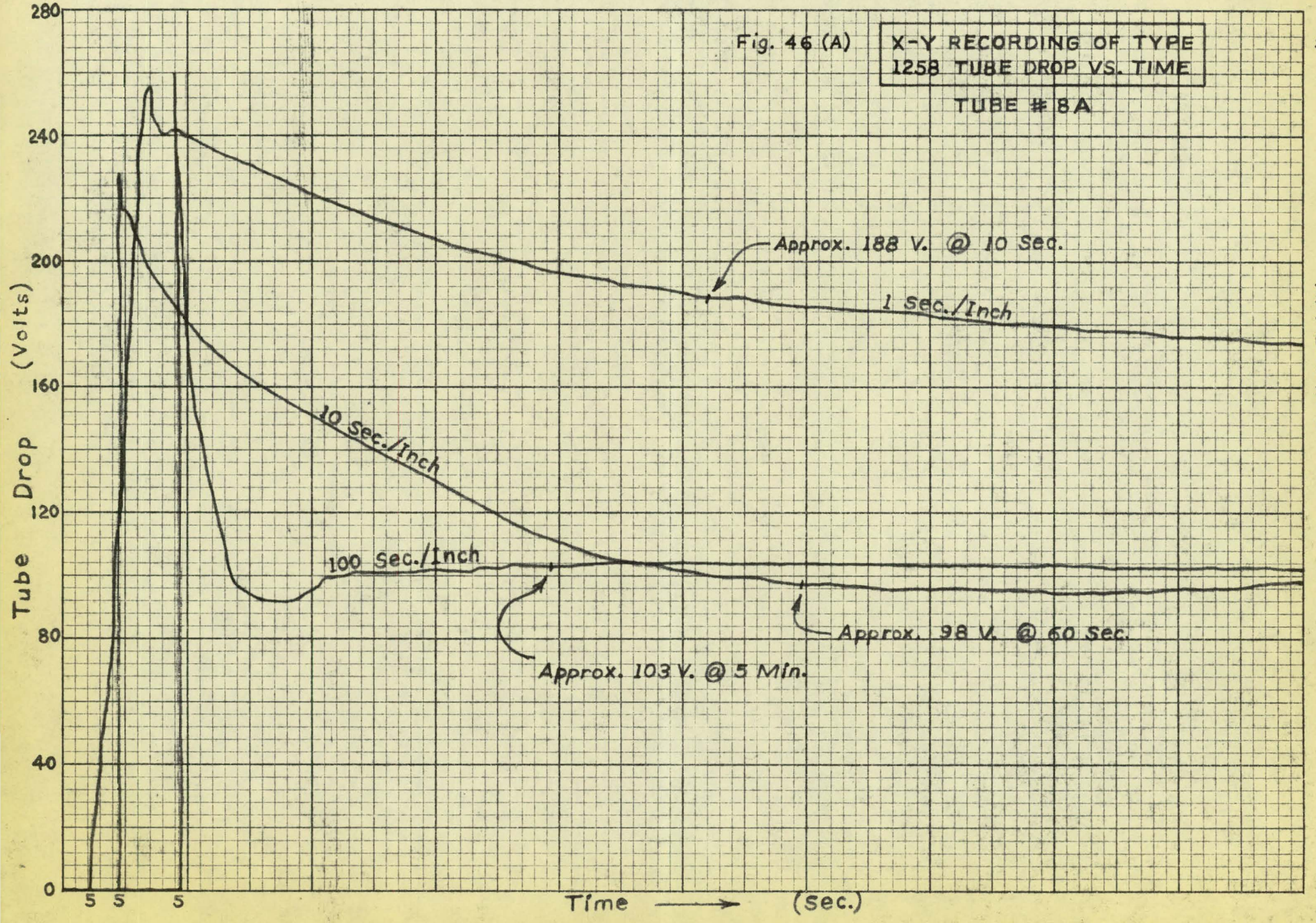

ELECTRO INSTRUMENTS, INC.
SAN DIEGO, CALIFORNIA
NO. R100-10
MADE IN U.S.A.

Fig. 46 (B)

X-Y RECORDING OF TYPE 1258 TUBE DROP VS. TIME

TUBE # 9A

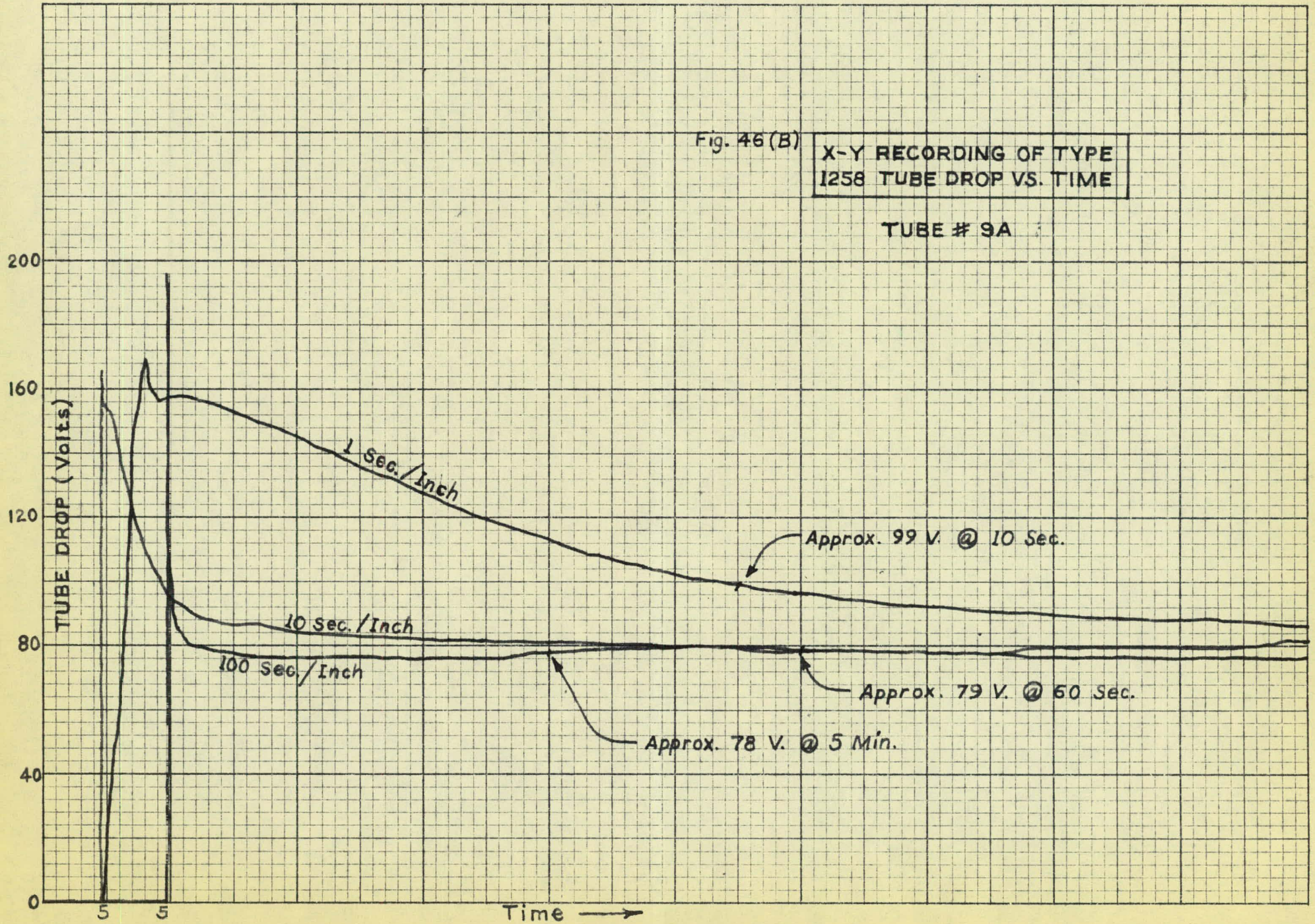

ELECTRO INSTRUMENTS, INC.
SAN DIEGO, CALIFORNIA
NO. R100-10
MADE IN U.S.A.

Fig. 46 (C)

X-Y RECORDING OF TYPE 1258 TUBE DROP VS. TIME

TUBE # 29A

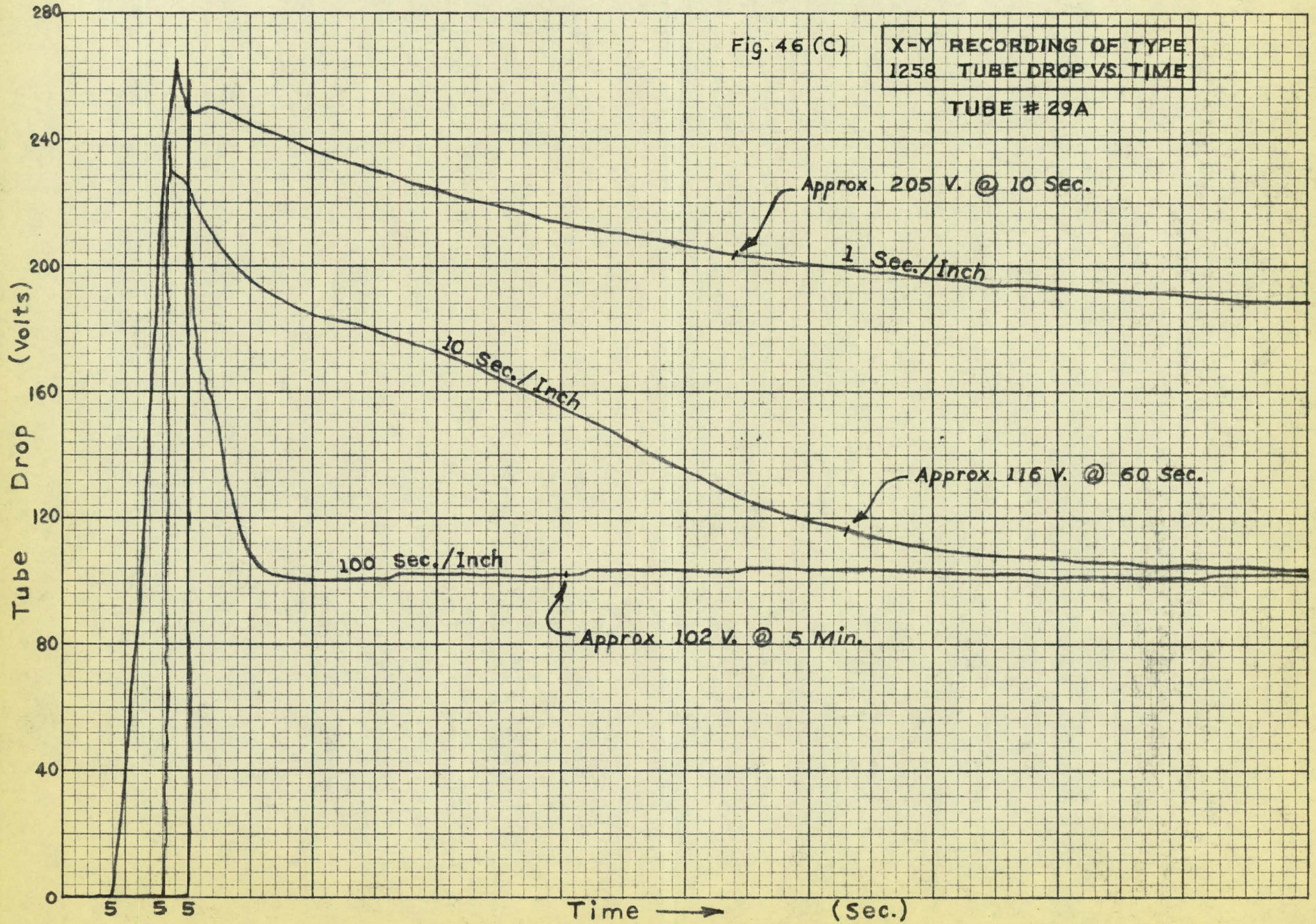

ELECTRO INSTRUMENTS, INC.
SAN DIEGO, CALIFORNIA
NO. R100-10
MADE IN U.S.A.

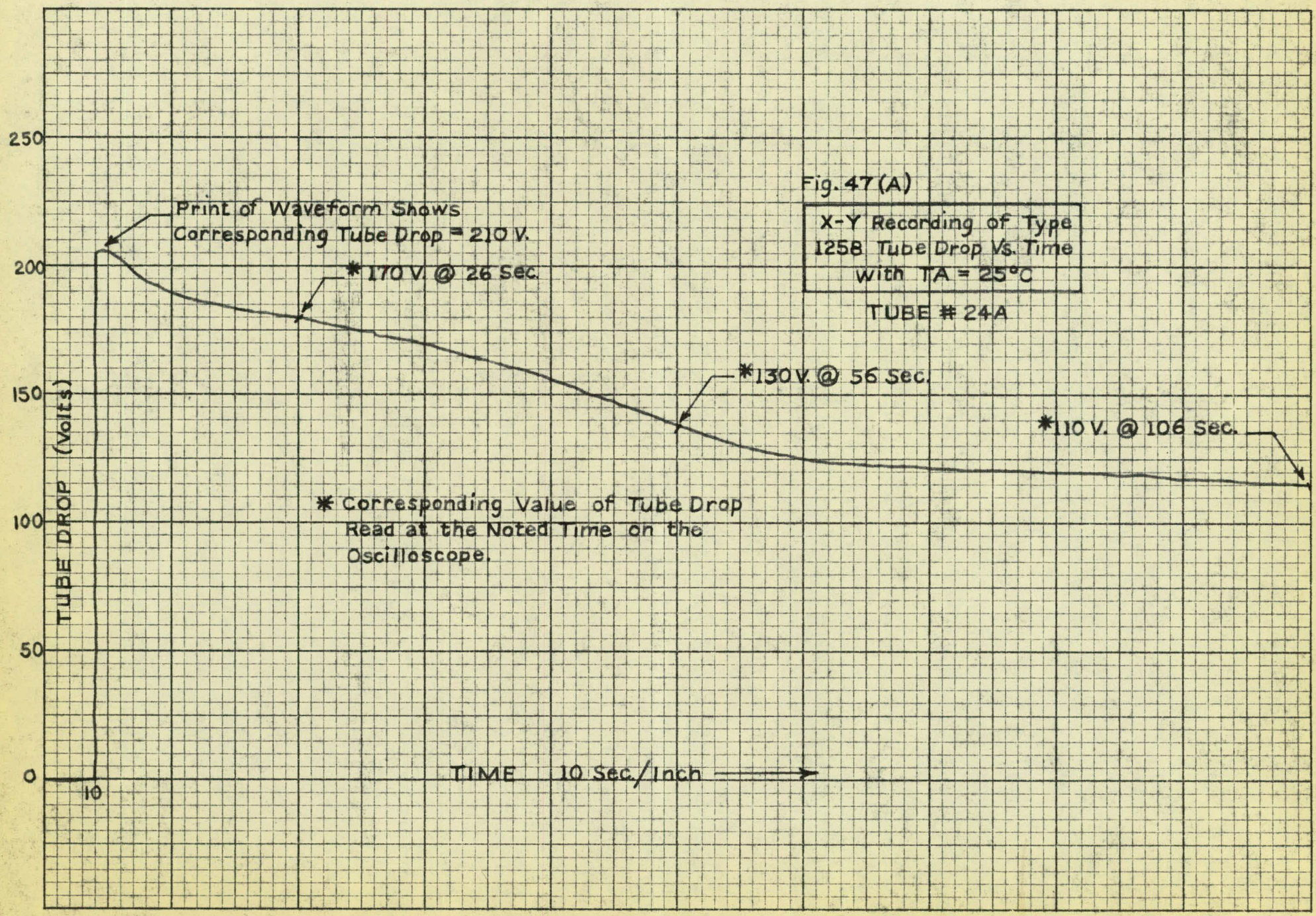

Fig. 47 (A)

X-Y Recording of Type 1258 Tube Drop Vs. Time with TA = 25°C

TUBE # 24A

ELECTRO INSTRUMENTS, INC.
SAN DIEGO, CALIFORNIA
NO. R100-10
MADE IN U.S.A.

Fig. 47(B)

X-Y Recording of Type 1258 Tube Drop Vs. Time with TA = 25°C

TUBE # 336

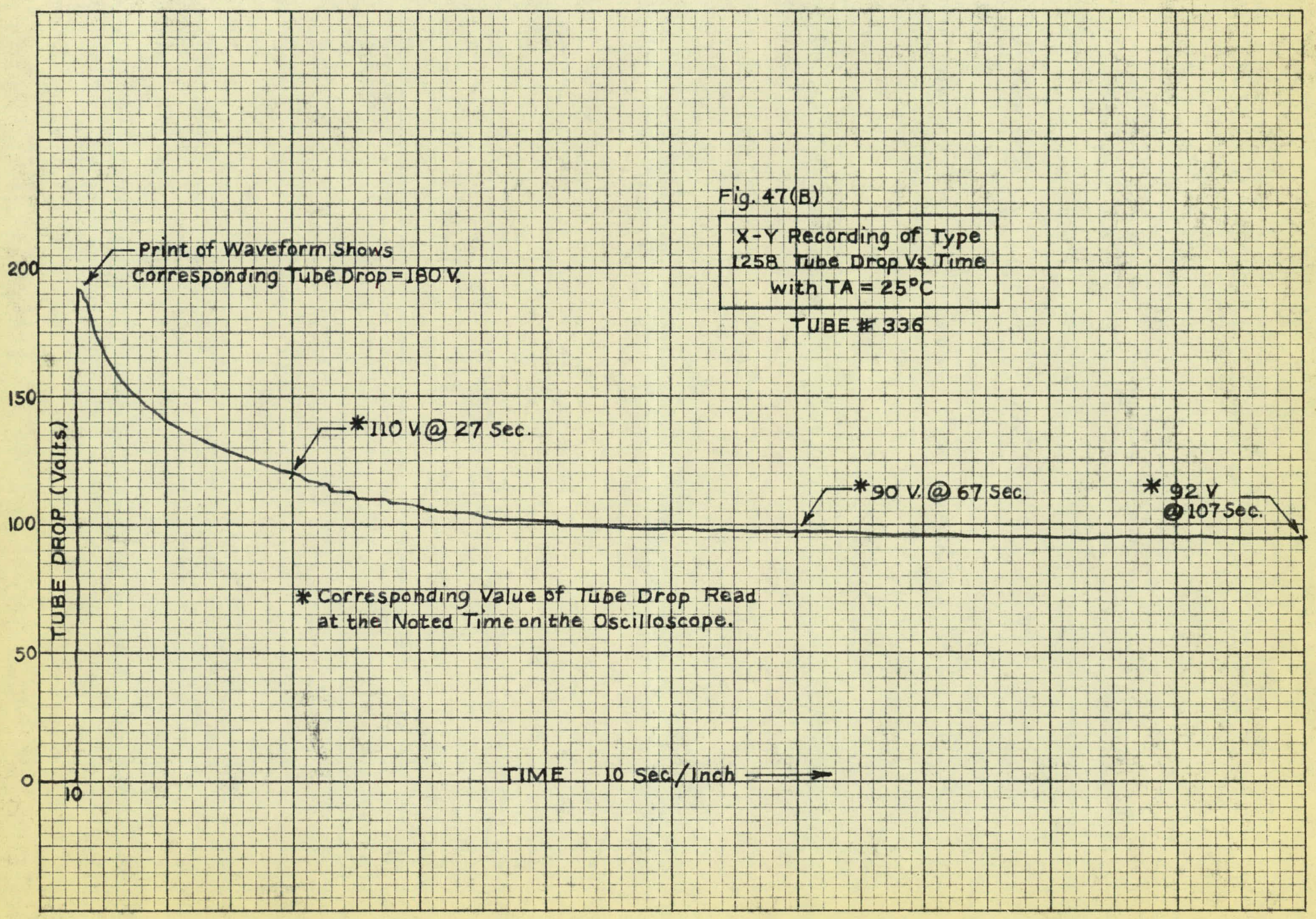

ELECTRO INSTRUMENTS, INC.
SAN DIEGO, CALIFORNIA
NO. R100-10
MADE IN U.S.A.

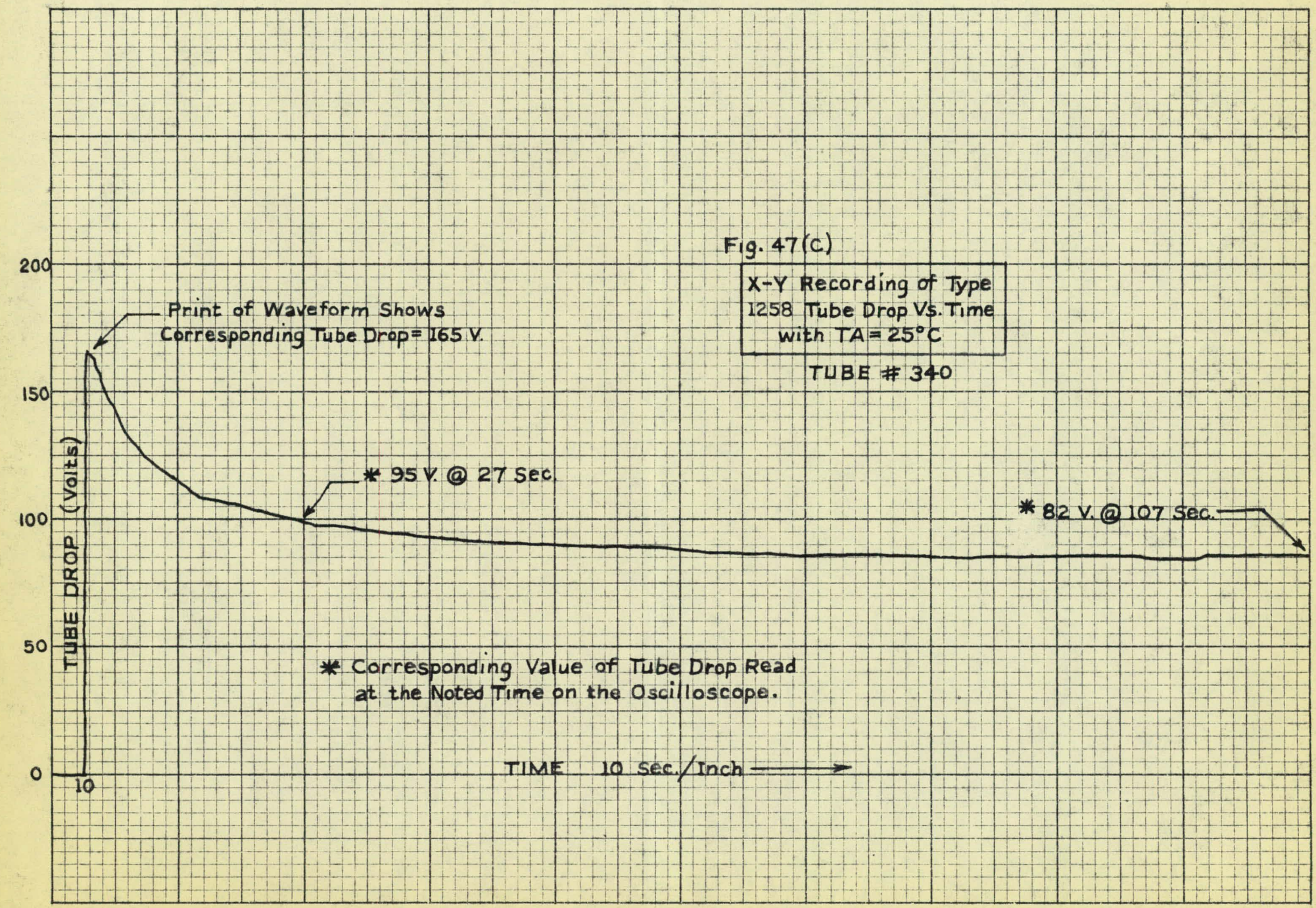

Fig. 47(C)

X-Y Recording of Type 1258 Tube Drop Vs. Time with TA = 25°C

TUBE # 340

ELECTRO INSTRUMENTS, INC.
SAN DIEGO, CALIFORNIA
NO. R100-10
MADE IN U.S.A.

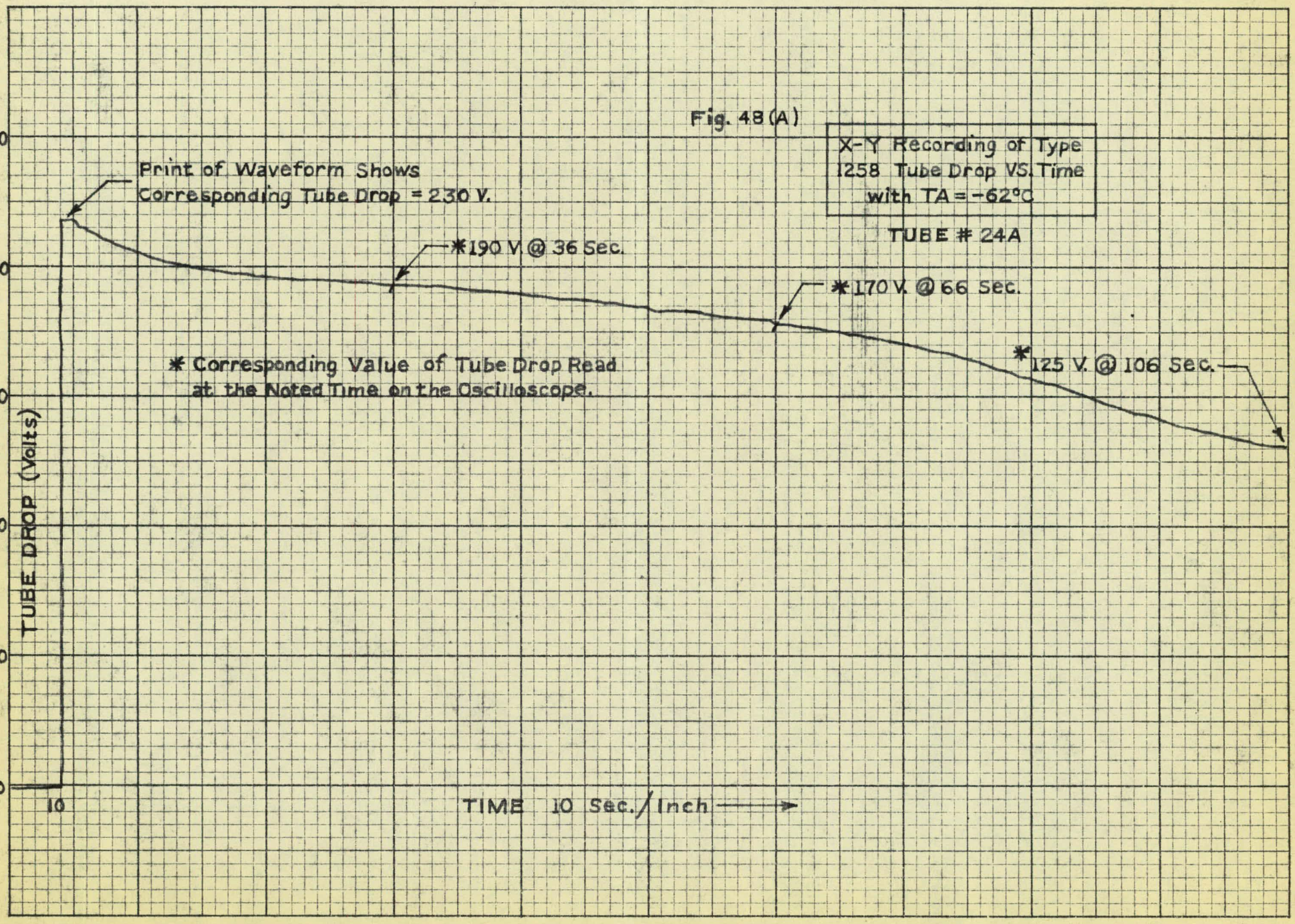

ELECTRO INSTRUMENTS, INC.
SAN DIEGO, CALIFORNIA
NO. R100-10
MADE IN U.S.A.

Fig. 48(B)

X-Y Recording of Type 1258 Tube Drop Vs. Time with TA = -62°C

TUBE # 336

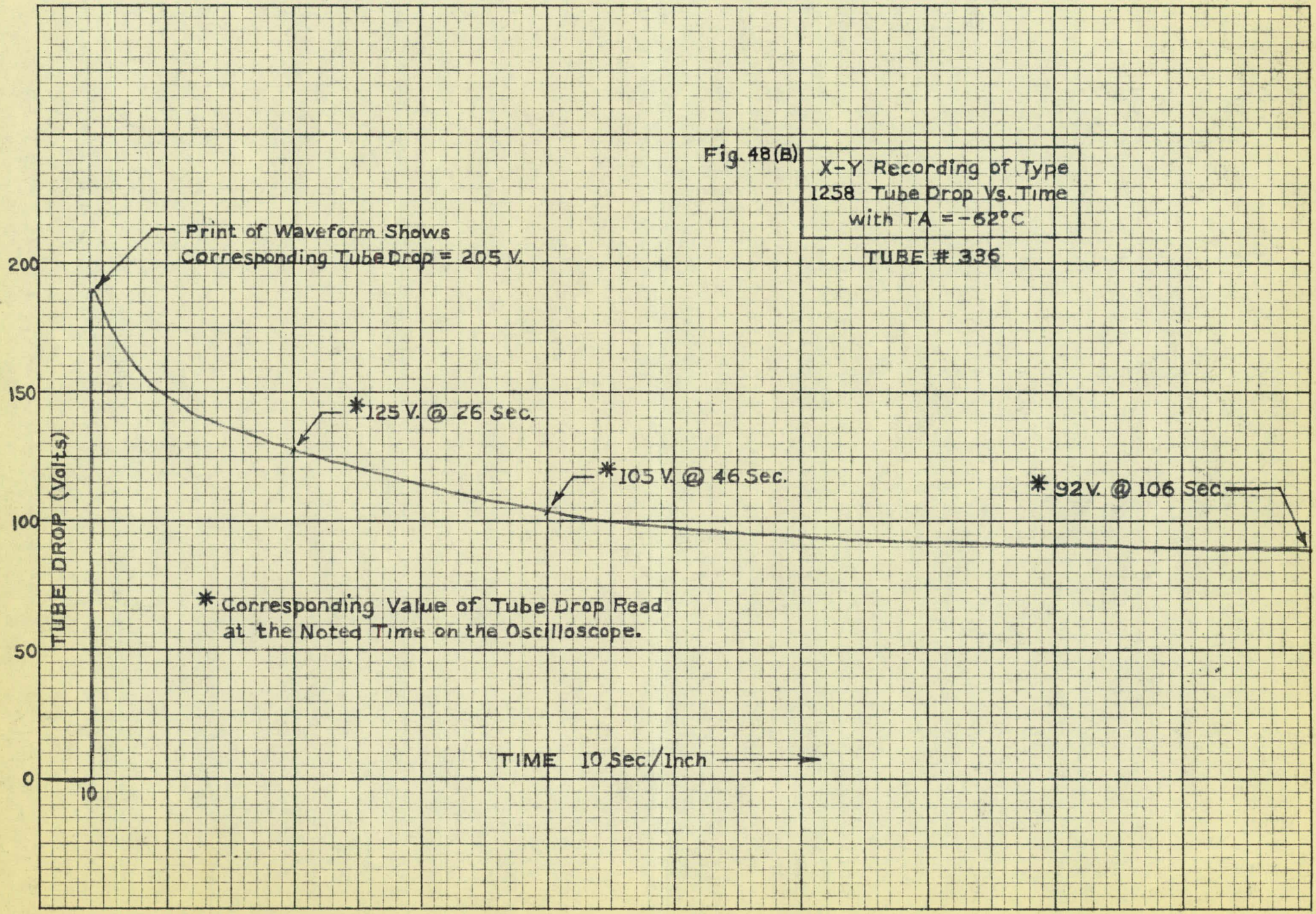

* Corresponding Value of Tube Drop Read at the Noted Time on the Oscilloscope.

ELECTRO INSTRUMENTS, INC.
SAN DIEGO, CALIFORNIA
NO. R100-10
MADE IN U.S.A.

Fig. 48(C)

X-Y Recording of Type 1258 Tube Drop Vs. Time with TA = -62°C

TUBE # 340

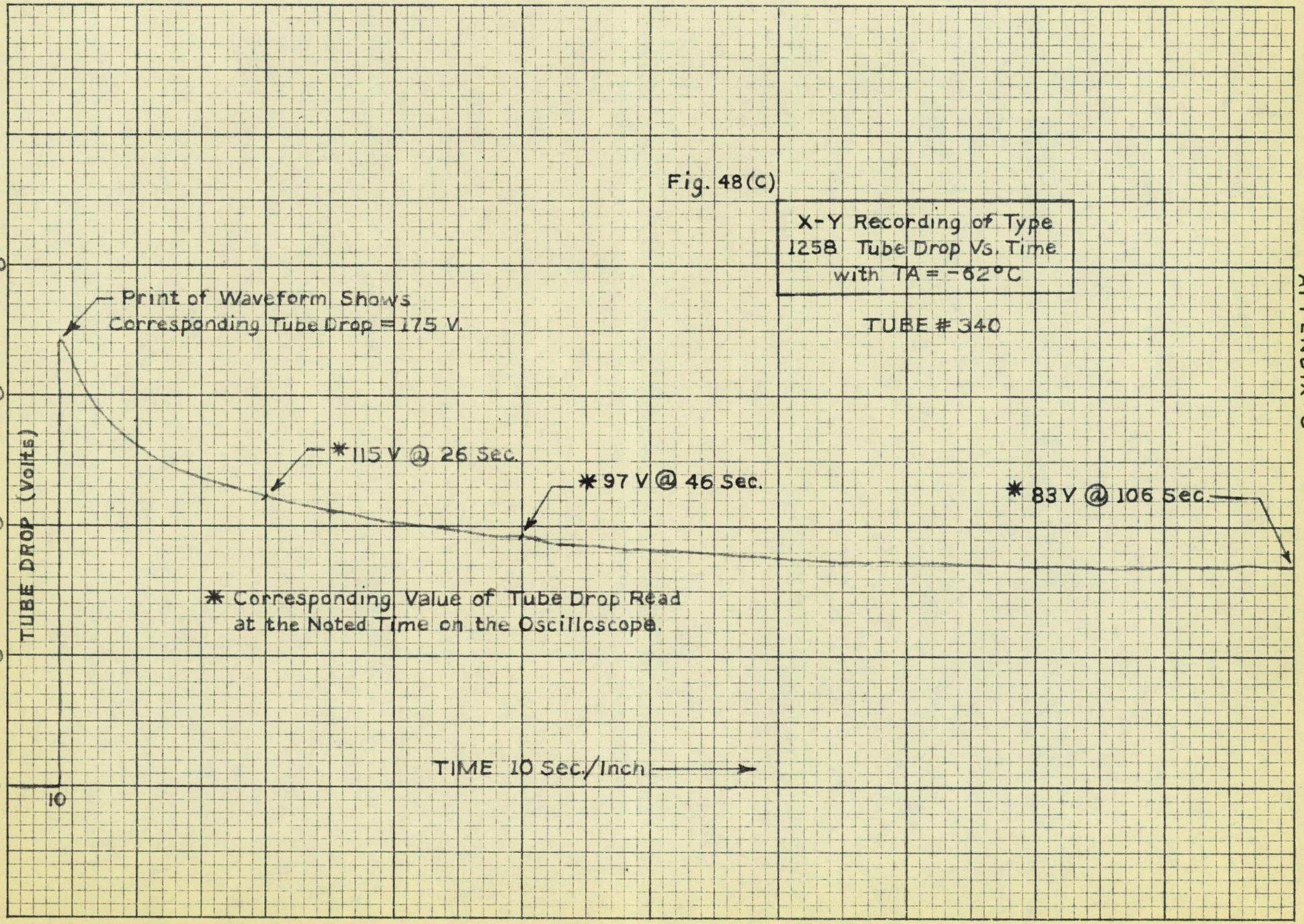

APPENDIX C

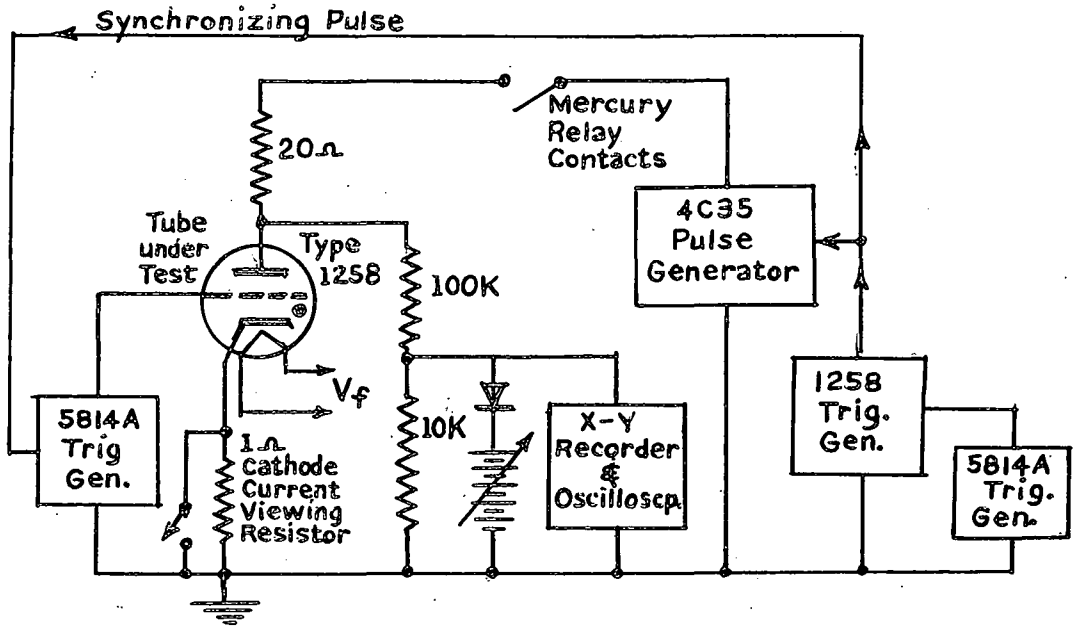

Fig. 49. Test Circuit for Measuring Tube Drop vs. Time

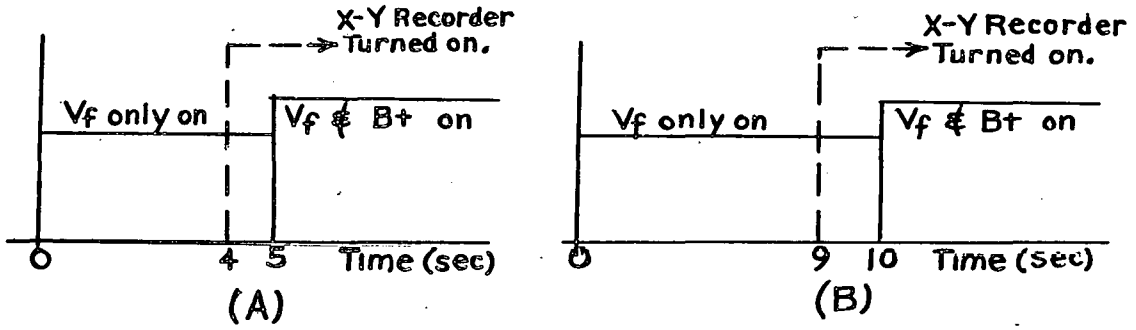

Fig. 50. Sequence of Electrode Voltage Turn-On

Procedure 1 (Figure 50A)

(1) Filament voltage V_f to tube under test turned on at time $t_o = 0$.

(2) X-Y recorder turned on at time $t_1 = 4$ seconds.

(3) Mercury relay contacts, applying pulse voltage to plate of tube under test turned on at time $t_2 = 5$ seconds. (Pulse voltage is

APPENDIX C

pre-set to value giving i_b = 13.5 amperes after 3 minute operation.)

(4) Tube drop vs time curves obtained for time-recording speeds of 1 sec/inch, 10 sec/inch, and 100 sec/inch.

Procedure 2 (Fig. 50B)

(1) Same as step (1) in Procedure 1.

(2) Same as step (2) in Procedure 1 except t_1 = 9 seconds.

(3) Same as step (3) in Procedure 1 except t_2 = 10 seconds.

(4) Same as step (4) in Procedure 1 except only the time-recording speed of 10 sec/inch was utilized.